

12-2007

# Fish Gelatin-Nanoclay Composite Film. Mechanical and Physical Properties, Effect of Enzyme Cross-Linking, and as a Functional Film Layer

Hojae Bae

Clemson University, hbae@clemson.edu

Follow this and additional works at: [https://tigerprints.clemson.edu/all\\_dissertations](https://tigerprints.clemson.edu/all_dissertations)



Part of the [Food Science Commons](#)

---

## Recommended Citation

Bae, Hojae, "Fish Gelatin-Nanoclay Composite Film. Mechanical and Physical Properties, Effect of Enzyme Cross-Linking, and as a Functional Film Layer" (2007). *All Dissertations*. 179.

[https://tigerprints.clemson.edu/all\\_dissertations/179](https://tigerprints.clemson.edu/all_dissertations/179)

This Dissertation is brought to you for free and open access by the Dissertations at TigerPrints. It has been accepted for inclusion in All Dissertations by an authorized administrator of TigerPrints. For more information, please contact [kokeefe@clemson.edu](mailto:kokeefe@clemson.edu).

FISH GELATIN-NANOCCLAY COMPOSITE FILM. MECHANICAL AND PHYSICAL  
PROPERTIES, EFFECT OF ENZYME CROSS-LINKING, AND AS A FUNCTIONAL  
FILM LAYER

---

A Dissertation  
Presented to  
the Graduate School of  
Clemson University

---

In Partial Fulfillment  
of the Requirements for the Degree  
Doctor of Philosophy  
Food Technology

---

by  
Ho Jae Bae  
December 2007

---

Accepted by:  
William S. Whiteside, PhD, Committee Chair  
Duncan O. Darby, PhD  
Robert M. Kimmel, PhD  
Hyun Jin Park, PhD

## ABSTRACT

The effect of clay content, homogenization RPM, and pH on the mechanical and barrier properties of fish gelatin/nanoclay composite films was investigated. The addition of clay increased the tensile strength (TS) from  $30.31 \pm 2.37$  MPa to  $40.71 \pm 3.30$  MPa. The nanoclay composite film had improved oxygen and water barrier properties when compared to neat fish gelatin film. Oxygen permeability decreased from  $0.0004028 \pm 0.0000007$  g·m/m<sup>2</sup>·day·atm to  $0.0001144 \pm 0.0000162$  g·m/m<sup>2</sup>·day·atm and the water vapor permeability decreased from  $0.0312 \pm 0.0016$  ng·m/m<sup>2</sup>·s·Pa to  $0.0081 \pm 0.0001$  ng·m/m<sup>2</sup>·s·Pa. The Small angle x-ray scattering (SAXS) and Transmission electron microscopy (TEM) observations confirmed that the ultrasonification treatment (30 min at 40% output) resulted in exfoliation of the silicates. Intercalation was achieved within the composite film without the ultrasonification treatment.

The fish gelatin solution was cross-linked by the addition of Microbial transglutaminase (MTGase) in an effort to measure the effect on film mechanical and barrier properties. The viscosity of the MTGase treated gelatin solution (2% w/w) increased from  $86.25 \pm 1.77$  cp (0 min) to  $243 \pm 12.37$  cp (80 min). Sodium dodecyl sulfate polyacrylamide gel electrophoresis (SDS-PAGE) results indicated that the molecular weight of fish gelatin solutions increased after treatment with MTGase. The increase of molecular weight imparted steric hindrance to intercalation, which also resulted in a marked decrease of intercalation. The tensile strength decreased from  $61.30 \pm 1.90$  MPa (0 min) to  $57.36 \pm 4.97$  MPa (50 min), and the elongation at break (EB) decreased from  $16.73 \pm 4.47\%$  (0 min) to  $13.34 \pm 5.13\%$  (50 min) at 2% (w/w) MTGase concentration. The

oxygen permeability and water vapor permeability were not significantly different as a function of treatment time at 2% (w/w) MTGase concentration. The incorporation of nanoclay to the MTGase treated film decreased oxygen permeability. The SAXS and TEM results suggested that the nanoclay was exfoliated in the MTGase treated fish gelatin film.

A three layer laminant film, utilizing the fish gelatin-nanoclay composite film as the functional barrier, was produced using a pilot scale laminator. The laminant film structure was low density polyethylene (LDPE), fish gelatin-nanoclay composite film, and polyester (PET). The fish gelatin-nanoclay laminant film showed excellent oxygen barrier (0~50% RH) when compared to a similar laminant structure utilizing an industry standard ethylene vinyl alcohol (EVOH) film as the barrier layer. In addition, the fish gelatin-nanoclay composite film exhibited sufficient bond strength (greater than 500 gr) to both the LDPE and the PET. Therefore, the fish gelatin-nanoclay barrier film has the potential to be used as a functional biopolymer barrier in laminant film structures for various food packaging applications.

## ACKNOWLEDGMENTS

It is very meaningful to me to complete each step of the learning process in my life. I thank God for helping me to finish my degree without any major obstacles, and also thank my friends, relatives, teachers, and colleagues whose advice encouraged me to work hard in my studies in foreign land.

I am extremely thankful to my committee members: Dr. Duncan O. Darby, Robert M. Kimmel, and Dr. Hyun J. Park for their friendly attitude, advice, guidance, and encouragements. I wish to express my special thanks Mr. Young J. Byun, Dr. Kay D. Cooksey, Ms. Seung I. Hong, Dr. Young T. Kim, and Mr. Jun B. Yi for their friendship and unselfish assistance and help. I want to extend my appreciation to the following people: Mr. Rijosh J. Cheruvathur, Mr. Christopher S. Hutchings, Mr. Derrick R. Jordan, Mrs. Patricia, D. G. Marcondes, Mr. Girard J. Stoner, Mrs. Alison Tusso for their excellent technical assistance and generous help in my research.

Appreciation is also extended to Mrs. Glenda S. Brown, Mrs. Linda H. Landreth, and Mrs. Linda L. Phelps for their kind secretarial assistance throughout doctoral studies.

## TABLE OF CONTENTS

	Page
TITLE PAGE .....	i
ABSTRACT .....	ii
ACKNOWLEDGMENTS .....	iv
LIST OF TABLES .....	viii
LIST OF FIGURES .....	ix
CHAPTER	
I. INTRODUCTION AND REVIEW .....	1
Biopolymer Films.....	1
Natural Biodegradable Polymers .....	2
Proteins .....	2
Polysaccharides.....	14
Lipids.....	18
Gelatin .....	19
Microbial Transglutaminase .....	25
Nanocomposites .....	27
Clays, Clay Minerals, and Clay Science .....	28
Structures and Mineralogy of Clay Materials – The 2:1 layer – Smectite .....	37
Swelling Property of Montmorillonite .....	41
Clay-Polymer Interactions and Formation of Nanocomposites .....	43
Delamination of Clay Using Ultrasonics.....	45
Biodegradable Nanocomposites.....	45
Nanoclay Complex with Proteins .....	47
Bibliography .....	48
II. RESEARCH HYPOTHESES.....	58
III. RESEARCH OBJECTIVES.....	59

Table of Contents (Continued)

	Page
IV. EFFECT OF CLAY CONTENT, HOMOGENIZATION RPM, pH, AND ULTRASONIFICATION ON MECHANICAL AND BARRIER PROPERTIES OF FISH GELATIN/MONTMORILLONITE NANOCOMPOSITE FILMS .....	61
Abstract.....	61
4.1. Introduction.....	62
4.2. Experimental Material and Method.....	66
4.3. Results and Discussion .....	72
4.4. Conclusion .....	79
4.5. References.....	80
4.6. Figure Captions .....	84
4.7. Table Captions .....	85
V. EFFECTS OF TRANSGLUTAMINASE INDUCED CROSSLINKING ON PROPERTIES OF FISH GELATIN-NANO CLAY COMPOSITE FILM.....	102
Abstract.....	102
5.1. Introduction.....	103
5.2. Experimental Material and Method.....	106
5.3. Results and Discussion .....	113
5.4. Conclusion .....	122
5.5. References.....	122
5.6. Figure Captions .....	126
5.7. Table Captions .....	127
VI. DEVELOPMENT AND CHARACTERIZATION OF PET/FISH GELATIN-NANOCCLAY COMPOSITE/ LDPE LAMINATE: GELATIN-NANOCCLAY FILM AS A FUNCTIONAL BARRIER LAYER.....	141
Abstract.....	141
6.1. Introduction.....	142
6.2. Experimental Material and Method.....	145
6.3. Results and Discussion .....	150
6.4. Conclusion .....	154

Table of Contents (Continued)

	Page
6.5. References.....	154
6.6. Figure Captions .....	157
6.7. Table Captions .....	158
VII. GENERAL CONCLUSION.....	169



## LIST OF TABLES

Table		Page
1.1	The contents of amino acids in gelatins .....	24
1.2	Current names of clays .....	31
1.3	Classification of planar hydrous phyllosilicates .....	33
1.4	Classification of non-planar hydrous phyllosilicates .....	34
1.5	Distinction between clay and clay mineral.....	35
1.6	Intercalation of proteins in micaceous silicates .....	48
4.1	Effect of clay content (0~9%) on color and haze of fish gelatin/ Cloisite NA+/glycerol/H <sub>2</sub> O films.....	100
4.2	Average values of TS, E, OP, and WVP of FG/glycerol/H <sub>2</sub> O, unultrasonified FG/Cloisite NA+ (5% w/w)/glycerol/H <sub>2</sub> O, and ultrasonified FG/Cloisite NA+ (5% w/w)/glycerol /H <sub>2</sub> O films .....	101
5.1	Effect of MTGase (2% w/w) on color and haze of fish gelatin/Cloisite NA+/glycerol/H <sub>2</sub> O films .....	140
6.1	Hunter L, a, b and haze (%) of produced PET/FG-nanoclay composite/LDPE and PET/EVOH/LDPE laminate films .....	166
6.2	Bond peel strength of LDPE / FG and LDPE / EVOH laminates .....	167
6.3	Bond peel strength of PET / FG and PET / EVOH laminates.....	168

## LIST OF FIGURES

Figure	Page
1.1 Repeating unit of general gelatin structure.....	20
1.2 Reactions catalyzed by transglutaminase (TGase) .....	26
1.3 Exfoliation and intercalation .....	28
1.4 Diagram of clay layer, particle, aggregate, and assembly of aggregates .....	36
1.5 Tetrahedron and tetrahedral sheet.....	39
1.6 Orientation of octahedral sheet.....	40
1.7 Models of 1:1 and 2:1 layer structure .....	40
1.8 Different layer structures.....	41
4.1 Flow diagram for preparation of film casting solution .....	86
4.2 Film applicator.....	87
4.3 Viscosity of film solution as a function of clay content and temperature.....	88
4.4 Tensile strength and E% of composite film as a function of clay content.....	89
4.5 Tensile strength and E% of composite film as a function of shear force .....	90
4.6 Tensile strength and E% of composite film as a function of pH.....	91
4.7 Oxygen permeability and water vapor permeability of composite films as a function of clay content .....	92
4.8 Oxygen permeability and water vapor permeability of composite films as a function of shear force.....	93
4.9 Oxygen permeability and water vapor permeability of composite films as a function of pH .....	94

## List of Figures (Continued)

Figure	Page
4.10 SAXS diffractograms of the FG/glycerol, Cloisite Na+, and nanocomposite films (FG/Cloisite Na+/glycerol, and ultrasonified FG/Cloisite Na+/glycerol) .....	95
4.11 TEM observation of ultrasonified FG/Cloisite NA+ (9% w/w)/glycerol/H2O film.....	96
4.12 TEM observation of ultrasonified FG/Cloisite NA+ (9% w/w)/glycerol/H2O film.....	97
4.13 TEM observation of unultrasonified FG/Cloisite NA+ (9% w/w)/glycerol/H2O film.....	98
4.14 TEM observation of unultrasonified FG/Cloisite NA+ (9% w/w)/glycerol/H2O film.....	99
5.1 Flow diagram for preparation of film casting solution .....	128
5.2 Effect of MTGase on viscosity as a function of MTGase concentration and time at 50 oC .....	129
5.3 Tensile strength and E% of film as a function MTGase treatment time (2% MTGase) .....	130
5.4 Oxygen permeability and water vapor permeability of composite films as a function of clay content .....	131
5.5 SAXS diffractograms of the FG/sorbitol/H2O, Cloisite Na+, and MTGase treated (0 and 50 min) nanocomposite films (ultrasonified FG/Cloisite Na+/sorbitol/H2O).....	132
5.6 TEM observation of MTGase treated (0 min) FG/Cloisite NA+ (5% w/w)/sorbitol/H2O film.....	133
5.7 TEM observation of MTGase treated (0 min) FG/Cloisite NA+ (5% w/w)/sorbitol/H2O film.....	134
5.8 TEM observation of MTGase treated (0 min) FG/Cloisite NA+ (5% w/w)/sorbitol/H2O film.....	135

## List of Figures (Continued)

Figure	Page
5.9 TEM observation of MTGase treated (50 min) FG/Cloisite NA+ (5% w/w)/sorbitol/H <sub>2</sub> O film.....	136
5.10 TEM observation of MTGase treated (50 min) FG/Cloisite NA+ (5% w/w)/sorbitol/H <sub>2</sub> O film.....	137
5.11 TEM observation of MTGase treated (50 min) FG/Cloisite NA+ (5% w/w)/sorbitol/H <sub>2</sub> O film.....	138
5.12 Electrophoretic profile of fish gelatin and MTGase treated fish gelatin .....	139
6.1 Flow chart of PET/FG/LDPE and PET/EVOH/LDPE laminate preparation .....	159
6.2 Observation of cross section of the laminates .....	160
6.3 TEM observation at 50,000 magnification of FG (glycerol) film containing 20% w/w clay content.....	161
6.4 TEM observation at 100,000 magnification of FG (glycerol) film containing 20% w/w clay content.....	162
6.5 TEM observation at 50,000 magnification of FG (sorbitol) film containing 20% w/w clay content.....	163
6.6 TEM observation at 100,000 magnification of FG (sorbitol) film containing 20% w/w clay content.....	164
6.7 Oxygen permeability of PET/FG/LDPE and PET/EVOH/LDPE laminates .....	165

CHAPTER ONE  
INTRODUCTION AND REVIEW

**Biopolymer Films**

Films are generally defined as stand-alone thin layers of materials (Han and Gennadios, 2005). They usually consist of polymers able to provide sufficient mechanical strength to the stand-alone thin structure. The film-forming mechanisms of biopolymers include interatomic forces such as covalent bonds (e.g., disulfide bonds and cross-linking) and/or electrostatic, hydrophobic or ionic interactions (Han and Gennadios, 2005). One of the important advantages is that the biopolymer films provide edibility and biodegradability not offered by conventional packaging materials (Cuq and others, 1995; Han, 2002). Films can form pouches, wraps, capsules, bags, or casings through further fabrication processes.

Biopolymer films can be made from three general raw materials; proteins, polysaccharides (carbohydrates or gums), or lipids. Films and coatings from these materials function as protective layers which enhance the quality and safety of food products, resulting in shelf-life extension. (Gennadios and Weller, 1990). Among these raw materials, protein-based edible films are the most appealing for two reasons. They are reported to provide nutritional value and in addition, protein-based films have improved gas barrier and mechanical properties compared to lipid and polysaccharide based films (Ou, Kwok, & Kang, 2004).

## **Natural Biodegradable Polymers**

Natural macromolecules such as proteins, celluloses, and starches are generally degraded rapidly by hydrolysis and the action of micro-organisms. As such they represent an alternative to more traditional petroleum-based plastics which can be relatively inert and take a significant amount of time to degrade (Paetau and others, 1994). In the 1990s, there was a considerable increase in research efforts for the development of biopolymer films and coatings from protein, polysaccharide, and lipid materials.

From a chemical perspective, biopolymers from natural origins can be classified into three groups: proteins, polysaccharides, lipids.

### **Proteins**

Proteins are large organic compounds made of amino acids arranged in a linear chain and joined together by peptide bonds between the carboxyl and amino groups of adjacent amino acid residues. For thousands of years, people have been using natural proteins such as wool, silk, and hair ( $\alpha$ -keratin) for clothes or adornment. The first industrial applications of using proteins as polymers were in the early 1930s and 40s with casein and soy protein (Clarival & Halleux, 2005). Proteins were mainly used in encapsulations (pharmaceutical), coatings (food), adhesives or surfactants (Guilbert, 2002). Proteins can be classified into two groups according to their source; animal proteins (casein, whey, keratin, collagen, and gelatin) and plant proteins (wheat, corn, soy, pea, and potato) (Chiellini and others, 2002).

## *Plant origin proteins*

### Zein

Zein is a prolamine (simple proteins having a high proline content) protein found in maize (corn). It is usually manufactured as a powder from corn gluten meal. Zein is composed of a group of prolamine found in the corn endosperm (nutritive tissue within seeds of flowering plants). It accounts for 50% or more of total endosperm protein, occurring in small and compact bodies embedded in the glutelin protein matrix and distributed mainly in the outer layers of the endosperm. Zein is one of the most well understood plant proteins (Momany and others, 2005) and has a variety of industrial and food uses (Lawton, 2002). Historically, it has been used in the manufacture of a wide variety of commercial products including coatings for paper cups, soda bottle cap linings, clothing fabric, buttons, adhesives, coatings, and binders. The dominant historical use of zein was in the textile fibers market where it was produced under the name “Vicara” (Lawton, 2002). Pure zein is clear, odorless, tasteless, hard, water-insoluble, and edible, making it invaluable in processed foods and pharmaceuticals. It is now used as a coating for candy, nuts, fruit, pills, and other encapsulated foods and drugs.

Zein films are easily cast from alcohol solutions. Zein is dissolved in warm (65~85°C) aqueous ethanol or isopropanol with added plasticizers (substance added to plastics or other materials to make or keep them soft or pliable). The solution is cooled to 40~50°C, allowing bubbling to cease prior to casting, and is then poured over a glass plate where a film is formed as the alcohol evaporates from the surface. The dried film is finally peeled off the casting plate (Gennadios and others, 1993). The most common

plasticizer for zein films is glycerol, however, it tends to migrate from the bulk of the film matrix to the food surface due to the fact that its interaction with protein molecules is weak (Park and others, 1994).

Zein films offer several advantages as biodegradable packaging material. They are resistant to rodent and insect attack and freezing and thawing cycles. Therefore, it is expected that there will be continued research focused on improving zein film properties, thus allowing future commercial applications (Buffo and Han, 2005).

### Soy Protein

Soy protein is generally regarded as the storage protein (proteins generated mainly during seed production and stored in the seed that serve as nitrogen sources for the developing embryo during germination) held in discrete particles called protein bodies, which are estimated to contain at least 60~70% of the total soybean protein. Soy protein used in the food industry is classified as soy flour, concentrate or isolate, based on the protein content. Defatted soy flour (DSF) contains 50~59% protein, and is obtained by grinding defatted soy flakes. Soy protein concentrate (SPC) contains 65~72% protein, and is obtained by aqueous liquid extraction or acid leaching processes. Soy protein isolate (SPI) contains more than 90% protein, and is obtained by aqueous or mild alkali extraction followed by isoelectric precipitation (Park and others, 2002).

Soy protein is a viable and renewable resource for producing edible and environmentally friendly biodegradable films. The use of soy protein as a film-forming agent can add value to soybeans by creating new markets for soy protein. In particular,



SPI despite its low cost and plentiful supply and is actually an under-utilized product despite its high protein quality (Raynes and others, 2000).

### Wheat Gluten

Wheat gluten proteins are generally very high molecular weight compounds that are markedly apolar (having no radiating processes). The complexity and diversity of their protein fractions allow to produce films with novel functional properties, such as selective gas-barrier properties and rubber-like mechanical properties. Wheat gluten based materials are homogeneous, transparent, mechanically strong, and with relatively water resistance. They are biodegradable, biocompatible, and edible when food-grade additives are used (Guilber and others, 2002).

Film formation from wheat gluten solutions or dispersions has been studied extensively (Gennadios and Weller, 1990; Gennadios and others, 1993; Park and Chinnan, 1995). Wheat gluten films can be obtained by casting from solution or by extrusion, the latter being more cost effective. Wheat gluten films have also been produced by collecting the surface skin formed during the heating of wheat gluten solutions to temperatures near boiling (Watanabe and Okamoto, 1976).

Application of wheat gluten based materials can be envisioned for the coating of seeds, pills, and foodstuffs, and for making cosmetic masks, polishes or drug capsules. It is important to note that the allergenic character of wheat gluten based products for people suffering from celiac disease could limit such applications to cereal based products (Guilbert and others, 2002).

## Cotton Seed Protein

Cotton has been cultivated in 70 different countries for centuries as a fiber crop. Cottonseed accounts for about 13% of world oilseed production, even though oil production accounts only for about 15% of the commercial value of the cottonseed crop. To enhance the usage of this low cost, oil and protein rich commodity, the film forming properties of cottonseed proteins could be used to produce biodegradable materials of economic and environmental interests (Wu and Bates, 1973).

Cotton seed is crushed to extract oil and to produce cake that is chiefly used for ruminant livestock (Zongo and Coulibaly, 1993). Given that this cake contains gossypol, a toxic compound, it cannot be used for human consumption. Cottonseed proteins make up 30-40% w/w of the cottonseed kernel. Other important cottonseed components include lipids, soluble carbohydrates, cellulose, minerals, phytates, and polyphenolic pigments. The protein components are mainly globulins (proteins that are found extensively in blood plasma, milk, and plant seeds and that are insoluble in pure water and half saturated ammonium sulfate, soluble in dilute salt solution, and coagulate when heated) (60%) and albumins (water-soluble proteins that can be coagulated by heat and found in egg white) (30%), with lower proportions of prolamins (8.6%) and gluteins (0.5%) (Saroso, 1989).

Cottonseed protein based films are obtained directly from cottonseed flour using a casting process (Marquié, 1995; Marquié and others, 1995, 1997, 1998). In contrast to protein isolates, the conditions required to obtain films from cottonseed flour based

solutions are difficult to determine because of the complex nature of the raw material, which contains proteins, lipids, ash, cellulose, and carbohydrates.

Cottonseed flour films may be suitable for certain applications in non-food packaging (e.g. compostable waste bags) where good mechanical resistance and insolubility in water are required. They could also be used for agricultural packaging and mulching films to protect crops and fixate seeds, and other applications where film color, porosity, and biodegradability are beneficial (Marquié and Guilbert, 2002). Cottonseed flour films also have potential in certain medical areas where biodegradability is necessary (e.g. prostheses and resorbable dressings). The ability of these films to absorb considerable amounts of moisture is a further advantage for exudates (any fluid that filters from the circulatory system into lesions or areas of inflammation) absorption (Marquié, 1995).

### Peanut Protein

Peanut protein concentrates and isolates are commercially produced from defatted peanut flour using several methods. Hydraulic pressing, screw pressing, solvent extraction, and pre-pressing followed by solvent extraction have been used for defatting (Natarajan, 1980; Woodroof, 1983). After oil removal, protein isolation and purification are necessary.

Two different methods have been used to prepare peanut protein films. The first method involves the formation of peanut protein lipid films on the surface of heated peanut milk (Wu and Bates, 1972; Aboagye and Stanley, 1985; Del Rosario and others,

1992). The second method involves casting of peanut protein concentrates (PPC) or peanut protein isolates (PPI) solutions

### Rice Protein

Rice protein concentrate can be prepared by alkaline extraction of rice flour or of broken rice kernels, a side product of rice milling. Alternatively, rice flour or kernels may be treated with enzymes to partially remove the starch component (Chen and Chang, 1984).

Films from rice bran protein solutions (70% protein, dry basis) have been prepared using glycerol as plasticizer (2% w/v), adjusting the pH to either 9.5 or 3.0, heated to 80°C, poured onto polyethylene plates and dried at 60°C (Gnanasambandam and others, 1997).

### Pea Protein

Pea proteins are separated from starch and fiber by multi step solubilization at pH 2.5-3.0, followed by centrifugation (Nickel, 1981). These protein isolates have a mean crude protein content of 85.3% and an ash content of 4.1-5.0%. They show a lower fat absorption than SPI, suggesting the presence of more numerous hydrophilic than hydrophobic groups on the surface of protein molecules (Nackz and others, 1986). Pea proteins consists primarily of globulins (>80% of total protein) and a small fraction of albumins. The globulins are storage proteins located in the cotyledons, whereas albumins

are cytoplasmic proteins consisting of many different subunits (Boulter, 1983; Mosse and Pernollet, 1983).

Films made from denatured pea protein isolate (ca. 85% protein) show physical and mechanical properties similar to those of soy protein and whey protein films, and possess relatively good strength and elasticity. Increasing the glycerol content as a plasticizer in the film decreases the tensile strength (TS) and elastic modulus, but increases the elongation at break (EB) and water vapor permeability (WVP). Very strong and stretchable films can be obtained from 70/30 and 60/40 pea protein concentrate/glycerol compositions, respectively. Film solubility is not affected by the amount of plasticizer (Choi and Han, 2001).

### Pistachio Protein

*Pistacia* is mainly grown in hot, dry climates, such as Western Asia, Asia Minor, Southern Europe, Northern Africa, and California. Its fruits (kernels) are used as edible nuts, for making a coffee-like drink, and as a source of oil and coloring (Crane, 1979). Between 35 and 40% of the raw kernel consists of protein, in which the hydrophilic amino acids predominate (e.g. glutamic and aspartic acids) (Ayranci and Dalgic, 1992).

### Grain Sorghum Protein

Grain sorghum ranks fifth among cereals produced in the world (Dendy, 1995). The main protein fraction in the sorghum kernel is prolamin, also known as kafirin.

Kafirin is similar to corn zein in molecular weight, solubility, structure, and amino acid composition (Shull and others, 1991).

Films have been prepared from laboratory extracted kafirin (89% protein) (Buffo, 1995). When dissolved in ethanol with glycerin and PEG added as plasticizers, the dry films have similar TS, EB, and WVP to those of films prepared from commercial corn zein.

### *Animal origin proteins*

#### Casein

Casein is the most predominant phosphoprotein (proteins which are chemically bonded to a substance containing phosphoric acid) found in milk and cheese. Casein consists of fairly high number of proline peptides, which do not interact. There are also no disulfide bridges. As a result, it has relatively little secondary structure or tertiary structure so therefore it cannot denature.

Commercial caseinates are produced by adjusting acid-coagulated casein to pH 6.7 using calcium or sodium hydroxide. Caseins are predominantly phosphoproteins that precipitate at pH 4.6 and at 20°C (Gennadios and others, 1994). Among the protein fractions of casein,  $\beta$ -casein is the most interesting fraction to produce films of low permeability to water vapor. The  $\alpha$ -casein fraction contains more charged residues and fewer hydrophobic residues than the  $\beta$ -casein fraction (Dalglish, 1989).

Caseins form films from aqueous solutions without further treatment due to their random-coil nature and their ability to hydrogen bond extensively. It is believed that

electrostatic interactions also play an important role in the formation of casein-based edible films (Gennadios and others, 1994). Pure caseinate/glycerol/CMC films are highly soluble in water (88%).

### Whey protein

Whey protein is a collection of globular proteins that can be isolated from whey, a by-product of cheese manufacturing industry. It is typically a mixture of beta-lactoglobulin (~65%), alpha-lactalbumin (~25%), and serum albumin (~8%), which are soluble in their native forms, independent of pH. Whey proteins represent around 20% of total milk proteins (Brunner, 1977) and contain five main proteins:  $\alpha$ -lactalbumin,  $\beta$ -lactoglobulin, bovine serum albumin (BSA), immunoglobulin, and proteose-peptones.

Formation of intact and insoluble whey protein films can be produced by heat denaturation of the proteins. Heating modifies the three-dimensional structure of the protein, exposing internal S-H and hydrophobic groups (Shimada and Cheftel, 1998), which promote intermolecular S-S bonds and hydrophobic interactions upon drying (McHugh and Krochta, 1994). McHugh and Krochta (1994) produced whey protein isolate (WPI) films by heat treatment using a protein concentration from 8-12% and heating temperatures between 75 and 100°C.

### Collagen and gelatin

Collagen is the main protein of connective tissue in animals and the most abundant protein in mammals making up about 25% of the total protein content (Di Lullo

and others, 2002). Collagen is a constituent of skin, tendon, and connective tissues. It is a fibrous protein, and represents about 30% of the total mass of the body (Gustavson, 1956). Collagen fibrils are produced by self-assembly of collagen molecules in the extracellular matrix, and provide tensile strength to animal tissues (Trotter and others, 2000). Collagen can be dissolved in dilute acid or alkali solutions and in neutral solutions. Two major components are identified;  $\alpha$  (MW 100,000 Da) and  $\beta$  (MW 200,000 Da), and consist of two different types of covalent cross-linked chain pairs  $\alpha 1-\alpha 1$  and  $\alpha 2-\alpha 2$  (Harrington, 1966).

Hydrolysis of collagen results in gelatin. The molecular weight of gelatin covers a broad range, from 3000-200,000 Da, depending on the raw material employed during gelatin production and handling conditions (Young, 1967). Edible coatings made with gelatin reduce the migration of moisture, oxygen, and oil.

Collagen is the most commercially successful edible protein film. Film-forming collagen has been traditionally used in the meat industry, for the production of edible sausage casings. This protein has largely replaced natural gut casings for sausages. Collagen films have good mechanical properties (Hood, 1987) and have excellent oxygen barrier property at 0% relative humidity, but oxygen permeability increases rapidly with increasing RH in a manner similar to cellophane (Liebermann and Guilbert, 1973). Different cross-linking chemical agents have been used to improve the mechanical properties to reduce the solubility, and to improve the thermal stability of these films. Carbodiimide, microbial transglutaminase, and glutaraldehyde are often used as cross-



linking agents (Jones and Whitmore, 1972; Takahashi and others, 1999; Taylor and others, 2002).

Gelatin is known to form clear, flexible, strong, and oxygen-impermeable films when cast from aqueous solutions in the presence of plasticizers (Gennadios and others, 1994). Industrial applications of gelatin include capsule coating and micro-encapsulation. Gelatin films exhibit good gas barrier, but poor water barriers due to their hydrophilic nature.

### Egg white

Egg white is common name for the clear liquid (also called the albumin or the glair/glaire) contained within an egg. It is the cytoplasm of the egg, which until fertilization is a single cell (including the yolk). It consists of about 15% proteins dissolved in water. Its primary natural purpose is to protect the egg yolk and provide additional nutrition for the growth of the embryo, as it is rich in proteins and has high nutritional value.

The surplus of egg-white products has created a reason to produce more edible films and coatings and led to development of new applications in the food industry. The use of egg white in film and coating production represents a nutritional interest, since it is an effective antioxidant (Negbenebor and Chen, 1985). Edible packaging made from egg white is clear and transparent, and has properties similar to other proteins. It has been reported that pH range from 10 to 12 is necessary to obtain homogeneous films

(Okamoto, 1978; Handa, 1999). Egg albumin has been studied for its potential to retain moisture inside raisins in cereal/raisin mixtures (Bolin, 1976) and inside meat products.

## **Polysaccharides**

Polysaccharides are relatively complex carbohydrates. They are polymers made up of many monosaccharides joined together by glycosidic bonds. They are therefore very large, often branched, macromolecules. They tend to be amorphous, insoluble in water, and have no sweet taste. Examples include, storage polysaccharides such as starch and glycogen and structural polysaccharides such as cellulose and chitin. Polysaccharides have a general formula of  $C_n(H_2O)_{n-1}$  where n is usually a large number between 200 and 2500. Considering that the repeating units in the polymer backbone are often six-carbon monosaccharides, the general formula can also be represented as  $(C_6H_{10}O_5)_n$  where n=40-3000.

## Starch

Starch is a mixture of amylose and amylopectin. Amylose is a nearly linear polymer of  $\alpha$ -1,4 anhydroglucose units, with a molecular weight of  $10^5$ - $10^6$  (Galliard and Bowler, 1987). Amylopectin is a highly branched polymer consisting of short  $\alpha$ -1,4 chains linked by  $\alpha$ -1,6 glucosidic branching points occurring every 25-30 glucose units, with a molecular weight of  $10^7$ - $10^9$ . The content of amylose in starch varies from 0 to 100%, depending on the botanical origins.

Preparing a clear starch solution is normally the first step when making edible starch films. While it is important to minimize or avoid hydrolysis and oxidation of starch, a solution-making process must ensure that starch polymers are completely gelatinized, disintegrated, and solubilized.

Aqueous starch solutions are normally unstable. In particular, those with a high solid concentration and/or high amylose starch tend to gel immediately upon cooling (Young, 1984), which makes casting more difficult. It is therefore necessary to keep the starch solution at a temperature above the gelation temperature prior to casting.

Self-supporting starch films are commonly produced by casting the starch solution upon a support with a smooth surface, on which it is dried until the film can be removed (Wolff and others, 1951). Drying is crucial to the appearance and performance of starch films. Rapid drying is normally undesirable, because it can induce cracks, warping, and concentric drying marks on the film, or even granulate the films. Over-drying should also be avoided to prevent the films from becoming too brittle.

Generally, amylose films exhibit improved mechanical properties over amylopectin films. However, it appears that the origin of starch has little effect on the mechanical properties of amylose films. Increasing amylose content normally leads to improved mechanical properties, including tensile strength and elongation.

Normally, starch films are good barriers to oxygen, since oxygen is a non-polar gas and cannot be dissolved in starch films (Rankin and others, 1958). In ambient environments, amylose and amylopectin films have very low oxygen permeability

comparable to ethylene vinyl alcohol (EVOH), which is recognized as a good commercial oxygen barrier film (Forsell and others, 2002).

### Cellulose

Cellulose is present in all land plants, being the structural material of cell walls. Cellulose is the most abundantly naturally occurring polymer on earth, and is an almost linear polymer of anhydroglucose. At a molecular level, cellulose is relatively simple polymer consisting of  $\beta$ -[1,4] linked D-glucose molecules in a linear chain. Because of its regular structure and array of hydroxyl groups, it tends to form strong hydrogen-bonded crystalline microfibrils, which are insoluble in many solvents. Cellulose is a cheap raw material, and is highly crystalline and insoluble. For film production, cellulose is dissolved in a mixture of sodium hydroxide and carbon disulfide (xanthation) and then recast into sulfuric acid to produce cellophane films.

### Chitosan

Chitosan is a polysaccharide derived from chitin, and is found in abundance in the shells of crustaceans. Chitosan is mainly composed of 2-amino-2-deoxy- $\beta$ -D-glucopyranose repeating units, but still retains a small amount of 2-acetamido-2-deoxy- $\beta$ -D-glucopyranose residues. Chitosan with a high amino content ( $pK_a \approx 6.2-7.0$ ) is water soluble in aqueous acids (Rinaudo and Domard, 1989). In general, chitosan has numerous uses; it can be used as a flocculent, clarifier, thickener, gas-selective membrane, promoter of plant disease resistance, wound-healing factor agent, and antimicrobial agent (Brine

and others, 1991). Chitosan also readily forms films, and in general produces materials with a high gas barrier.

### Alginate

Alginate is a polysaccharide derived from brown seaweed known as Phaeophyceae, considered to be a (1->4) linked polyuronic. It contains containing three types of block structure: M block ( $\beta$ -D-mannuronic acid), G block (poly  $\alpha$ -L-gluronic acid), and MG block (containing both polyuronic acids). The relative amounts of the two uronic acid monomers and their sequential arrangement along the polymer chain vary widely, depending on the origin of the alginate. Alginates produce uniform, transparent and water-soluble films, Divalent cations are used as gelling agents in alginate film formation to induce ionic interactions followed by hydrogen bonding. Films and coatings can be made from a sodium alginate solution by a rapid reaction with calcium in the cold, forming intermolecular associations involving the G-block regions. The treatment of an alginate film with multivalent cation (i.e. calcium) solutions converts the film to insoluble. Alginates possess good film-forming properties, but tend to be quite brittle when dry; however, they may be plasticized with the inclusion of glycerol.

### Carrageenan

Carrageenan is derived from red seaweed, and is a complex mixture of several polysaccharides. The three principal carrageenan fractions are kappa ( $\kappa$ ), iota ( $\iota$ ), and, lambda ( $\lambda$ ), which differ in the sulfate ester and 3, 6-anhydro  $\alpha$ -D-galactopyranosyl

content.  $\kappa$ -carrageenan fractions contain the lowest number of sulfate groups and the highest concentrations of the 3, 6-anhydro  $\alpha$ -D-galactopyranosyl units. The  $\iota$ -carrageenan fractions have an additional sulfate group at the 2-position.

Carrageenan-based coatings have been applied for a long time to a variety of foods to carry antimicrobials or antioxidants, and to reduce moisture loss, oxidation, or disintegration. Defrosted whole chickens, with a carrageenan based coating, have a better resistance against off-flavor development during storage at 4°C. The incorporation of gallic acid or ascorbic acid as an antioxidant in a carrageenan based coating was able to maintain the sensorial qualities of frozen mackerel fillets over 8 months of storage at -18°C (Stoloff and others, 1949).

## **Lipids**

Lipids can be broadly defined as any fat-soluble (hydrophobic), naturally-occurring molecules. The term is more-specifically used to refer to fatty-acids and their derivatives (including tri-, di-, and monoglycerides and phospholipids) as well as other fat-soluble sterol-containing metabolites such as cholesterol. Lipids have many functions in living organisms including nutrients, energy storage, structural components of cell membranes, and important signaling molecules. Although the term *lipid* is sometimes used as a synonym for fat, fats are in fact a subgroup of lipids called triglycerides and should not be confused with the term fatty acid.

Plant oils and animal fat are mostly unsaturated fatty acids. Some of these oily products are already well known from their use in paint (e.g., flax(linseed); tung oils are

drying oils used in paints, varnishes and enamels) or in soaps, detergents, cosmetics, and lubricant applications. Plant oils are becoming an increasing source of raw material to produce thermoset resins that can be mixed with natural fibres in order to achieve light and resistant composite materials. When combined with bio-based resins with natural fibres (plant poultry) or lignin, they can produce new low-cost composites that are economical in many high volume applications (Beckwith, 2003). These composites are used in agricultural equipment, automotive sheet-moulding compounds (SMCs), civil and rail infrastructures, marine applications, housing, and the construction industry (Wool, 2003).

Plant oils represent about 80% of the worldwide lipid production. Soybean and palm oils are the most important ones, but European oils (rapeseed, sunflower, and linseed) contain more than 90% unsaturated fatty acid.

## **Gelatin**

Gelatin (also called gelatine) is prepared by the thermal denaturation of collagen, isolated from animal skin and bones, with very dilute acid. It can also be extracted from fish skins.

The structure of collagen, the raw material source of gelatin, is a right handed triple-helix with the three individual protein strands in the left-handed polyproline-II helix conformation. The three strands of helices are staggered by one residue, allowing for inter-chain hydrogen bonds. Each helix in a single collagen molecule forms a rod ( $\sim 3,000 \text{ \AA}$  long and  $\sim 15 \text{ \AA}$  in diameter). Formation of the triple-helix conformation requires

the presence of a repeated Gly-Xaa-Yaa sequence, the most common repeating sequence being Gly-Pro-Hyp. All peptide bonds in collagen are believed to be in a *trans*-conformation.

Gelatin contains many glycine (almost 1 in 3 residues, arranged every third residue), proline and 4-hydroxyproline residues. A typical structure is -Ala-Gly-Pro-Arg-Gly-Glu-4Hyp-Gly-Pro-.

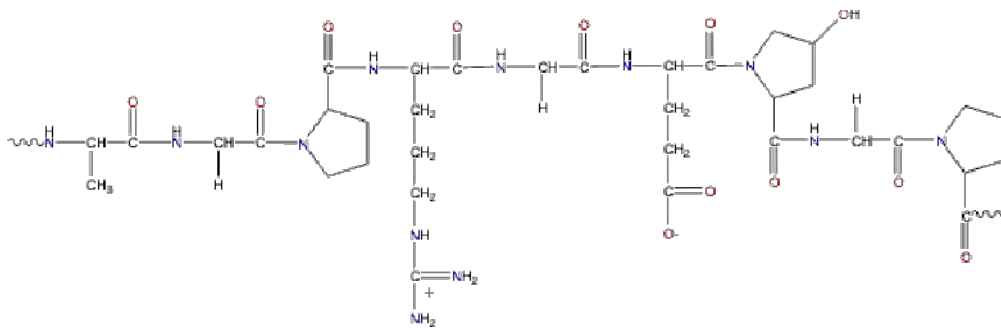


Figure 1.1. Repeating unit of general gelatin structure

### Molecular structure

Gelatin is a heterogeneous mixture of single or multi-stranded polypeptides, each with extended left-handed proline helix conformations and containing between 300 - 4000 amino acids. The triple helix of type I collagen extracted from skin and bones, as a source for gelatin, is composed of two  $\alpha 1(I)$  and one  $\alpha 2(I)$  chains, each with molecular mass  $\sim 95$  kD, width  $\sim 1.5$  nm and length  $\sim 0.3$   $\mu\text{m}$ . Gelatin consists of mixtures of these strands together with their oligomers and breakdown (and other) polypeptides. Solutions undergo coil-helix transition followed by aggregation of the helices by the formation of collagen-like right-handed triple-helical proline/hydroxyproline rich junction zones.



Higher levels of these pyrrolidines result in stronger gels. There is some dispute over whether each of the three chains in the helical structure has a 10/1 helix (the three strands forming a 10/3 helix) with a 85.8 Å axial repeat or a 7/1 helix (the three strands forming a 7/2 helix) with a 60 Å axial repeat, with tripeptides forming each unit. Although the former view seems prevalent at the present time, recent evidence indicates the latter to be correct (Okuyama and others, 2006). Each of the three strands in the triple helix require about 21 residues to complete one turn; typically there would be between one and two turns per junction zone (Oakenfull, and others, 2003). Gelatin films containing greater triple-helix content swell less in water and are consequentially much stronger (Bigi and others, 2004). Chemical cross-links can be introduced, to alter the gel properties, using transglutaminase to link lysine to glutamine residues (Babin, and others, 2001) or by use of glutaraldehyde to link lysine to lysine.

### Functionality

Gelatin is primarily used as a gelling agent (Ledward, 1986) forming transparent elastic thermoreversible gels on cooling below about 35°C. It can be dissolved at low temperature to give 'melt in the mouth' products with useful flavor-release. In addition, the amphiphilic nature of the molecules endows them with useful emulsification (for example, whipped cream) and foam-stabilizing properties (for example, mallow foam). Upon dehydration, irreversible conformational changes take place (Mogilner and others, 2002) that may be used in the formation of surface films. Such films are strongest when

they contain greater triple-helix content. Gelatin is also used as a fining agent to clarify wine and fruit juice.

Although gelatin is by far the major hydrocolloid used for gelling, current concerns about the possibility of an animal-derived product containing the prions that cause Creutzfeldt-Jakob Disease (CJD), plus the need generated by vegetarians and certain religious prohibitions has encouraged the serious search for alternatives. The combination of the melt in the mouth, elastic and emulsification characteristics of gelatin gels is, however, difficult to reproduce.

Gelatin is nutritionally lacking as a protein being deficient in isoleucine, methionine, threonine and tryptophan.

#### Classification of gelatin

Commercial gelatin is classified into two types: Type A and Type B gelatin. Gelatin type A and gelatin type B are made by acidic and alkaline pretreatment, respectively, before heat processing. The difference between Gelatin A and B is that the alkaline pretreatment converts amide residues of glutamine and asparagines into glutamic and aspartic acid, which leads to a 25% higher carboxylic acid content for gelatin B than for gelatin A. Acid pretreatment (Type A gelatin) uses pigskin whereas alkaline treatment (Type B gelatin) makes use of cattle hides and bones.

## Fish gelatin

Fish gelatin has gained great interest in recent years as the demand for non-bovine and non-porcine gelatin has increased due to the bovine spongiform encephalopathy (BSE) crisis and for religious and social reasons. Production of gelatin from pig skins is not acceptable for Judaism and Islam and gelatin from beef is acceptable only if it has been prepared according to religious requirements. In contrast, fish gelatin is acceptable for Islam and with a minimum restriction for Judaism. Secondly, fish skin is a major by-product of the fish-processing industry and this by product could provide a valuable source of gelatin. Limited research has been carried out regarding gelatins obtained from different fish species or their behavior in processed foods.

The commercial interests in fish gelatin have been relatively low so far due to sub-optimal physical properties compared to mammalian gelatin. Common problems connected with fish gelatin from cold water species (representing the majority of the industrial fisheries) are low gelling temperatures, low melting temperature and low gel modulus. This makes these gelatins unsuited as mammalian gelatin replacements, especially since they typically gel below 8 °C. The differences in the physical properties between mammalian gelatin and from cold water species based gelatins are due to a lower content of the amino acids proline (Pro) and hydroxyproline (Hyp). Calf skin gelatin contains approximately 94 Hyp and 138 Pro residues per 1000 total amino acid residues, while cod skin gelatin contains approximately 53 and 102 amino acids of Hyp and Pro, respectively, per 1000 total residues. Gelatins from warm water fish species, like fish gelatin from tilapia, contain approximately 70 and 119 residues of Hyp and Pro,

respectively, per 1,000 total residues, and have physical properties more equal to those of mammalian gelatins.

Table 1.1. The contents of amino acids in gelatins (residues per 1000 total residues)

Source	Bovine Corium Collagen <sup>a</sup>	Pig Skin <sup>b</sup>	Cattle Hide <sup>b</sup>	Cattle Bone <sup>b</sup>	Cod Skin <sup>b</sup>	Tilapia Skin <sup>b</sup>	Vyse Fish gelatin <sup>c</sup>
Extraction process	-	Acid	Alkali	Alkali	Auto-claving	Acid	Acid
Aspartic acid	47	46	46	47	52	46	53
Glutamic acid	72	72	71	73	75	67	98
Hydroxyproline	94	91	98	93	53	76	73
Serine	39	35	37	33	69	37	27
Glycine	337	330	333	335	345	340	233
Histidine	5	4	5	4	8	9	-
Arginine	48	49	46	48	51	54	91
Threonine	17	18	17	18	25	26	31
Alanine	107	111	112	116	107	120	107
Proline	129	132	129	124	102	119	130
Tyrosine	5	3	2	1	4	3	5
Valine	20	26	20	22	19	17	19
Methionine	4	4	6	4	13	9	9
Cystine	-	-	-	-	<1	-	<1
Isoleucine	11	10	12	11	11	8	11

Leucine	24	24	23	24	23	23	22
Hydroxylysine	5	6	6	4	6	8	-
Phenylalanine	13	14	12	14	13	12	20
Tryptophane	-	-	-	-	-	-	-
Lysine	25	27	28	28	25	25	34

---

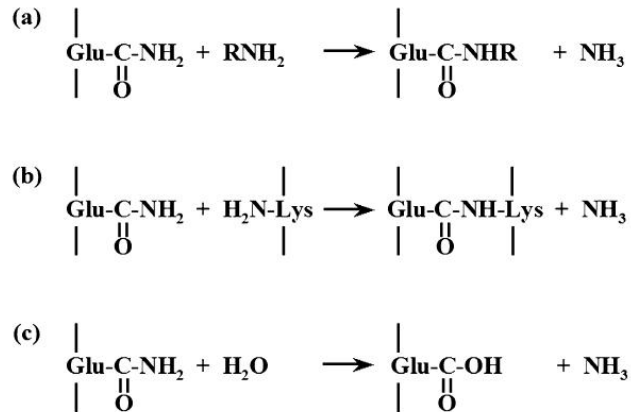
<sup>a</sup>(Arvanitoyannis 2002), <sup>b</sup>(Podczeck and Jones 2004), <sup>c</sup>(Vyse gelatin)

### Microbial transglutaminase

Transglutaminase (TGase; protein-glutamine  $\gamma$ -gluamyl-transferase, EC 2.3.2.13) catalyzes an acyl transfer reaction between the  $\gamma$ -carboxamide group of a peptide bound glutamyl residue (acyl donors) and a variety of primary amines (acyl acceptors), including the amino group of lysine (figure 1.2). In the absence of amine substrates, TGase catalyzes the hydrolysis of the  $\gamma$ -carboxamide group of the glutamyl residue, resulting in deamination. When the  $\epsilon$ -amino group of a peptide bound lysyl residue is the substrate, peptide chains are covalently connected through  $\epsilon$ -( $\gamma$ -glutamyl)lysine (G-L) bonds. TGases are present in most animal tissue and body fluids, and are involved in several biological processes, including blood clotting, wound healing, epidermal keratinization, and stiffening of the erythrocyte membrane (Aeschlimann and Paulsson, 1994).

Microbial transglutaminases catalyze the displacement of the amide ammonia at the  $\gamma$ -position in glutamine residues by replacing it with another amine, usually a  $\epsilon$ -amino group from a suitable lysine residue (figure 1.2). The formation of  $\epsilon$ -( $\gamma$ -

glutamyl)lysine isopeptide bonds results in the incorporation of inter- or intramolecular covalent cross-links into food proteins, leading to improving the physical and textural properties of many food proteins, such as tofu, boiled fish paste, and sausage.



(a)Acyl transfer (b)Crosslinking of Gln and Lys residues in proteins or peptides. The resulting bridge is called an  $\epsilon$ -( $\gamma$ -glutamyl)lysine (G-L bond) (c)Deamination

Figure 1.2. Reactions catalyzed by transglutaminase (TGase).

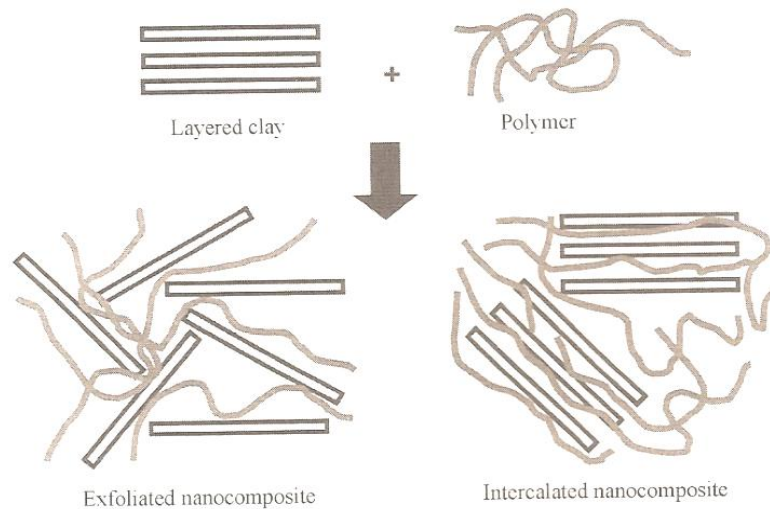
The optimum pH for MTGase activity is between 5 and 8. However, MTGase has shown some activity at pH 4 or 9 (Ando and others, 1989), and was thus considered to be stable over a wide pH range. The optimum temperature for enzymatic activity is 55 °C (for 10 min at pH 6.0); it maintains full activity for 10 min at 40 °C, but loses activity within a few minutes at 70 °C. It is active at 10 °C, and retains some activity at near-freezing temperatures.

## Nanocomposites

Nanocomposites are materials that are created by introducing nanoparticles (often referred to as *filler*) into a macroscopic sample material (often referred to as *the matrix*). This is a growing field of nanotechnology. Upon the addition of nanoparticulates to the matrix material, the resulting nanocomposite may exhibit dramatically enhanced properties. For example, adding carbon nanotubes tends to add to the electrical and thermal conductivity. Other certain matrix materials of nanoparticulates may result in enhanced optical properties, dielectric properties or mechanical properties such as stiffness and strength. In general, the nanoparticle is dispersed into the matrix during processing. The percentage by weight (called *mass fraction*) of the nanoparticles introduced is typically very low (on the order of 0.5% to 5%) due to the incredibly high surface area to volume ratio of nanoparticulates. Considerable research is focused on developing more efficient combinations of matrix and filler materials and better control of the production process.

There are two types of nanocomposite structures which may be formed, termed intercalated and exfoliated nanocomposites (Figure 1.3). In an intercalated nanocomposite, often a single polymer chain will be driven between the nanosubstance layers, but the system still remains quite well ordered in a stacked type of arrangement. In an exfoliated nanocomposite, the nanosubstance layers are completely delaminated from each other and are well dispersed. It is this second type, the exfoliated nanocomposite, has been shown to exhibit the most significant improvements in physical properties (Usuki and others, 1993; Kojima and others, 1993; Vaia and Giannelis, 1997; Giannelis,

1998). The degree of intercalation and exfoliation of layered silicates in polymer nanocomposites can be quantified using wide-angle X-ray diffraction (WAXS) and transmission electron microscopy (TEM).



**Schematic of exfoliated and intercalated nanocomposite formation (Martin and others, 1991)**

Figure 1.3. Exfoliation and intercalation

### **Clays, Clay Minerals, and Clay Science**

*Clay* is defined as a ‘material’ composed primarily of fine-grained minerals which is generally plastic at appropriate water contents and will harden when dried or fired.

Clay is also defined as phyllosilicae minerals and minerals which impart plasticity to clay and which harden upon drying or firing (Auerbach, Carrado, & Dutta, 2004).

Clay has been known and used by humans for thousands of years. Indeed, clay has been implicated in the prebiotic synthesis of biomolecules, and the very origins of life on earth. Clay has also become indispensable to modern living. It is the primary material



of many kinds of ceramics, such as porcelain, bricks, tiles, and sanitary ware as well as an essential constituent of plastics, paints, paper, rubber, and cosmetics. Clay is considered nonpolluting and can be used as a depolluting agent. Of great importance in the near future is the potential of some clays to be dispersed as nanometer-size unit particles in a polymer phase, forming novel nanocomposite materials with superior thermomechanical properties. The diversity of structures and properties of clays, and their wide-ranging applications, make it difficult to compile a comprehensive reference text on clay science (Bergaya, and Lagaly, 2006).

### Clay

There is, as yet, no uniform nomenclature for clay and clay materials. Georgius Agricola (1494-1555), the founder of geology, was apparently the first to have formalized a definition of clay (Guggenheim and Martin, 1995). The latest effort in this direction was made nearly five centuries later by the joint nomenclature committees (JNCs) of the Association Internationale pour l'Etude des Argiles (AIPEA) and the Clay Minerals Society (CMS). The JNCs have defined 'clay' as "...a naturally occurring material composed primarily of fine-grained minerals, which is generally plastic at appropriate water contents and will harden with dried or fired" (Guggenheim and Martin, 1995). By this definition, synthetic clays and clay-like materials are not regarded as clay even though they may be fine grained, and display the attributes of plasticity and hardening on drying and firing.

Although particle size is a key parameter in all definitions of clay, there is no generally accepted upper limit. Some disciplines and professions, however, have conventionally set a maximum size of clay particles. In pedology (study of soils in its natural environment. It is one of two branches of soil science), for example, the 'clay fraction' refers to a class of materials whose particles are smaller than 2  $\mu\text{m}$  in equivalent spherical diameter (e.s.d.). In geology, sedimentology, and geoen지니어ing the size limit is commonly set at  $<4 \mu\text{m}$  e.s.d. (Moore and Reynolds, 1997), while in colloid science the value of  $<1 \mu\text{m}$  is generally accepted. Indeed, Weaver (1989) has suggested that the term 'clay' should only be used in the textural sense to indicate material that is finer than 4  $\mu\text{m}$ .

Table 1.2. Current names of clays

Current Names of clays	Origin	Main clay Mineral Constituents	Remarks
Ball clay	Sedimentary	Kaolinite	Highly plastic, white burning (Grim, 1962)
Bentonite	Volcanic rock alteration or authigenic	Montmorillonite	
Bleaching earth	Acid-activated bentonite	Decomposed montmorillonite	
Common clay	Sedimentary or by weathering	Various, often illite/smectite mixed-layer minerals	General for ceramics excluding porcelain
China clay	Hydrothermal	Kaolinite	Kaolins from Coenwall plastic, white burning
Fire clay	Sedimentary	Kaolinite	Plastic, high refractoriness (Grim, 1962)
Flint clay	Sedimentary with subsequent diagenesis	Kaolinite	Non-slaking, not plastic, used for refractories (Frim, 1962; Keller, 1978, 1981, 1982)
Fuller's earth	Sedimentary, residual, or hydrothermal	Montmorillonite, sometimes palygorskite, sepiolite	
Primary kaolin	Residual or by hydrothermal alteration	Kaolinite	
Secondary kaolin	Authigenic sedimentary	Kaolinite	
Refractory clay	Authigenic sedimentary	Kaolinite	With low levels of iron, alkali, and alkali earth cations for refractories (Grim, 1962)
Laponite	Synthetic	Hectorite-type smectite	
Nanoclay		Mostly montmorillonite	

(Bergaya and Lagaly, 2006)

## Clay Mineral

As a first approximation, the term ‘clay mineral’ signifies a class of hydrated phyllosilicates making up the fine-grained fraction of rocks, sediments, and soils. The definition that the JNCs have proposed is “...phyllosilicate minerals and minerals which impart plasticity to clay and which harden upon drying or firing” (Guggenheim and Martin, 1995). Since the origin of the material is not part of the definition, clay mineral (unlike clay) may be synthetic.

In the JNCs’ definition of clay material, the grain size does not attribute as a decisive factor. Accordingly, phyllosilicates of any size, such as macroscopic mica, vermiculite, and chlorite may be regarded as clay minerals. Indeed, much of the basic and detailed understanding of clay mineral structures is derived from X-ray diffraction analysis of macrocrystalline forms, notably the micas and vermiculites. A similar concept was advocated by Weaver (1989) who suggested the term ‘physils’ for the whole family of phyllosilicates (including palygorskite and sepiolite) irrespective of grain size.

The JNCs have further proposed that non-phyllosilicate minerals would qualify as clay minerals if they impart plasticity to clay, and harden on drying or firing.

Table 1.3. Classification of planar hydrous phyllosilicates

Interlayer Material <sup>a</sup>	Group	Octahedral (polyhedron with eight faces) Character <sup>b</sup>	Species
<i>1:1 clay materials</i>			
None or H <sub>2</sub> O only, $\zeta \sim 0$	Serpentine kaolin	Tri	Amesite, berthierine, brindleyite, cronstedtite, fraipontite, kellyite, lizardite, nepouite,
		Di	Dickite, halloysite (planar), kaolinite, nacrite,
		Di-tri	Odinite
<i>2:1 clay minerals</i>			
None, $\zeta \sim 0$	Tale-pyrophyllite	Tri	Kerolite, pimelite, talc, willemsite
		Di	Ferripyrophyllite, pyrophyllite
Hydrated exchangeable cations, $\zeta \sim 0.2 \sim 0.6$	Smectite	Tri	Hectorite, saponite, sauconite, stevensite, swinefordite
		Di	Beidellite, montmorillonite, nontronite, volkonskoite
Hydrated exchangeable cations, $\zeta \sim 0.6 \sim 0.9$	Vermiculite	Tri	Diocahedral vermiculite
Non-hydrated monovalent cations, $\zeta \sim 0.6 \sim 1.0$	True (flexible) mica	Tri	Biotite, lepidolite, phlogopite, etc.
		Di	Celadonite, illite, glauconite, muscovite, paragonite, etc.
Non-hydrated divalent cations, $\zeta \sim 1.8 \sim 2.0$	Brittle mica	Tri	Anandite, bityite, clintonite, kinoshitalite
		Di	Margarite
Hydroxide sheet, $\zeta$ variable	Chlorite	Tri	Baileychlore, chamosite, clinochlore, nimite, pennantite
		Di	Donbassite
		Di-tri	Cookeite, sudoite
<i>Regularly interstratified 2:1 clay minerals</i>			
$\zeta$ Variable		Tri	Aliettite, corrensite, hydrobiotite, kulkeite
		Di	Rectorite, tosudite

(Martin and others, 1991)

Table 1.4. Classification of non-planar hydrous phyllosilicates

Modulated Component	Linkage Configuration	Unit layer $c \sin \beta$ Value	Traditional Affiliation	Species
<i>1:1 Minerals with modulated structures</i>				
Tetrahedral sheet	Strips	0.7 nm	Serpentine	Antigorite, bementite
	Islands	0.7 nm	Serpentine	Caryopilite, ferropyrosmalite, friedelite, greenalite, manganpyrosmalite, mcgillite, nelenite, pyrosmalite, schallerite
	Other		None	
<i>2:1 Minerals with modulated structures</i>				
Tetrahedral sheet	Strips	0.95 nm	Talc	Minnesotaite
		1.25 nm	Mica	Eggletonite, ganophyllite
	Islands	0.96-1.25 nm	Mica/ complex	Ferristilpnomelane, ferrostilpnomelane, lennilenapeite, parsettensite, stilpnomelane, zussmanite
	Other	1.23 nm	None	Bannisterite
		1.4 nm	Chlorite	Gonyerite
Octahedral sheet	Strips	1.27-1.34 nm	Pyribole	Falcondoite, loughlinitite, palygorskite, sepiolite, yofortierite
<i>1:1 Minerals with rolled and spherical structures</i>				
None	Trioctahedral		Serpentine	Chrysolite, percoraite
	Dioctahedral		Kaolin	Halloysite (nonplanar)

(Martin and others, 1991)

Table 1.5. Distinction between clay and clay mineral

Clay	Clay mineral
Natural	Natural and synthetic
Fine-grained (< 2 um or <4 um)	No size criterion
Phyllosilicates as principal constituents	May include non-phyllosilicates
Plastic	Plastic
Hardens on drying or firing	Hardens on drying or firing

(Bergaya and Lagaly, 2006)

For simplicity, assembly of layers is often referred to as a ‘particle’ and an assembly of particles as an ‘aggregate’. The arrangement of the particles or aggregates leads to different morphologies, such as platelets, tubules, laths, and fibres. All phyllosilicates are therefore porous, containing pores of varied size and shape.

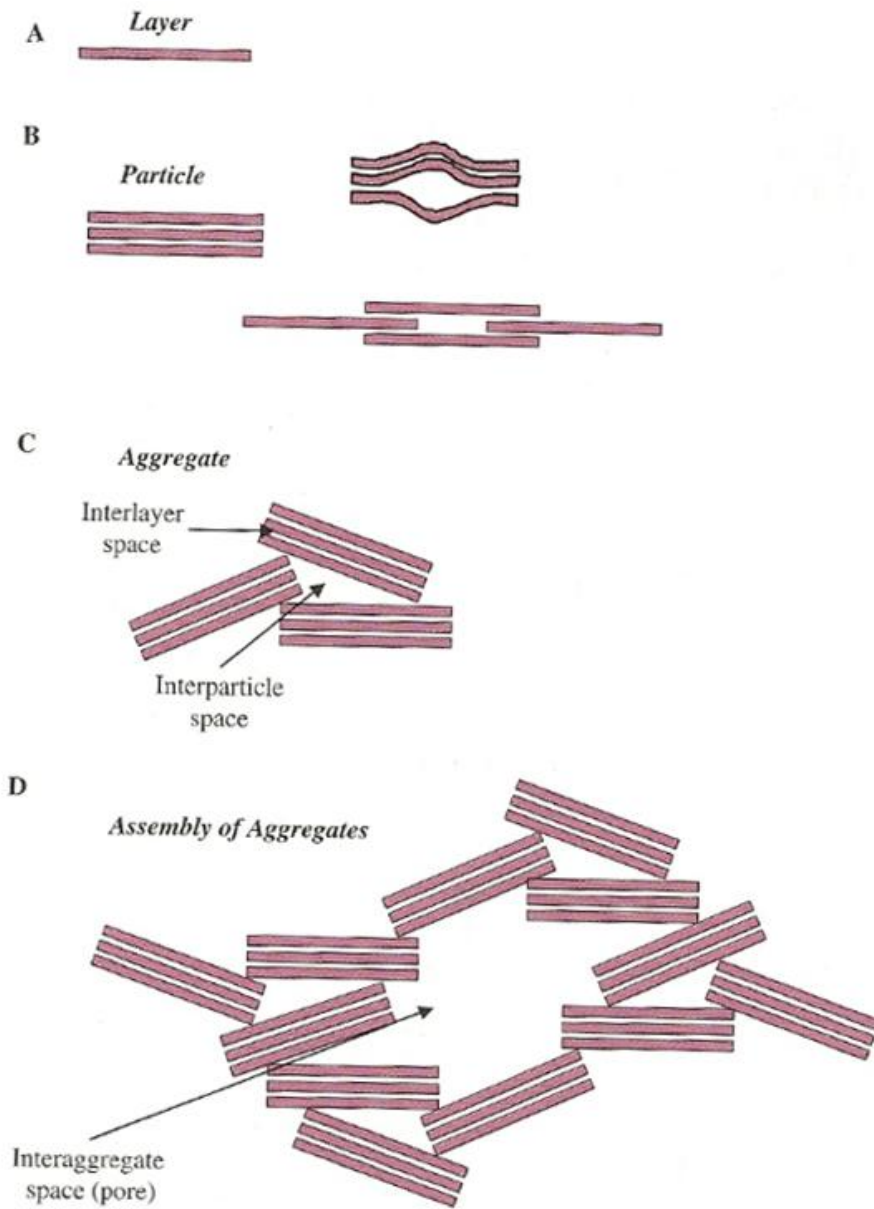


Diagram showing (A) a clay mineral layer; (B) a particle, made up of stacked layers; layer translation and deformation can give rise to a lenticular pore; (C) an aggregate, showing an interlayer space and an interparticle space; and (D) an assembly of aggregates, enclosing an interaggregate space (pore). (Bergaya and Lagaly, 2006)

Figure 1.4. Diagram of clay layer, particle, aggregate, and assembly of aggregates



## Clay science

Clay minerals are unique in the sense that these materials are studied by, and used in, many disciplines for fundamental and applied research. The multidisciplinary approach is at the frontier between materials science and colloid science, while the multi-scale approach linking nano-, micro-, and macro- scale studies is a challenge for the future of clay science. Clay research is being actively pursued by many people and in many countries, and the future of clay science looks bright, exciting, and promising.

### **Structures and Mineralogy of Clay Materials - The 2:1 layer – Smectite**

The silicate minerals make up the largest and most important class of rock-forming minerals. They are classified based on the structure of their silicate ion group. Phyllosilicates, formerly called disilicate, is compound with a structure in which silicate tetrahedrons (a central silicon atom surrounded by four oxygen atoms at the corners of a tetrahedron) are arranged in sheets. The layer of 2:1 phyllosilicates consists of an octahedral sheet sandwiched between two opposing tetrahedral sheets. In pyrophyllite (dioctahedral) and talc (trioctahedral), the layer is electrically neutral. In the other 2:1 phyllosilicates (e.g. smectite, vermiculite, mica, chlorite), the layer is usually negatively charged. The magnitude of the layer charge (X) measures the deviation of charge from neutrality. For true micas (group of sheet delicate minerals which include several closely related materials having highly perfect basal cleavage) X is close to -1, while for brittle micas it is approximately equal to -2. In both cases, the space between the adjacent layers is occupied by anhydrous cations. Illite is a micaceous clay mineral that occurs widely in

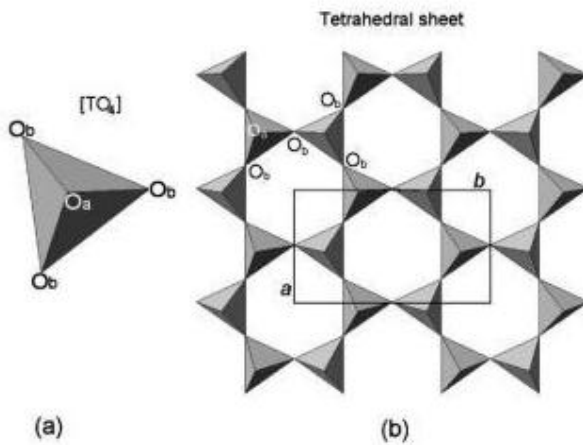
soils and sediments. A fractional value for layer charge and the presence of hydrated cations in the interlayer space characterize the most common 2:1 clay minerals, such as smectites and vermiculites. In smectites, the negative charge per half-unit-cell ranges from 0.2 to 0.6, while in vermiculites this value is between 0.6 and 0.9. In chlorite, the negative layer charge is neutralized by the presence of a positively charged octahedral sheet in the interlayer space. Most chlorites are trioctahedral; dioctahedral chlorites, and intermediate forms with alternating dioctahedral and trioctahedral sheets, are rare. As in 1:1 phyllosilicates, the 2:1 layer structure can be non-planar. For example, minnesotaite (traditionally considered as a variety of talc) has a modulated structure with tetrahedral strips. Other 2:1 layer silicates, such as sepiolite, palygorskite, and loughlinitite also show a modulated structure but the strips are made up of octahedral sheets (Martin and others, 1991).

### Smectite

Smectites are 2:1 phyllosilicates with a total (negative) layer charge between 0.2 and 0.6 per half unit cell. Except for the layer charge and hydration of the interlayer cations, their structure is similar to that of other 2:1 phyllosilicates. The octahedral sheet may either be dominantly occupied by trivalent cations (dioctahedral smectites) or divalent cations (trioctahedral smectites).

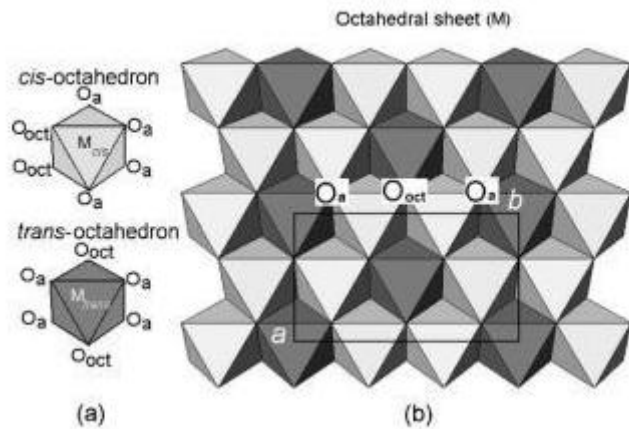
Most of the technological uses of smectite are related to reactions that take place in the interlayer space. Positive ions,  $\text{Na}^+$ ,  $\text{K}^+$ ,  $\text{Ca}^{2+}$ , and  $\text{Mg}^{2+}$ , which balance the negative 2:1 layer charge, are commonly hydrated and interchangeable. Smectites contain

water in several forms. The water held in pores may be removed by drying under ambient conditions. Water may also be associated with layer surfaces and in interlayer spaces (Güven, 1992). Usually, three modes of hydration (recognized as pH-dependent) are distinguished: (i) interlayer hydration (of internal surfaces) of primary clay mineral particles; (ii) continuous hydration relating to an unlimited adsorption of water on internal and external surfaces; and (iii) capillary condensation of free water in micropores. The main elements of interlayer hydration are (i) hydration of interlayer cations, (ii) interaction of clay surfaces with water molecules and interlayer cations, and (iii) water activity in the clay-water system.



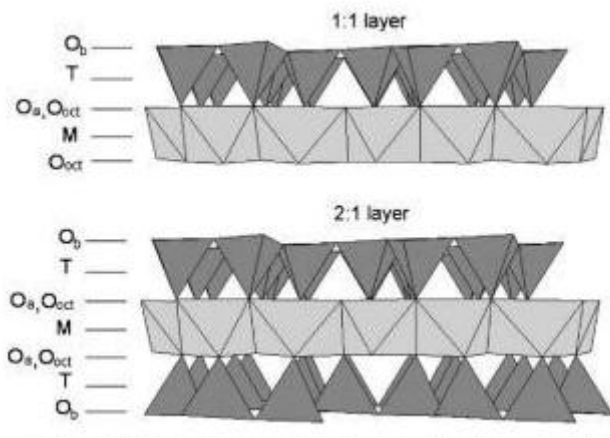
(a) Tetrahedron [TO<sub>4</sub>]; (b) tetrahedral sheet, O<sub>a</sub> and O<sub>b</sub> refer to apical and basal oxygen atom, respectively. a and b refer to unit-cell parameters. (Bergaya and Lagaly, 2006)

Figure 1.5. Tetrahedron and tetrahedral sheet



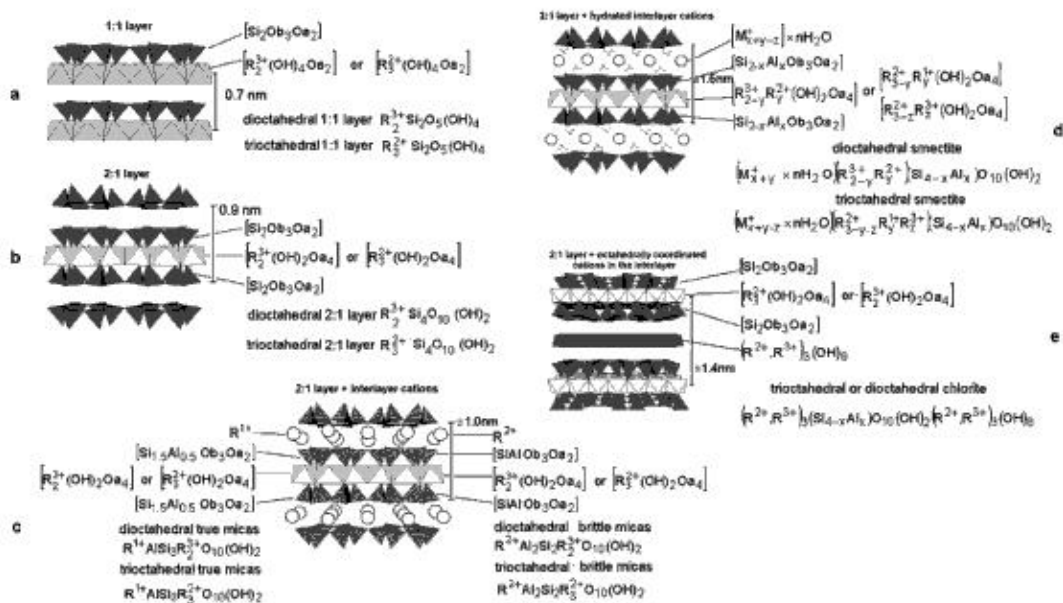
(a)  $O_{oct}$  (OH, F, Cl) orientation in *cis*-octahedron and *trans*-octahedron; (b) location of *cis*- and *trans*-sites in the octahedral sheet.  $O_a$  and  $O_b$  refer to apical and basal oxygen atoms, respectively.  $a$  and  $b$  refer to unit cell parameters. (Bergaya and Lagaly, 2006)

Figure 1.6. Orientation of octahedral sheet



Models of a 1:1 and 2:1 layer structure.  $O_a$ ,  $O_b$ , and  $O_{oct}$  refer to tetrahedral basal, tetrahedral apical, and octahedral anionic position, respectively. M and T indicate the octahedral and tetrahedral cation, respectively. (Bergaya and Lagaly, 2006)

Figure 1.7. Models of 1:1 and 2:1 layer structure



Different layer structures: (a)1:1 layer (i.e., kaolinite- and serpentine- like layer); (b)2:1 layer (i.e., pyrophyllite- and talc- like layer); (c)2:1 layer with anhydrous interlayer cations (i.e., the mica-like layer); (d)2:1 layer with hydrated interlayer cations (i.e., smectite- and and vermiculite- like layer); (e)2:1 layer with octahedrally coordinated interlayer cations (i.e., chlorite- like layer). (Bergaya and Lagaly, 2006)

Figure 1.8. Different layer structures

## Swelling Property of Montmorillonite

Montmorillonite is a very soft phyllosilicate mineral that typically forms in microscopic crystals, forming clay. It is a member of the smectite family (2:1 clay) meaning that it has 2 tetrahedral sheets sandwiching a central octahedral sheet. The particles are plate-shaped with an average diameter of approximately 1 micrometer. Montmorillonite is capable of intercalating a number of water layers through which the basal spacing (distance between similar faces of adjacent layers) increases stepwise from ~1 to ~2.2 nm, corresponding to interlayer separations of ~0 to ~1.2 nm. This type of expansion is referred to as intracrystalline, or simply, crystalline swelling, signifying that the gross crystal morphology is preserved. Other terms used for this process are “region

1” and “stage 1” swelling as distinct from those events which may take place on subsequent uptake of water. Swelling in this region is primarily due to hydration of the interlayer cations which probably take up positions midway between two opposing silicate layers. Montmorillonite saturated with polyvalent cations does not normally expand beyond an interlayer separation of ~1 nm, presumably because the repulsive effect of ion hydration is more than offset by electrostatic attraction between cation and silicate layer.

On the other hand, montmorillonites containing small, monovalent cations, such as  $\text{Li}^+$  and  $\text{Na}^+$ , can take up more water under suitable conditions. The interlayer spacing then increases abruptly to 3-4 nm and continues to rise more or less linearly to some tens of nanometers with water content. This is termed region 2 or stage 2 swelling and is ascribable to the formation of diffuse electrical double layers on interlayer surfaces. The interaction of these layers generates a repulsive, osmotic force which is opposed only to a limited extent by Van der Waals forces. For the most part, the osmotic force is restrained by frictional forces arising from edge-to-face particle (layer) association. At this stage, the consistency on the nanoscale of the clay –water systems is that of a paste or thick gel.

In the near absence of edge-to-face bonding or when this type of particle association has been disrupted by gentle shaking, the system passes into region 3 or stage 3 swelling. The individual silicate layers are separated by large distances, the extent of separation being limited only by the volume of water in the system. When this is large, the system is a dilute sol in which the particles are kept apart mainly through thermal

motion. In relatively concentrated suspensions or gels, diffuse double layer interaction is the stabilizing factor together with some residual edge-to-face and edge-to-edge bonding.

### **Clay – Polymer Interactions and Formation of Nanocomposites**

Blumstein (1961) demonstrated that the possibility of forming polymer/clay intercalation compounds by in situ polymerization of various monomers, such as acrylonitrile, vinyl acetate, and methyl methacrylate, previously intercalated into smectites in the presence of an initiator. The resulting products are stable organic-inorganic materials that nowadays are known as polymer-clay nanocomposites (PCNs) (Blumstein, 1961). Friedlander (1961) demonstrated that layered silicates containing transition metal ions with redox properties as exchangeable cations could also induce the polymerization of unsaturated monomers, resulting in materials where the polymer remains strongly associated with the mineral substrate.

As in conventional composites, there are structural and functional nanocomposites. The main interest of the first group concerns mechanical or rheological properties, such as nylon-clay nanocomposites (Fukushima and others, 1988), where as the latter group refers to nanostructured materials showing a specific chemical or physical behavior, such as conductive nanocomposites (Ruiz-Hitzky and others, 2000).

A classification of methods for preparing polymer-layered inorganic solid compounds takes into account the main processes involved in the synthesis of the final hybrid material. The nature of both 2D host solid and the guest polymer determines the pathway applicable to obtain a particular nanocomposite and, in certain cases, is decisive

in the behavior of the resulting material. In general, the synthetic routes commonly employed have been classified into four groups:

1. Direct intercalation of the polymer by (a) adsorption from solutions, (b) ion exchange reactions, or (c) polymer melt intercalation.
2. In situ intercalative polymerization in the interlayer spaces, which requires the previous intercalation of the monomer/s and a second step to induce their polymerization-usually activated by a thermal treatment or by addition of a catalyst.
3. Delamination and entrapping-restacking of clay is a method that profits from the possibility of swelling the host solids by separation of their layers using an appropriated solvent or some specific treatment and then adding the monomer or the polymer to be intercalated.
4. Templating synthesis is a method that can be used when the layered host matrix could be synthesized in the presence of the polymer that acts as a template agent remaining between the layers of the assembled solid.

The selection of method depends on the characteristics of both host and guest species. An important factor that must be considered is the necessity of compatibility between the organic macromolecule and the interlayer space of the layered solid. Thus, due to the organophilic character of most polymers, it is usually necessary to modify such regions to ensure affinity between polymer and inorganic substrate (Ruiz-Hitzky and others, 2004).



### **Delamination of Clay Using Ultrasonics**

Sonifiers and ultrasonic baths have been used to improve the level of intercalation and exfoliation particularly for in-situ polymerized nanocomposites (Artzi and others, 2002; Liao and others, 2001; Okamoto and others, 2000). If a sound wave is of sufficient energy, cavitation bubbles are created at sites of rarefaction as the liquid fractures or tears because of the negative pressure of the sound wave in the liquid. As the wave fronts pass, the cavitation bubbles can eventually grow to be unstable under the influence of positive pressure. The high-speed collapse of the cavitation bubbles results in implosions, which cause shock waves to be radiated from the sites of the collapse. High temperatures and pressures can be generated at the implosion sites of cavitation bubbles.

### **Biodegradable Nanocomposites**

Montmorillonite, hectorite, and saponite are frequently used pristine layered silicates which are combined with polymeric materials to form nanocomposites (Sinha Ray and Okamoto, 2003). These clays usually contain hydrated sodium or potassium ions (Giannelis, 1998) and in this state these silicates are miscible only with hydrophilic polymers such as poly(ethylene oxide) (PEO), poly(vinyl alcohol) (PVA), and natural polymers such as starches and proteins (Sinha Ray and Okamoto, 2003). Cationic surfactants (e.g. alkyl ammonium ions) may be ion exchanged with these hydrated ions to enable the intercalation of numerous engineered polymers. The alkyl ammonium cations in the layered silicates improve the wetting characteristics with the polymer and can

provide functional groups that can react with the polymer or initiate polymerization of monomers to improve the strength of the interface between the inorganic component and the polymer (Vaia and Giannelis, 1997; Giannelis. 1998; Alexandre and Dubois. 2000).

The literature available for natural biodegradable nanocomposite materials is quite limited. Park and others (2002, 2003) reported on the preparation and properties of starch/montmorillonite clay nanocomposites. In this work, the naturally occurring Na<sup>+</sup> montmorillonite (Cloisite Na<sup>+</sup>) and three alkyl ammonium modified clays (Cloisite 30B, 10A, and 6a) were used to form the nanocomposites. Initially, the starches were gelatinized with glycerol and water, and then allowed to sit for one hour prior to processing on a Haake mixer at 110°C, after which the gelatinized starch was cooled and cut into small pieces. The gelatinized starch pieces and the various clays were then dry mixed in a roller mixer for 20 minutes. WAXS showed some broadening of the d-<sub>001</sub> peak indicative of partial exfoliation, but the peaks essentially remained in the same position.

Fischer (2001, 2003) also investigated starch/clay nanocomposites. In this work, a number of experimental pathways were investigated, including the dispersion of Na<sup>+</sup> montmorillonite clay in water, followed by blending in an extruder at a temperature of 85-105°C with a premixed powder of potato starch, glycerol, and water. The resulting material appeared to be fully exfoliated and exhibited a reduction in hydrophobicity and improved stiffness, strength, and toughness.

## **Nanoclay Complex with Proteins**

The fact that proteins can become incorporated in montmorillonites and other micaceous layer silicates, has for many years been used to eliminate clouding proteins from beer and wine. The fixation (the act of uniting chemically) characteristics of proteins to minerals vary with the type of mineral and with the kind of proteins involved. Aside from their basic properties, the proportions of hydrophobic residues in proteins are determining factors. It is noteworthy that pre-expanded sodium montmorillonites have a larger exchange capacity for proteins than the non-expanded variety. X-ray diagrams, however, suggest a lower crystallinity in such instances. The reaction products can simply be described in terms of cationic and anionic polyelectrolyte precipitates. For the strong protamines (any of a class of proteins, rich in arginine, found in the sperm of fish. It is used to control the action of insulin) the uptake increases strongly with rising pH of the equilibrium solution. This suggests that the protein is picked up as a cation. Increases in pH raise the ratio of free amino groups to ammonium groups. Consequently, more protein becomes incorporated in order to substitute all interlayer cations by ammonium ions.

Table 1.6. Intercalation of proteins in micaceous silicates, (1) Ca-montmorillonite from Geisenheim, (2) nontronite from the Ficht mine, (3) montmorillonite from Unterrupsroth, (4) Na-montmorillonite from Geisenheim

Protein	Basic concentration g protein/1 L solution	pH value	Linked protein mg protein/1 g silicate	Layer distance of the dehydrated sample (110°C)
Salmin	6.0	8.0	266(1)	16.9
		8.3	289(3)	17.3
		11.4	285(2)	17.5
Serum albumin	3.1	5.1	215(1)	12.5
		5.2	607(4)	16.0
Egg albumin	20.0	4.0	215(1)	14.8
		4.0	412(4)	15.5
		4.0	548(3)	15.8
Zein	15.3	3.9	95(3)	13.5
		4.0	107(1)	12.6
		6.1	83(2)	12.4
Gliadin	3.8	6.1	82(2)	12.4
		6.8	138(3)	15.0
		6.8	168(1)	13.2
Gelatin	10.0	2.2	62	14.3
Human albumin	10.0	2.2	49	14.2
Pepsin	8.0	2.2	26	13.6
Hemoglobin		2.6	50	

## Bibliography

Abogaye, Y. and Stanley, D. W. (1985). *Can. Inst. Food Sci. Technol. J.* 18, 12-20.

Aeschlimann, D. and Paulsson, M. (1994). Transglutaminases: protein cross-linking enzymes in tissues and body fluids. *Thromb Haemost* 71, 402-415.

- Alexandre, M. and Dubois, P. (2000). Polymer-layered silicate nanocomposites: preparation, properties and uses of a new class of materials. *Materials Science and Engineering* 28(1-2), 1-63.
- Ando, H., Adachi, M., Umeda, K., Matsuura, A., Nonaka, M., Uchiro, R., Tanaka, H., and Motoki, M. (1989). Purification and characteristics of a novel transglutaminase derived from microorganism. *Agric. Biol. Chem.* 53, 2613-2617.
- Arvanitoyannis, I.S. (2002). Formation and Properties of Collagen and Gelatin Films and Coatings, In: A. Gennadios (ed.) *Protein-Based Films and Coatings*: 275. Boca Raton: CRC.
- Auerbach, S. M., Carrado, K. A., and Dutta, P. K. (2004). Handbook of Layered Materials, New York, Marcel Dekker, pp. 1-2.
- Ayranci, E. and Dalgic, A. C. (1992). *Lebensm. Wiss. U. Technol.* 25, 442-444.
- Artzi, N. Nir, Y., Narkis, M., and Siegmann, A. (2002). Melt blending of ethylene-vinyl alcohol copolymer/clay nanocomposites: Effect of the clay type and processing conditions. *Journal of polymer Science Part B: Polymer Physics* 40(16), 1741-175.
- Babin, H. ad Dickinson, E. (2001). Influence of transglutaminase treatment on the thermoreversible gelation of gelatin. *Food Hydrocolloids*, 15, 271-276.
- Beckwith, S. W. (2003). Natural Fiber – Reinforcement Materials, lower cost for composite applications, *composite fabrication*, November/December, 1-6.
- Bergaya, F. and Lagaly, G. (2006). General Introduction: Clays, clay minerals, and clay science, In: Bergaya, F, Theng, B. K. G., and Lagaly, G. (eds) Handbook of clay science, pp. 1-18. Elsevier, Academic Press.
- Bigi, A., Panzavolta, S., and Rubini, K. (2004). Relationship between triple-helix content and mechanical properties of gelatin films. *Biomaterials*, 25, 5675-5680.
- Blumstein, A. (1961). *Bull. Soc. Chim. France* 899-905.
- Bolin, H. R. (1976). Texture and crystallization control in raisins. *J. Food Sci.* 41, 1316-1319.
- Boulter, D. (1983). In: (M. S. Peterson and A. H. Johnson, eds) *Encyclopedia of Food Science*, pp. 221-224. Martinus Nijhoff Publishers, The Hague, The Netherlands.

- Brunner, J. R. (1977). Milk proteins. In: (J. R. Witaker and S. R. Tannenbaum, eds) *Food Proteins*, pp. 175-208. AVI Publishers, Westport, CT.
- Buffo, R. A. (1995). MS thesis, Department of Food Science and Technology, University of Nebraska, Lincoln, NE.
- Buffo, R. A. and Han, J. H. (2005). *Edible films and coatings from plant origin proteins*, In: Jung H. Han(ed.) *Innovations in Food Packaging*: 239. Elsevier Academic Press.
- Chen, W. P. and Chang, Y. C. (1984). *J. Sci. Food Agric.* 35, 1128-1135.
- Choi, W. S. and Han, J. H. (2001). *J. Food Sci.* 67(4), 1399-1406.
- Crane, J. C. (1979). In: (J. G. Woodroof, ed.) *Tree Nuts: Production, Processing, Products*, pp. 572-603. The AVI Publishing Co., Westport, CT.
- Cuq, B. Gontard, N., and Guilbert, S. (1995). Edible films and coatings as active layers. In: M. Rooney(ed.) *Active Food Packaging*, pp. 111-142. Blackie, Glasgow, UK.
- Dalgleish, D. G. (1989). Milk proteins – chemistry and physics. In: (J. E. Kinsella and W. G. Soucie, eds) *Food Proteins*, pp. 155-178. American Oil Chemists Society, Champaign, IL.
- Dendy, D. A. V. (1995). In: (D. A. V. Dendy, ed.) *Sorghum and Millets: Chemistry and Technology*, pp. 11-26. American Association of Cereal Chemists, St Paul, MN.
- Del Rosario, R. R., Rubio, M. R., Maldo, O. M., Sabiniano, N. S., Real, M. P. N., and Alcantara, V. A. (1992). *Philippine Agriculturist* 75, 93-98.
- Di llulo, G. A., Sweeney, S. M., KÖrkkÖ, J., Ala-Kokko, L., and San Atonio, J. D. (2002). Mapping the Ligand-binding Sites and Disease-associated Mutations on the Most Abundant Protein in the Human, Type I Collagen. *J Biol Chem*, 277(6), 4223-4231.
- Fischer, H. (2003). Polymer nanocomposites: from fundamental research to specific applications. *Materials Science and Engineering: C* 23(6-8), 763-772.
- Fischer, H. and Fischer, S. (2001). *Biodegradable thermoplastic material*. WO 01/68762A1.
- Friedlander, H. Z. (1961). *ACS Div. Polym. Chem. Reprints* 4, 300-306.

- Fukushima, Y., Okada, A., Kawasumi, M., Kurauchi, T., and Kamigaito, O. (1988). *Clay Miner.* 23, 27-34.
- Galliard, T. and Bowler, P. (1987). Morphology and composition of starch. In: *Starch: Properties and Potential* (T. Galliard, ed.), pp. 55-78. John-Wiley & Sons, New York, NY.
- Gennadios, A. and Weller, C. L. (1990). Edible films and coatings from wheat and corn proteins. *Food Technol* 44(10), 63-69.
- Gennadios, A., Park, H. J., and Weller, C. L. (1993). *Trans. ASAE*, 36, 1867-1872.
- Gennadios, A., McHugh, T., Weller, C., and Krochta, J. M. (1994). Edible coatings and films based on proteins. In: (J. M. Krochta, E. A. Baldwin, and M. Nisperos-Carriedo, eds) *Edible coatings and Films to Improve Food Quality*, pp. 231-247. Technomic Publishing, Lancaster, PA.
- Giannelis, E. P. (1998). Polymer-layered silicate nanocomposites: synthesis, properties, and applications. *Applied Organometallic Chemistry* 12(10-11), 675-680.
- Gnanasambandam, R. Hettiarachchy, N. S., and Coleman, M. (1997). *J. Food Sci.* 62, 395-398.
- Guggenheim, S., Martin, R. T., (1995). Definition of clay and clay mineral: joint report of the AIPEA nomenclature and CMS nomenclature committees. *Clays and Clay Minerals* 43, 255-256 and *Clay Minerals* 26, 237-243.
- Guilbert, S., Gontard, N., Morel, M. H., Chalier, P., Micard, V., and Redl, A. (2002). In: A. Gennadios(ed.) *Protein-based films and coatings*, pp. 69-121. CRC Press, Boca Raton, FL.
- Gustavson, K. H. (1956). *The Chemistry and Reactivity of Collagen*. Academic Press, New York, NY.
- Guven, N. (1992). Molecular aspects of clay-water interactions. In: Guven, N., Pollastro, R. M. (eds) *Clay-Water Interface and its Rheological Implications*, CMS Workshop Lectures, vol. 4, pp. 1-80. The Clay minerals Society, Boulder, CO.
- Han, J. H. (2002). Protein-based edible films and coatings carrying antimicrobial agents. In: A. Gennadios(ed.) *Protein-based films and coatings*, pp. 485-499. CRC Press, Boca Raton, FL.
- Han, J. H., and Gennadios, A. (2005). *Edible films and coatings: a review*, In: Jung H. Han(ed.) *Innovations in Food Packaging*: 239. Elsevier Academic Press.

- Handa, A., Gennadios, A., Froning, G. W., Kuroda, N., and Hanna, M. A. (1999). Tensile, solubility, and electrophoretic properties of egg white films as affected by surface sulfhydryl groups. *J. Food Sci.* 64, 82-85.
- Harrington, W. F. (1966). Collagen. In: (H. F. Mark, N. G. Gaylord, and N. M. Bikales, eds) *Encyclopedia of Polymer Science and Technology*, Vol. 4, *Plastics, Resins, Rubbers, Fibers*, pp. 1-16. Interscience Publishers, New York, NY.
- Hood, L. L. (1987). Collagen in sausage casting. In: (A. M. Pearson, T. R. Dutson, and A. J. Bailey, eds) *Advances in Meat Research*, pp. 109-129. Van Nostrand Reinhold, New York, NY.
- Johnston-Banks, F.A. (1990). Gelatine, in P. Harris (ed.) *Food Gels: 275*. Boca Raton: CRC.
- Kojima, Y., Usuki, A., Kawasumi, M., Okada, A., Fukushima, Y., Kurauchi, Y., and Kamigaito, O. (1993). Mechanical properties of nylon 6-clay hybrid. *J. Mater. Res.* 8(5), 1185-1189.
- Liao, Y., Wang, Q., and Xia, H. (2001). Preparation of poly(butyl methacrylate)/gamma-Al<sub>2</sub>O<sub>3</sub> nanocomposites via ultrasonic irradiation. *Polymer International* 50(2), 207-212.
- Liebaerman, E. R. and Guilbert, S. G. (1973). Gas permeation of collagen films as affected by cross-linkage, moisture and plasticizer content. *J. Polym. Sci. Symp.* 41, 33-43.
- Jones, H. W. and Whitmore, A. (1972). US Patent 3,694,234.
- Lawton, J. W. (2002). Zein: A history of processing and use. *Cereal Chem.* 79(1), 1-18.
- Lieberman, E. R. and Guilbert, S. G. (1973). Gas permeation of collagen films as affected by cross-linkage, moisture and plasticizer content. *J. Polym. Sci. Symp.* 41, 33-43.
- Le Chatelier, H. (1887). De l'action de la chaleur sur les argiles. *Bulletin de la Société Française de Minéralogie.* 10, 204-211.
- Ledward, D. A. (1986). Gelation of gelatin, in *Functional properties of food macromolecules*, ed. J. R. Mitchell and D. A. Ledward, Elsevier Applied Science Publishers Ltd, pp. 171-201.
- Marquié, C. (1995). Breve déposé au nom du Cirad du 07 Mars, No. 9502640.



- Marquié, C., Aymard, C., Cuq, J. L., and Guilbert, S. (1995). *J. Agric. Food Chem.* 43, 2762-2767.
- Marquié, C., and Guilbert, S. (2002). In: (A. Gennadios ed.) *Protein-based Films and Coatings*, pp. 139-157. CRC Press, Boca Raton, FL.
- Marquié, C., Tessier, A. M., Aymard, C., and Guilbert, S. (1997). *J. Agric. Food Chem.* 45, 922-926.
- Marquié, C., Tessier, A. M., Aymard, C., and Guilbert, S. (1998). *Nahrung* 42, 264-265.
- Martin, R. T., Bailey, S. W., Eberl, D. D., Fanning, D. S., Guggenheim, S., Kodama, H., Pevear, D. R., Srodon, J., and Wicks, F. J. (1991). Report on the Clay Monerals Society nomenclature committee: revised classification of clay minerals. *Clays and Clay Minerals* 39, 333-335.
- McHugh, T. H. and Krochta, J. M. (1994). Water vapor permeability properties of edible whey protein-lipid emulsion films. *J. Am. Oil Chem. Soc.* 71, 307-312.
- Mogilner, I. G., Ruderman, G., and Grigera, J. R. (2002). Collagen stability, hydration and native state. *J. Mol. Graphics Modeling.* 21, 209-213.
- Momany, F. A., Sessa, D. J., Lawton, J. C., Selling, G. W. Hamaker, S. A. H., and Willwtt, J. L. (2006). Structural characterization of  $\alpha$ -Zein. *J. Agric. Food Chem.*, **54** (2), 543 -547.
- Moore, D. M., Reynolds, R. C. Jr. (1997). *X-ray Diffraction and the Identification and Analysis of Clay Minerals*, 2<sup>nd</sup> edition. Oxford University Press, Oxford.
- Mosse, J. and Pernollet, J. C. (1983). In: (S. K. Akora, ed.) *Chemistry and Biochemistry of Legumes*, pp. 111-193. Oxford & IBH Publishing, New Delhi, India.
- Nackz, M., Rubin, L. J., and Shahidi, F. (1986). *J. Food Sci.* 51, 1245-1247.
- Natarajan. K. R. (1980). In: (C. O. Chichester, E. M. Mrak, and G. F. Stewart, eds) *Advances in Food Research*, Vol. 26, pp. 215-273. Academic press, New York, NY.
- Negbenebor, C. A. and Chen, T. C. (1985). Effect of ovalbumen on TBA values of cornminuted poultry meat. *J. Food Sci.* 50, 270-271.
- Nickel, G. B. (1981). Canadian Patent 1,104,871.
- Oakenfull, D. and Scott, A. (2003). Gelatin gels in deuterium oxide. *Food Hydrocoll.* 17, 207-210.

- Okamoto, S. (1978). Factors affecting protein film formations. *Cereal Food World* 23, 256-262.
- Okamoto, M., Morita, S., Taguchi, H. Kim, Y. H., Kotaka, T., and Tateyama, H. (2000). Synthesis and structure of smectic clay/poly(methyl methacrylate) and clay/polystyrene nanocomposites via in situ intercalative polymerization. *Polymer* 41(10), 3887-3890.
- Okuyama, K., Wu, G., Jiravanichanun, N., Hongo, C., and Noguchi, K. (2006). Helical twists of collagen model peptides. *Biopolymers*, 84, 421-432.
- Okuyama, K., Xu, X., Iguchi, M., and Noguchi, K. (2006). Revision of collagen molecular structure. *Biopolymers*, 84, 181-191.
- Ou, S. Y., Kwok, K. C., and Kang, Y. J. (2004). Changes in in vitro digestibility and available lysine of soy protein isolate after formation of film. *Journal of Food Engineering*, 64(3), 301-305.
- Paetau, I., Chen, C.-Z., and Jane, J. (1994). Biodegradable plastic made from soybean products. 1. Effect of preparation and processing on mechanical properties and water absorption. *Industrial & Engineering Chemistry Research*, 33(7):1821-1827.
- Park, H. J., Bunn, J. M., Weller, C. L., Vergano, P. J., and Testin, R. F. (1994). *Trans. ASAE*, 37, 1281-1285.
- Park, H. J. and Chinnan, M. S. (1995). *J. Food Engr.* 25, 497-507.
- Park, H. M., Li, X., Jin, C.-Z., Park, C.-Y., Cho, W.-J., and Ha, C.-S. (2002). Preparation and Properties of Biodegradable Thermoplastic Starch/Clay Hybrids. *Macromolecular Materials and Engineering* 287(8), 553-558.
- Park, H. M., Lee, W.-K., Park, C.-Y., Cho, W.-J., and Ha, C.-S. (2003). Environmentally friendly polymer hybrids Part I Mechanical, thermal, and barrier properties of thermoplastic starch/clay nanocomposites.. *Journal of Materials Science* 38(5), 909-915.
- Park, S. K., Hettiarachchy, N. S., Ju, J. Y., and Gennadios, A. (2002). In: A. Gennadios(ed.) *Protein-based Films and Coatings*, pp. 123-137. CRC Press, Boca Raton, FL.
- Raynes, M., Ciolfi, V., Maves, B., Stedman, P., and Mittal, G. S. (2000). *J. Sci. Food Agric.*, 80, 777-782.

- Ruiz-Hitzky, E. and Aranda, P., (2000). Electroactive Polymers Intercalated in Clays and Related Solids. Chapter 2. pp. 19-46 In: Pinnavaia, T. J., Beall, G. W. (eds) Polymer-Nanocomposites. New York, USA, Marcel Dekker.
- Ruiz-Hitzky, E., Aranda, P., and Serratosa, J. M. (2004). Clay-Organic Interactions. Chapter 3. pp. 122-123 In: Auerbach, S. M., Carrado, K. A., and Dutta, P. K. (eds) Handbook of Layered Materials. West Sussex, UK, Wiley.
- Saroso, B. (1989). *Ind. Crop Res. J.* 1, 60-65.
- Shimada, K. and Cheftel, J. C. (1998). Sulfhydryl group disulfide bond interchange during heat induced gelation of whey protein isolate. *J. Agric. Food Chem.* 37, 161-168.
- Shull, J. M., Watterson, J. J., and Kirlies, A. W. (1991). *J. Agric. Food Chem.* 39, 83-87.
- Sinha Ray, S. and Okamoto, M. (2003). Polymer/layered silicate nanocomposites: areview from preparation to processing. *Progress in Polymer Science* 28(11), 1539-1641.
- Stoloff, L. S., Puncochar, J. F., and Crowther, H. E. (1949). Curb mackerel fillet rancidity. *Food Ind.* 20, 1130-1132.
- Takahashi, K., Nakata, Y., Someya, K., and Hattori, M. (1999). Improvement of the physical properties of pepsin-solubilized elastin collagen film by crosslinking. *Biosci. Biotechnol. Biochem.* 63, 2144-2149.
- Taylor, M. M., Liu, C. K., Latona, N., Marmer, W. N., and Brown, E. M. (2002). Enzymatic modification of hydrolysis products from collagen using a microbial transglutaminase. II. Preparation of films. *J. ALCA* 97, 225-234.
- Trotter, J. A., Kadler, K. E., and Holmes, D. F. (2000). Echinoderm collagen fibrils grow by surface-nucleation and propagation from both centers and ends, *J. Mol. Biol.* 300, 531-540.
- Usuki, A., Kojima, Y., Kawasumi, M., Okada, A., Fukushima, Y., Kurauchi, T., and Kamigaito, O. (1993). Synthesis of nylon 6-clay hybrid. *J. Mater. Res.* 8(5), 1179-1184.
- Vaia, R. A., and Giannelis, E. P. (1997). Polymer Melt Intercalation in Organically Modified Layered Silicates: model Predictions and Experiment. *Macromolecules* 30(25), 8000-8009.
- Watanabe, K. and Okamoto, S. (1976). *New Food Ind.* 18(4), 65-77.

- Weaver, C. E. (1989). *Clays, Muds, and Shales*. Elsevier, Amsterdam.
- Wolff, I. A., Davis, H. A., Cluskey, J. E., Gundrum, L. J., and Rist, C. E. (1951). Preparation of films from amylase. *Ind. Eng. Chem.* 43, 915-919.
- Woodroof, J. G. (1983). In: (J. G. Woodroof, ed.) *Peanuts: Production, Processing, Products*, 3<sup>rd</sup> edn., pp. 165-179. The AVI Publishing Company, Westport, CT.
- Wool, R. (2003). Affordable bio-based materials from renewable resources, *Business Briefing*, CPI Technology, 32-36.
- Wu, L. C. and Bates, R. P. (1972). *J. Food Sci.* 37, 36-44.
- Yannas, I. V. (1972). *J. Macromol. Sci.-Rev. Macromol. Chem.*, C7 (1): 49-104.
- Young, A. H. (1984). Fractionation of starch. In: *Starch: Chemistry and Technology* (R. L. Whistler, J. N. BeMiller, and E. F. Paschall, eds), pp. 249-284. Academic Press, New York, NY.
- Young, H. H. (1967). Gelatin. In: (H. F. Mark, N. G. Gaylord, and N. M. Bikales, eds) *Encyclopedia of Polymer Science and Technology*, Vol. 7, *Plastics, Resins, Rubbers, Fibers*, pp. 456-460. Interscience Publishers, New York, NY.
- Zongo, D. and Coulibaly, M. (1993). *Tropicultura* 11, 95-98.

## CHAPTER TWO

### RESEARCH HYPOTHESES

The following hypotheses are the basis of this study.

1. Fish gelatin film can be manufactured in good quality by casting method and thus can be qualified for commercial application.
2. The physical and mechanical properties can be enhanced by adding nano-sized layered clay materials when certain conditions (content, mixing force, pH, clay type, pre-treatment of clay) are met.
3. The 2:1 type montmorillonite clay has large surface area ( $760 \cdot 10^3 \text{ m}^2 \text{ kg}^{-1}$ ) and high cation exchange capacity ( $\sim 1 \text{ mol kg}^{-1}$  monovalent cations) which is largely independent of salt concentration and pH. Therefore, it easily forms an interlayer complex with a wide variety of simple and polymeric organic molecules (charged or uncharged).
4. The montmorillonite clays saturated with small, monovalent cations ( $\text{Li}^+$ ,  $\text{Na}^+$ ) may show extensive interlayer expansion in dilute aqueous solutions of their respective cation salt and in water, and under optimum conditions the layers can dissociate completely.
5. The adsorption of amino acids by clay and soil systems is extremely sensitive to variations in the pH of the medium (e.g. anionic form of amino acids is relatively unreactive towards the negatively charged clay surfaces).

6. The increased degree of cross-linking in polymer matrix enhances the rigidity of polymer molecules and also increases the molecular weight.
7. The type of mechanisms of clay-organic interactions are electrostatic, van der waals forces, hydrogen bonding, water bridges, ion dipole and coordination, proton transfer, electron transfer, and covalent bonding.

## CHAPTER THREE

### RESEARCH OBJECTIVES

The overall objectives of this study were to develop fish gelatin-nanoclay composite film as an barrier layer and characterize its physical, mechanical, and clay dispersion properties using sophisticated instruments.

The specific objectives of each section were:

#### Section 1

1. To investigate the effect of clay content, homogenization RPM, ultrasonification, and pH of gelatin on physical and mechanical properties of fish gelatin-nanoclay composite film.
2. To enhance physical and mechanical properties of fish gelatin based film and find the optimum condition (e.g. content, homogenization RPM, pH) for the addition of clay.
3. To characterize (e.g. are the clays intercalated? Or exfoliated? What is their  $d_{001}$  spacing?) the clay dispersion using XRD and TEM.

#### Section 2

1. To investigate the effect of MTGase treatment on fish gelatin-nanoclay composite film.
2. To further enhance the physical and mechanical properties of fish gelatin-nanoclay composite film by MTGase treatment.

### Section 3

1. To develop a laminate film comprised of PET/FG-clay composite/LDPE using conventional laminating machine for the application in retort pouch production.
2. Investigate bond peel strength between each layer of produced PET/FG-clay composite/LDPE laminate film.
3. To investigate oxygen barrier property of produced PET/FG-clay composite/LDPE laminate film at 0, 25, 50, 75% relative humidity.
4. Produce laminate film comprised of PET/EVOH/LDPE and compare bond peel strength and oxygen barrier properties with PET/FG-clay composite/LDPE laminates.



## CHAPTER FOUR

### EFFECT OF CLAY CONTENT, HOMOGENIZATION RPM, pH, AND ULTRASONIFICATION ON MECHANICAL AND BARRIER PROPERTIES OF FISH GELATIN/MONTMORILLONITE NANOCOMPOSITE FILMS

Ho J. Bae<sup>1</sup>, Young J. Byun<sup>1</sup>, Seung I. Hong<sup>2</sup>, Duncan. O. Darby<sup>1</sup>,  
Robert. M. Kimmel<sup>1</sup>, and William. S. Whiteside<sup>1\*</sup>

<sup>1</sup> Department of Packaging Science, Clemson University, Clemson, SC 29634-0320,  
USA.

<sup>2</sup> Graduate School of Biotechnology, Korea University, 5-Ka, Anam-Dong, Sungbuk-Ku,  
Seoul 136-701, Korea

\* To whom all correspondence should be sent:

Dr. William Scott Whiteside, Associate Professor  
Department of Packaging Science,  
Clemson University, Clemson, SC 29634-0370, USA.  
Telephone: +1-864-656-6246, fax: +1-864-656-4395  
e-mail: wwhtsd@clemson.edu

#### **Abstract**

The effect of clay content, homogenization RPM, and pH on the mechanical and barrier properties of fish gelatin/nanoclay composite films was investigated. The addition of 5% nanoclay (w/w) increased the tensile strength from 30.31±2.37 MPa to 40.71±3.30 MPa. The 9% nanoclay (w/w) film exhibited the largest improvements in oxygen and water

barrier properties. Oxygen permeability decreased from  $0.0004028 \pm 0.0000007$   $\text{g}\cdot\text{m}^2\cdot\text{day}\cdot\text{atm}$  to  $0.0001144 \pm 0.0000162$   $\text{g}\cdot\text{m}^2\cdot\text{day}\cdot\text{atm}$  and the water vapor permeability decreased from  $0.0312 \pm 0.0016$   $\text{ng}\cdot\text{m}^2\cdot\text{s}\cdot\text{Pa}$  to  $0.0081 \pm 0.0001$   $\text{ng}\cdot\text{m}^2\cdot\text{s}\cdot\text{Pa}$ . The incorporation of nanoclay improved both barrier and mechanical properties of fish gelatin films. The WAXS and TEM observation suggested that the ultrasonification treatment (30 min at 40% output) resulted in exfoliation of the silicates.

Key words: Fish gelatin, nanoclay, film, ultrasonification, biopolymer

#### **4.1. Introduction**

Food packaging materials composed of synthetic polymeric materials developed in the past 50 – 60 years are durable and inert in the presence of microorganisms (Mali, Grossmann, Garcia, Martino, & Zaritzky, 2002) and have gained a solid position in the food packaging industry (Guilbert, 1986). Packaging materials account for approximately 30% by weight of municipal solid waste and two-thirds of the volume in trash cans due to their bulk. Among the 30% packaging waste, 13% is due to plastic materials that are not biodegradable even though they are convenient, safe, strong, and economical (Han, 2001). Moreover, the depletion of petrochemical streams is also an important environmental fact.

Since the 1970s, environmental concerns have prompted several studies of different polar biopolymers as potential alternatives for synthetic polymers in the flexible packaging industries (Garcia, Martino, & Zaritzky, 2000). Numerous studies have been

conducted investigating the properties of various protein, polysaccharide, and lipid-based biopolymer materials. These materials have successfully been formed into films or coatings (Gontard, Guilbert, & Cuq, 1993; Park & Chinnan, 1995; Kim, Ko, & Park, 2002; Lawton, 1996; Arvanitoyannis, Nakayama, & Aiba, 1998; McHugh & Krochta, 1994; Gontard, Thibault, Cuq, & Guilbert, 1996; Chen, 1995; Lourdin, Valle, & Colonna, 1995; Gennadios, Weller, & Testin, 1993; Mchugh, Aujard, & Krochta, 1994; Park, Weller, Vergano, & Testin, 1993).

Natural biopolymers have the advantage of being biodegradable, renewable, and often edible. However, biopolymer films have exhibited relatively poor mechanical and water vapor barrier properties when compared to traditional polymeric films, therefore limiting their commercial use. Also, the use of additives such as plasticizers, which are necessary to achieve flexible films, affect barrier properties (Mchugh & Krochta, 1994). Due to inherent hydrophilic properties, biopolymer films absorb large quantities of water at elevated relative humidity (RH) conditions, resulting in plasticized film matrices that have weakened barrier and mechanical properties (Lim, Mine, & Tung, 1999). Numerous studies have been conducted in an effort to improve the properties of biopolymer films utilizing a variety of modifications (Chen, Embree, Brown, Taylor, & Payne, 2003; Uresti, Ramirez, Lopez-Arias, & Vazquez, 2003; Haug, Draget, & Smidsrod, 2004; Tanaka, Iwata, Sanguandeeikul, Handa, & Ishizaki. 2001; Veiga-Santos, Oliveira, Cereda, & Scamparini, 2007). Even after such modifications, the physical and mechanical properties of these biopolymer films can still be inadequate for many applications.

The focus of this research is gelatin. Gelatin is a complex polypeptide widely used in the food, pharmaceutical, photographic, and cosmetic manufacturing. Gelatin was one of the initial materials used for the formation of biopolymer films and continues to be used in edible film studies given the abundance of raw material, low production cost, global availability, and excellent film forming properties (Vanin, Sobral, Menegalli, Carvalho, & Habitante, 2005). Gelatin is obtained by thermal or acid/alkali denaturation of collagen from animal skin, bones, and cartilages (Darder, Ruiz, Aranda, Damme, Ruiz-Hitzky, 2006; Podczeczek & Jones, 2004; Veiga-Santos, Oliveira, Cereda, & Scamparini, 2007). Traditional sources of gelatin have been primarily pig skin and cowhide, however for a number of reasons such as religious prohibition and concerns over the spreading of bovine spongiform encephalopathy (commonly known as mad cow disease), alternatives for these mammalian based gelatins are increasing in demand.

Among the many possible alternatives (Park & Chinnan, 1995; Park, Lee, Jung, & Park, 2001; Kim, Ko, & Park, 2002), the characteristics and properties of fish gelatin have been studied in recent years as a potential mammalian gelatin alternative. (Yi, Kim, Bae, Whiteside, & Park, 2006) One of the limitations of fish gelatin is that it has relatively low gelling and melting temperatures along with poor mechanical properties when compared to mammalian gelatin. This is primarily due the fact that fish gelatin contains lower amounts of the proline and hydroxyproline.(Yi, Kim, Bae, Whiteside, & Park, 2006; Bower, Avena-Bustillos, Olsen, Mchugh, & Bechtel, 2006)

Recently, the emerging research area of polymer nanocomposites has received great interest due to the ability of nano-sized material fillers to significantly improve

polymer properties when compared with polymer alone or micro-scale composites. A polymer nanocomposite is a hybrid material consisting of a polymer matrix reinforced with a fiber, platelet or particle having at least one dimension on the nanometer scale ( $10^{-9}$  m). It is believed that when the domain size is comparable to the size of a molecule, the atomic and molecular interactions can have a significant influence on the macroscopic properties of that material (Rao, 2007). The potential improvements include enhanced mechanical strength, weight reduction, increased heat-resistance and improved barrier properties. (Ray & Okamoto, 2003)

The enhanced mechanical properties of polymer/nanoclay composite films have attracted a great deal of research focus in the last decade (Usuki, 1995; Usuki, Kojima, Okada, Fukushima, Kurauchi, & Kamigaito, 1993; Usuki, Kojima, Kawasumi, Okada, Fukushima, & Kurauchi, 1993; Krook, Gallstedt, & Henedqvist, 2005; Ke, Long, & Qi, 1999; Noh & Lee, 1999; Lan, Kaviratna, & Pinnavaia, 1996; Aranda & Ruiz-Hitzky, 1999; Rao and Pochan, 2007). Among studied minerals, the expanding 2:1 type layer silicates, of which montmorillonite is an example, were of particular interest in view of their ability to intercalate a huge list of compounds (Ruiz-Hitzky, Darder, & Aranda, 2005). A relatively small amount of nanoclay, typically in the range of 3-5 wt%, can produce significant improvements in the mechanical and thermal properties of the nanoclay/polymer nanocomposites. (Lam, Lau, Cheung, & Ling, 2005) Product development of these type of composites have increased globally. For example, a Toyota research group showed improvement in the thermal and mechanical properties of a polyamide 6-montmorillonite composite material (Usuki, 1995; Usuki, Kojima, Okada,

Fukushima, Kurauchi, Kamigaito, 1993; Usuki, Kojima, Kawasumi, Okada, Fukushima, Kurauchi, 1993; Krook, Gallstedt, & Henedqvist, 2005).

In this research, fish gelatin was combined with layered silicates, specifically homoionic smectites (Na-montmorillonite), in order to enhance the mechanical properties and the barrier properties against oxygen and water vapor. Research has shown that two factors, the intercalation of the clay sheets and the dispersion of the intercalated platelets, determine the change in properties (Rao, 2007). The resulting fish gelatin-nanoclay composite film was characterized according to the clay content, amount of shear force applied at pretreatment of clay solution, pH, and ultrasonification applied at pretreatment of clay solution.

## **4.2. Experimental Material and Method**

### 4.2.1. Materials

The following raw materials were used to develop gelatin-clay composite films: Gelatin 200 bloom-fish-8 mesh (Vyse Gelatin Company, Illinois, USA); Cloisite® NA<sup>+</sup> (Southern clay Products, Texas, USA); Glycerol, Anhydrous (J. T. Baker, New Jersey, USA); Tris(hydroxymethyl)aminomethane, 99% (Alfa Aesar, Massachusetts, USA); Hydrochloric acid (Fisher Scientific, Pennsylvania, USA).

### 4.2.2. Solution Preparation

Warm-water gelatin was used for solution preparation because cold-water gelatins behave as a viscous liquid at room temperature (Avena-Bustillos, Olsen, Olson, Chiiou,

Yee, Bechtel, & Mchugh, 2006), which limits their application for casting technique, The film solution preparation and development procedure is reported in Figure 1. The nanoclay solutions were prepared by first dissolving 10 g of glycerol in 100 mL of 50°C degassed, distilled, and deionized water and stirred for 30 min at 50±5°C. The concentration of glycerol was 0.2 g glycerol/g gelatin. Various amounts of clay were added and stirred by magnetic stirrer for 30 min at 50±5°C. The solution was then homogenized for 5 min. This was followed by sonification using Branson sonifier (Model S-450D), which was used to aid intercalation and exfoliation of the clay and plasticizers. A standard 1/2 in diameter tapped flat horn tip was used at approximately 40% output for 30 min. The gelatin solution was prepared separately. Fifty grams of biopolymer was dissolved in 100 mL of 60 °C degassed, distilled, and deionized water and stirred for 2 hr at 60±5°C. Finally, the clay solution was added to gelatin solution in droplets and gently stirred for 24 hr at 35±5°C before casting.

#### 4.2.3. Film Casting

Approximately 35 mL of the prepared film solution was cast onto a BYTAC<sup>®</sup> (Norton Performance Plastics Corporation, Wayne, NJ, USA) coated 8” x 16” glass plate which was formed utilizing a custom designed film applicator as shown in Figure 2. After drying, films were peeled off from the glass plates and cut into test specimens. The test specimens were immediately placed into a constant temperature and humidity chamber (25°C, 50% RH) and held for 48 hr prior to testing.

#### 4.2.4. Film Thickness

Film thickness was measured with a Digimicro MFC105 micrometer (Nikon, Japan). Measurements for testing mechanical properties were taken at five different locations on the film samples for each test. For testing oxygen and water barrier properties, measurements were made at nine different locations. The mean thickness was used to calculate the mechanical and barrier properties of film.

#### 4.2.5. Viscosity

The viscosity of film casting solution was measured by dial reading viscometer (LVT, Brookfield, Mass., USA) at temperature range from 25 °C ~ 50 °C. The spindle type used was LV-3C at speed 6, and the amount of the sample used was 500 mL.

#### 4.2.6. Color

Hunter L, a, and b values of films were measured by using ColorQuest II Spectrophotometer with Universal Software version 3.73 (Hunter Associates Laboratory, Inc., Reston, VA, USA). The machine was calibrated using a white standard plate (standard no. C6006) and a gray standard plate (standard no. C6006-G). The film specimen was placed on white standard plate (standard no. C6006) having color value of  $L = 94.62$ ,  $a = -0.91$  and  $b = 0.64$  and mounted at the reflectance port. Color values were measured at three random positions including the center of the film specimen. The L axis runs from top to bottom. The maximum for L is 100, which would be a perfect reflecting diffuser. The minimum for L would be zero, which would be black. The a and b axes



have no specific numerical limits. Positive a is red. Negative a is green. Positive b is yellow. Negative b is blue (HunterLab Applications Note, 1996). Total color difference (E) was calculated by substituting acquired Hunter L, a and b values into the equation below. The  $\Delta E$  is a single value that takes into account the differences between L, a, and b of the sample and standard (HunterLab Applications Note, 1996).

$$\Delta E = [(L_{\text{film}} - L_{\text{standard}})^2 + (a_{\text{film}} - a_{\text{standard}})^2 + (b_{\text{film}} - b_{\text{standard}})^2]^{0.5} \quad (1)$$

#### 4.2.7. Haze

The haze of films was determined using ColorQuest II Spectrophotometer with Universal Software Version 3.73 (Hunter Associates Laboratory, Inc., Reston, VA, USA). The haze measurement was made in transmission mode and calculated using following equation. The white plate (Standard No. C6006, X = 81.77, Y = 86.72, Z = 92.18) provided by the manufacturer was used for calibration and background. The values were expressed by

$$\text{Haze} = \frac{Y_{\text{Diffuse transmission}}}{Y_{\text{Total transmission}}} \times 100$$

#### 4.2.8. Mechanical Properties

The tensile strength (TS) and elongation (E) at break of the films were determined with an Instron Universal Testing Machine (Model 4201, Instron Corp., Canton, MA, U.S.A.). Forty specimen samples, 10 cm x 2.54 cm, were cut from film samples prepared on glass plates (8" x 16"). Samples were conditioned for 48 hr at 25°C and 50% relative

humidity (RH) in a constant temperature and humidity chamber before the measurement. Initial grip separation and cross-head speed were set at 5 cm and 25 mm/min, respectively. TS was calculated by dividing the maximum load by the cross-sectional area of the film, and E was calculated and expressed as percentage of change of the original length of a specimen between grips (5 cm) according to the ASTM standard method D882-88 (ASTM 1989).

#### 4.2.9. Oxygen Permeability

Oxygen permeability was measured at  $23 \pm 1$  °C and RH condition of 50% and done in triplicate to get the average mean value. The oxygen transmission rate was determined in an OX-TRAN 2/20 (Mocon, Inc., Minneapolis, MN, USA). The samples were equilibrated at  $50 \pm 1$ % relative humidity ( $23 \pm 1$  °C) for a period of 48 hr before analysis. The gas flow rate was fixed at (10 mL/min) and the difference in pressure across the film corresponded to atmospheric pressure (101.3 kPa). Oxygen permeability ( $\text{cc}\cdot\text{m}/\text{m}^2\cdot\text{day}\cdot\text{atm}$ ) was calculated by multiplying the oxygen transmission rate by the film thickness.

#### 4.2.10. Water Vapor Permeability (WVP)

A MOCON Permatran-W3/31 Water Vapor Permeation Measurement System with an IR detector was used to measure and analyze the water vapor transmission rate. The test film was first placed into the two test cells. Carrier gas,  $\text{N}_2$ , was passed through HPLC grade water to adjust the RH and flowed into the test cell. As the water vapor

diffused through the test film, it was carried by nitrogen carrier gas to the detector, and the water vapor transmission rate (WVTR) was continuously recorded. The nitrogen gas flow was set at 100 sccm (standard cubic centimeters per minute). The Permatran response was calibrated using a reference film provided by the manufacturer. The permeability coefficient ( $P$ ) was calculated according to  $P = \text{WVTR} \times (\text{film thickness}/\text{vapor partial pressure})$ . The test was done in triplicate and average mean value was used.

#### 4.2.11. Characterization

XRD studies of the samples were carried out using a Scintag XDS 2000 (Scintag Inc., USA) with a germanium detector equipped with Scintag DMSNT Version 1.37 software. In order to monitor the  $d_{-001}$  spacing corresponding to the interlayer spacing of the clay, the samples were scanned from the start angle of  $1^\circ$  and stop angle of  $20^\circ$  at step size 0.02 and preset time 0.7 sec.

#### 4.2.12. Transmission Electron Microscopy (TEM)

For TEM observation, 90-100 nm sections of the samples were microtomed at room temperature using an Ultracut E microtome at a cutting speed of 10 mm/s. The sections were cut perpendicular to the casting direction of the casted film. The observations were made using the transmission electron microscopy (H-7600T, HITACHI, Japan) at 120 kV using magnifications from 20,000 to 300,000 times to study dispersions of clay particles.

#### 4.2.13. Statistical Analysis

Measurements were replicated three times for each film, with individually prepared films as the replicated experimental units. Statistics on a completely randomized design were performed with the analysis of variance (ANOVA) procedure in SAS (Release 9.1, SAS Institute Inc., Cary, NC) software. Duncan's Multiple Range Test ( $p < 0.05$ ) was used to detect differences among film property mean values.

### 4.3. Results and Discussion

#### 4.3.1. Viscosity

The viscosity of the nanocomposite solution was measured at 20% (w/w) concentration at 50 °C, and at pH 6. As shown in Figure 3, the viscosity of the solution increased significantly ( $P < 0.05$ ) as the amount of clay (1 to 9% w/w) increased and as the temperature (25 to 50 °C) decreased, respectively. There was a significant ( $P < 0.05$ ) increase in viscosity for solutions containing 3%, 5%, 7%, and 9% (w/w) clay content below temperature of 40 °C. Gelatin solution viscosity containing 1% (w/w) clay and pure gelatin solution was not affected compared to solution with higher clay content. On the basis of viscosity observations, the temperature of 40 °C was selected for fish gelatin-nanoclay composite film preparation and subsequent analyses due to the convenience in preparing film samples using casting method.

#### 4.3.2. Color and Haze

The color and haze value of films are depicted in table 1. In this observation, the color of films was significantly affected by an increase in clay content. The lightness ( $L$ ) of films was not affected significantly by clay content, however, the red/green values ( $a$ ) and yellow/blue values ( $b$ ) varied from  $0.05 \pm 0.01$  to  $-0.04 \pm 0.01$  and  $-0.14 \pm 0.03$  to  $0.44 \pm 0.03$ , respectively. These results suggested that the color of films became more greenish and yellowish as the clay content increased, but these changes were not evident by a visual observation. The haze value of films did not change significantly according to increased clay content. These results suggested that the high degree of exfoliation resulted in lack of distinction of haziness between samples with different clay content. This finding is supported by the X-ray diffraction, where there was an absence of a broad series of peaks from interlayer spacings from  $10 \text{ \AA}$  to  $60 \text{ \AA}$  from the WAXS (Figure. 10) data. This indicates exfoliation of nanoclay. Dean and Yu (2005) reported disappearance of broad series of peaks (from  $10 \text{ \AA}$  to  $60 \text{ \AA}$ ) from WAXS data for soy protein nanoclay composite films and concluded that it was the indication of nanoclay exfoliation. Rao (2007) reported that when high-aspect-ratio clay such as Cloisite is used, then the gelatin-clay nanocomposite stays exfoliated up to 10%.

#### 4.3.3. Mechanical Properties

*Effect of clay content:* Tensile strength (TS) and elongation at break (EB) are used to describe how the mechanical properties of film materials relate to their chemical structure (Ninnemann, 1968). The mechanical properties of fish gelatin-clay composite

films as a function of clay content, shear force, and pH are presented in Figure 4, 5, and 6 respectively. The effects of composite formation are reflected in the mechanical property improvements, where the most significant improvement in TS is observed in the 5 wt % clay sample (Figure 4). Results indicated that increasing the clay content increased the TS of composite film and made the films more brittle. The control gelatin film had TS of  $30.31 \pm 2.37$  MPa. The TS of clay composite generally increased ( $40.71 \pm 3.30$  MPa) up to 5 wt % clay, and leveling out, with a slight dip at 7%. At a 9 wt % clay, TS of the composite film was higher than that of gelatin control film. Increasing the clay content dropped the E% of the fish gelatin-clay composite film. The EB dropped from  $48.24 \pm 4.00\%$  (control) to  $20.16 \pm 5.44\%$  (9 wt % clay).

*Effect of shear rate:* The difference in shear rate (0~5000 rpm) for the nanocomposite formation did not result in substantial changes in the TS or EB of the films (Figure 5). The TS decrease ( $36.36 \pm 2.17$  MPa and  $34.69 \pm 1.41\%$ ) as rpm was increased to 500 rpm ( $34.88 \pm 2.56$  MPa and  $30.15 \pm 3.84\%$ ), but increases up to  $36.92 \pm 1.17$  MPa at 1000 rpm followed by decrease at 3000 and 5000 rpm ( $34.87 \pm 2.4$  and  $33.44 \pm 1.81$  MPa). The E% of the films decreased as shear rate increased to 500 rpm, but increases along with the further increase of rpm. Although there were minor movements in both TS and EB as a function of shear rate, the degree of these movements was small in magnitude. It can be concluded that the composite film is independent of the level of mechanical force applied prior to sonification process.

*Effect of pH:* The tensile strength and elongation at break as a function of film solution pH were measured to reveal the importance of pH and are depicted in Figure 6.

It can be seen that the TS is the highest at lower pH values. The highest levels of TS and EB were observed at a pH of 5. Further increases in pH of the film solution decreased the TS and E%. The TS decreased from  $19.66 \pm 3.02$  MPa (pH 4) to  $13.04 \pm 1.38$  MPa (pH 9) and the E% decreased from  $46.69 \pm 8.41\%$  (pH 4) to  $34.33 \pm 6.91\%$  (pH 9). At pH 7, significant decrease of TS ( $12.89 \pm 1.38$  MPa) was observed. In the case of EB, significant decrease ( $36.36 \pm 7.64$ ) was observed at pH 6. The solubility of proteins is the lowest near their isoelectric point (pI) since intramolecular electrostatic interactions would be maximal at this point, causing the dipolar molecule to adopt the most compact conformation. It can be suggested that the increase of electrostatic interactions decreased contacts between protein and nanoclay and therefore resulted in decreased mechanical properties at pI (pH 6~7) of fish gelatin.

These findings are confirmed by the work of others in the literatures. Research has shown that the intercalation of gelatin in Na-homoionic smectites occurs at low pH values, which are necessary to protonate amino groups belonging to the amino acids of the protein. Thus, the positively charged gelatin is able to replace totally or partially the sodium ions which are mainly located on the interlayer space of the smectites (Ruiz-Hitzky, Darder, & Aranda, 2005).

It has been remarked earlier by Ensminger and Giesecking (1939, 1941) that complex formation between protein and montmorillonite primarily involved an exchange between the cationic ( $-\text{NH}_3^+$ ) groups on the amino acid side chains of the protein and the  $\text{Na}^+$  ion occupying exchange sites at the montmorillonite surface.

Mclaren and others (1958) studied the reactions of gelatin dissolved in buffer solutions of different pH and ionic strength, with Na-montmorillonite suspensions. They found that the process was characterized by determining the adsorption isotherms for the gelatin in function of pH and relating the basal spacing of the resulting complexes to the amount adsorbed. They reported decrease in adsorption at  $\text{pH} > \text{pI}$  which can be ascribed to electrostatic repulsion between the protein anion and the negatively charged montmorillonite surface. Moreover, this effect is further enhanced by the cations in solution (e.g.  $\text{Na}^+$ ) competing with the protein for the surface.

#### 4.3.4. Oxygen Barrier Properties (OP)

*Effect of clay content:* The effect of clay content on oxygen barrier properties is shown in Figure 7. As clay content increased, oxygen permeability decreased significantly. The control (0 % clay) gelatin film had oxygen permeability of  $0.0004028 \pm 0.0000007 \text{ cc}\cdot\text{m} / \text{m}^2 \cdot \text{day}\cdot\text{atm}$  and oxygen permeability decreased to maximum of  $0.0001144 \pm 0.0000162 \text{ cc}\cdot\text{m} / \text{m}^2 \cdot \text{day}\cdot\text{atm}$  at 9 wt % clay content (about 75% decrease).

*Effect of shear rate:* Changing the shear rate did not significantly influence oxygen permeability (Figure 8). Although differences were statistically significant, there appeared to be a trend of slight decrease of oxygen permeability up to 1000 rpm (from  $0.0001924 \pm 0.0000102 \text{ cc}\cdot\text{m} / \text{m}^2 \cdot \text{day}\cdot\text{atm}$  to  $0.0001713 \pm 0.0000025 \text{ cc}\cdot\text{m} / \text{m}^2 \cdot \text{day}\cdot\text{atm}$ )



followed by slight increase up to 5000 rpm (from  $0.0001713 \pm 0.0000025$  cc·m / m<sup>2</sup>·day·atm to  $0.0001964 \pm 0.0000085$  cc·m / m<sup>2</sup>·day·atm).

*Effect of pH:* The effect of pH on oxygen barrier properties is shown in Figure 9. The overall oxygen permeability decreased as film solution pH increased. The highest oxygen permeability was observed at pH 5 ( $0.0002480 \pm 0.0000046$  cc·m / m<sup>2</sup>·day·atm) and the lowest at pH 8 ( $0.0002073 \pm 0.0000102$  cc·m / m<sup>2</sup>·day·atm).

#### 4.3.5. Water Vapor Barrier Properties (WVP).

*Effect of clay content:* The effect of clay content on water vapor barrier property is shown in Figure 7. The addition of clay significantly enhanced the water vapor barrier properties of fish gelatin-clay composite film. The pure gelatin film had a WVP of  $0.0312 \pm 0.0016$  ng·m / m<sup>2</sup>·s·Pa and 9 wt % clay composite film had the maximum WVP decrease of  $0.0081 \pm 0.0001$  ng·m / m<sup>2</sup>·s·Pa (about 75% decrease).

*Effect of shear rate:* Varying the shear rate did not impart significant differences in water vapor permeability (Figure 8). Although differences were not significant, there was a trend of slight decrease of oxygen permeability up to 1000 rpm (from  $0.0131 \pm 0.0009$  ng·m / m<sup>2</sup>·s·Pa to  $0.0123 \pm 0.0005$  ng·m / m<sup>2</sup>·s·Pa) followed by slight increase up to 5000 rpm (from  $0.0123 \pm 0.0005$  ng·m / m<sup>2</sup>·s·Pa to  $0.0138 \pm 0.0010$  ng·m / m<sup>2</sup>·s·Pa) similar to the trend for OP.

*Effect of pH:* The effect of pH on water vapor barrier property was shown in Figure 9. The overall water vapor permeability decreased as the pH of the film solution

increased. The highest water vapor permeability was observed at pH 5 ( $0.0156 \pm 0.0007$  ng·m / m<sup>2</sup>·s·Pa) and the lowest at pH 7 ( $0.0124 \pm 0.0001$  ng·m / m<sup>2</sup>·s·Pa).

### 3.6. SAXS

The assessment of the dispersion of the clays in the fish gelatin-nanoclay composite films was done using SAXS (Figure. 10). This allowed monitoring of the d-001 spacing according to the interlayer spacing of the clay and allowed observation of whether clay was intercalated or exfoliated. The observed d-001 for neat Cloisite NA<sup>+</sup> was 11.7Å as was indicated by the manufacturer. The SAXS results of non-ultrasonicated sample and ultrasonicated sample showed significantly different behavior. From the diffractogram of the unultrasonified FG/Cloisite NA<sup>+</sup>/glycerol/H<sub>2</sub>O, a broad series of peaks was observed which corresponded to interlayer spacings from about 10Å to 60Å. The broad series of peaks were not observed from the diffractogram of ultrasonicated FG/Cloisite NA<sup>+</sup>/glycerol/H<sub>2</sub>O film. This suggests that the added nanoclay was exfoliated. Dean and Yu (2005) reported similar diffractogram for non-ultrasonified and ultrasonified soy protein/Cloisite NA<sup>+</sup> composite film which had been plasticized by glycerol. They reported a broad band from 10Å to 60Å for their untreated sample and disappearance of broad band for their ultrasonicated sample. Rao (2007) reported that in the exfoliated state, the diffraction from the clay interlayer spacing disappears, and it is believed that the two clay platelets are at least 70 Å apart.

#### 4.3.7. Transmission Electron Microscopy

Along with the SAXS, the TEM is one of the main tools used for determination of the dispersion of the clay nanoparticles. The acquired TEM image correlated well with the SAXS result. The TEM images of the non-ultrasonified and ultrasonified fish gelatin-clay composite film containing 9 wt % clay were shown in Figure. 11~Figure. 14. As can be seen in the Figure, large agglomerates are clearly visible along with tactoids (2~3 particles) of silicates. However, no large agglomerates were visible from TEM images of ultrasonicated samples. No agglomerates were observed, but mostly single exfoliated silicates were observed. The TEM results are in agreement with the XRD diffractogram results where no broad series of peaks corresponding to particular interlayer spacings were observed.

#### 4.3.8. Effect of Ultrasonification

In addition to the TEM images, the effects of ultrasonification are also shown in Table 2, especially in the oxygen barrier property data. Ultrasonified film showed improved barrier property against oxygen with about 11% improvement. From this result, it can be suggested that increased degree of exfoliation of nanoclay in film samples lead to improved barrier property against oxygen permeation. The result of TS, E%, and WVP showed somewhat different outcomes. The shown values were not significantly different ( $p < 0.05$ ) under each properties. The ultrasonification treatment did not affect TS, E%, and WVP properties as much as it did for OP.

#### 4.4. Conclusion

In this research, protein-based nanocomposites have been successfully developed from a fish gelatin. In the blends, the unmodified sodium montmorillonite clay was initially treated with a high-powered ultrasonifier in a solution of glycerol and distilled water. The nano-clay solution was then added to a fish gelatin solution and casted using a mechanical film caster. This ultrasonically treated nanocomposite film exhibited an exfoliated type structure and with improved tensile strength and barrier properties and the films produced were uniform in thickness and relatively transparent. The result gathered by XRD and TEM observations confirms that the majority of clay particles are in an exfoliated state. This study promotes the fact that clean ultrasonic energy contributes to the intercalation and exfoliation of unmodified montmorillonite clays. The complete exfoliation of clay silicates without the use of chemical modification is significant both in terms of cost and biodegradability.

#### **4.5. References**

- Aranda, P. and Ruiz-Hitzky, E. (1999). Poly(ethylene oxide)/NH<sub>4</sub><sup>+</sup>-smectite nanocomposites, *Appl Clay Sci*, 15, 119-135.
- Arvanitoyannis, I. S., Nakayama, A., Aiba, S. (1998). Chitosan and gelatin based edible films: state diagrams, mechanical and permeation properties. *Carbohydr Polym*, 37, 371-382.
- Avena-Bustillos, R. J., Olsen, C. W., Olson, D. A., Chiou, B., Yee, E., Bechtel, P. J., and Mchugh T. H. (2006). Water Vapor Permeability of Mammalian and fish gelatin films, *J Food Sci*, 71(4), 202-207.
- Bower, C. K., Avena-Bustillos, R. J., Olsen, C. W., Mchugh, T. H., and Bechtel, P. J. (2006). Characterization of Fish-Skin Gelatin Gels and Films Containing the Antimicrobial Enzyme Lysozyme, *J Food Sci*, 71(5), 141-145.

- Chen, H. Functional Properties and Applications of Edible Films Made of Milk Proteins. *J Dairy Sci*, 1995, 78, 2563-2583.
- Chen, T., Embree, H., Brown, E., Taylor, M., and Payne, G. (2003). Enzyme-catalyzed gel formation of gelatin and chitosan : potential for in situ applications, *Biomaterials*, 24(17), 2831-2841.
- Darder, M., Ruiz, A. I., Aranda, P., Van Damme, H., and Ruiz-Hitzky, E. (2006). Bio-nanohybrids based on layered inorganic solids: Gelatin nanocomposites *Current nanoscience*, 2(3), 231-241.
- Dean and Yu (2005). Ch In (R. Smith ed.) *Biodegradable polymers for industrial applications*. Boca Raton : CRC Press; Cambridge: Woodhead.
- Ensminger, L. E. and Gieseking, J. E. (1939). The adsorption of proteins by montmorillonitic clays. *Soil Science*, 48, 467-471.
- Ensminger, L. E. and Gieseking, J. E. (1941). The adsorption of proteins by montmorillonitic clays and its effect on base-exchange capacity. *Soil Science*, 51, 125-132.
- Garcia, M. A., Martino, M. N., and Zaritzky, N. E. Microstructural Characterization of Plasticized Starch-Based Films. *Starch/Stärke*, 2000, 52, 118-124.
- Gennadios, A., Weller, C. L., and Testin, R. F. Temperature Effect on Oxygen Permeability of Edible Protein-based Films. *J Food Sci*, 1993, 58, 212-219.
- Gontard, N., Guilbert, S., and Cuq, J. Water and Glycerol as Plasticizers Affect Mechanical and Water Vapor Barrier Properties of an Edible Wheat Gluten Film, *J Food Sci*, 1993, 58(1), 206-211.
- Gontard, N., Thibault, R., Cuq, B., and Guilbert, S. Influence of Relative Humidity and Film Composition on Oxygen and Carbon Dioxide Permeabilities of Edible Films, *Journal Agr Food Chem*, 1996, 44, 1064-1069.
- Guilbert, S. *Technology and application of edible protective films in Food Packaging and Preservation*, Elsevier Applied Science, London, 1986, 371-394.
- Han, J. H. Design of Edible and Biodegradable Films/Coatings Containing Active Ingredients. Pre-Congress Short Course of IUFoST 'Active Biopolymer Films and Coatings for Food and Biotechnological Uses', Korea University, Seoul, Korea. 2001.

- Haug, I. J., Draget, K. I., and Smidsrod, A. (2004). Physical behavior of fish gelatin-kapp-carrageenan mixtures, *Carbohyd Polym*, 56(1), 11-19.
- Ke, Y., Long, C., and Qi, Z. (1999). Crystallization, Properties, and Crystal and Nanoscale Morphology of PET-Clay Nanocomposites. *J Appl Polym Sci*, 71(7), 1139-1146.
- Kim, K. W., Ko, C. J., and Park, H. J. (2002). Mechanical Properties, Water Vapor Permeabilities and Solubilities of Highly Carboxymethylated Starch-Based Edible Films. *J Food Sci*, 67(1), 218-222.
- Krook, M., Gallstedt, M., and Hedenqvist, M. S. (2005). A Study on Montmorillonite/Polyethylene Nanocomposites Extrusion-coated Paperboard. *Packag Technol Sci*, 18, 11-20.
- Lam, C., Lau, K., Cheung, H., and Ling, H. Effect of Ultrasound Sonication in Nanoclay Clusters of Nanoclay/Epoxy Composites. *Mater Lett*, 2005, 59, 1369-1372.
- Lan, T., Kaviratna, P. D., and Pinnavaia, T. J. (1996). Epoxy Self-Polymerization in Smectite Clays, *J Phys Chem Solids*, 57, 1005-1010.
- Lawton, J. W. (1996). Effect of Starch Type on the Properties of Starch Containing Films, *Carbohyd Polym*, 29, 203-208.
- Lim, L. T., Mine, Y., and Tung, M. A. Barrier and Tensile Properties of Transglutaminase Cross-linked Gelatin Films as Affected by Relative Humidity, Temperature, and Glycerol Content, *J. Food Sci*, 1999, 64(4), 616-622.
- Lourdin, D., Valle, G. D., and Colonna, P. Influence of amylose content on starch films and foams, *Carbohyd Polym*, 1995, 27, 261-270.
- Mali, S., Grossmann, M. V. E., Garcia, M. A., Martino, M. N., and Zaritzky, N. E. Microstructural characterization of yam starch films, *Carbohyd Polym*, 2002, 50, 379-386.
- McHugh, T. H. and Krochta, J. M. (1994). Sorbitol- vs Glycerol-Plasticized Whey Protein Edible Films: Integrated Oxygen Permeability and Tensile Property Evaluation, *J Agr Food Chem*, 42, 841-845.
- McHugh, T. H., Aujard, J. F., and Krochta, J. M. Plasticized Whey Protein Edible Films: Water Vapor Permeability Properties, *J Food Sci*, 1994, 59(2), 416-419.

- Mclaren, A. D., Peterson, G. H., and Barshad, I. (1958). The adsorption and reactions of enzymes and proteins on clay minerals. IV. Kaolinite and montmorillonite. *Soil Science Society of America Proceedings*, 22, 239-244.
- Ninnemann, K. W. (1968). Measurement of physical properties of flexible films. In: Sweeting OJ, editors. *The Science and Technology of Polymer Films*. London, England: Interscience, 546-649.
- Noh, M. W. and Lee, D. C. (1999). Synthesis and characterization of PS-clay nanocomposite by emulsion polymerization. *Polym Bull*, 42, 619-626.
- Park, H. J., Chinnan, M. S. (1995). Gas and Water Vapor Barrier Properties of Edible Films from Protein and Cellulosic Materials. *Journal of Food Engineering*, 25, 497-507.
- Park, H. J., Weller, C. L., Vergano, P. J., and Testin, R. F. (1993). Permeability and Mechanical Properties of Cellulose-Based Edible Films. *J Food Sci*, 58(6), 1361-1370.
- Park, S.Y., Lee, B.I., Jung, S.T., and Park, H.J. (2001). Biopolymer composite films based on k-carrageenan and chitosan. *Mater Res Bull*, 36, 511-519.
- Podczec, F. and Jones, B. E. (2004). In Jones, R. T., editor. Pharmaceutical capsules, 2<sup>nd</sup> ed. London: *The Pharmaceutical Press*, 45-46.
- Rao, Y. (2007). Gelatin-clay nanocomposites of improved properties, *Polymer*, 48, 5369-5375.
- Rao, Y. and Pochan, J. M. (2007) Mechanics of Polymer-Clay Nanocomposites, *Macromolecules*, 40, 290-296.
- Ray, S. S., and Okamoto, M. (2003). Polymer/layered silicate nanocomposites: a review from preparation to processing. *Prog Polym Sci*, 28, 1539-1641.
- Ruiz-Hitzky, E., Darder, M., and Aranda, P. (2005). Functional Biopolymer Nanocomposites Based on Layered Solids. *J Mater Chem*, 15, 3650-3662.
- Tanaka, M., Iwata, K., Sanguandeeikul, R., Handa, A., and Ishizaki, S. (2001). Influence of plasticizers on the properties of edible films prepared from fish water-soluble proteins, *Fisheries Sci*, 67(2), 346-351.
- Uresti, R., Ramirez, J., Lopez-Arias, N., and Vazquez, M. (2003). Negative effect of combining microbial transglutaminase with low methoxyl pectins on the

- mechanical properties and colour attributes of fish gels, *Food Chem*, 80(4), 551-556.
- Usuki, A. (1995). The chemistry of polymer-clay hybrids. *Mater Sci Eng*, C3, 109-115.
- Usuki, A., Kojima, M., Okada, A., Fukushima, Y., Kurauchi, T., and Kamigaito, O. (1993). Synthesis of nylon 6-clay hybrid. *J Mater Res*, 8(5), 1179-1184.
- Usuki, A., Kojima, M., Kawasumi, M., Okada, A., Fukushima, Y., Kurauchi, T., and Kamigaito, O. (1993). Mechanical properties of nylon 6-clay hybrid. *J Mater Res*, 8(5), 1185-1189.
- Vanin, F. M., Sobral, P. J. A., Menegalli, F. C., Carvalho, R. A., and Habitante, A. M. Q. B. (2005). Effects of plasticizers and their concentrations on thermal and functional properties of gelatin-based films. *Food Hydrocolloid*, 19, 899-907.
- Veiga-Santos, P., Oliveira, L. M., Cereda, M. P., Scamparini, A. R. P. (2007). Sucrose and inverted sugar as plasticizer. Effect on cassava starch-gelatin film mechanical properties, hydrophilicity and water activity, *Food Chem*, 103, 255-262.
- Yi, J. B., Kim, Y. T., Bae, H. J., Whiteside, W. S., and Park, H. J. (2006). Influence of Transglutaminase-Induced Cross-Linking on Properties of Fish Gelatin Films. *J Food Sci*, 71(9), 376-383.

#### **4.6. Figure Captions**

**Figure 4.1.** Flow diagram for preparation of film casting solution.

**Figure 4.2.** Film applicator.

**Figure 4.3.** Viscosity of film solution as a function of clay content and temperature.

**Figure 4.4.** Tensile strength and E% of composite film as a function of clay content.

**Figure 4.5.** Tensile strength and E% of composite film as a function of shear force.

**Figure 4.6.** Tensile strength and E% of composite film as a function of pH.

**Figure 4.7.** Oxygen permeability and water vapor permeability of composite films as a function of clay content.



**Figure 4.8.** Oxygen permeability and water vapor permeability of composite films as a function of shear force.

**Figure 4.9.** Oxygen permeability and water vapor permeability of composite films as a function of pH.

**Figure 4.10.** SAXS diffractograms of the FG/glycerol, Cloisite Na<sup>+</sup>, and nanocomposite films (FG/Cloisite Na<sup>+</sup>/glycerol, and ultrasonified FG/Cloisite Na<sup>+</sup>/glycerol).

**Figure 4.11.** TEM observation of ultrasonified FG/Cloisite NA<sup>+</sup>(9% w/w)/glycerol/H<sub>2</sub>O film.

**Figure 4.12.** TEM observation of ultrasonified FG/Cloisite NA<sup>+</sup>(9% w/w)/glycerol/H<sub>2</sub>O film.

**Figure 4.13.** TEM observation of unultrasonified FG/Cloisite NA<sup>+</sup>(9% w/w)/glycerol/H<sub>2</sub>O film.

**Figure 4.14.** TEM observation of unultrasonified FG/Cloisite NA<sup>+</sup>(9% w/w)/glycerol/H<sub>2</sub>O film.

#### **4.6. Table Captions**

**Table 4.1.** Effect of clay content (0~9%) on color and haze of fish gelatin/Cloisite NA<sup>+</sup>/glycerol/H<sub>2</sub>O films.

**Table 4.2.** Average values of TS, E, OP, and WVP of FG/glycerol/H<sub>2</sub>O, unultrasonified FG/Cloisite NA<sup>+</sup> (5% w/w)/glycerol/H<sub>2</sub>O, and ultrasonified FG/Cloisite NA<sup>+</sup> (5% w/w)/glycerol/H<sub>2</sub>O films.

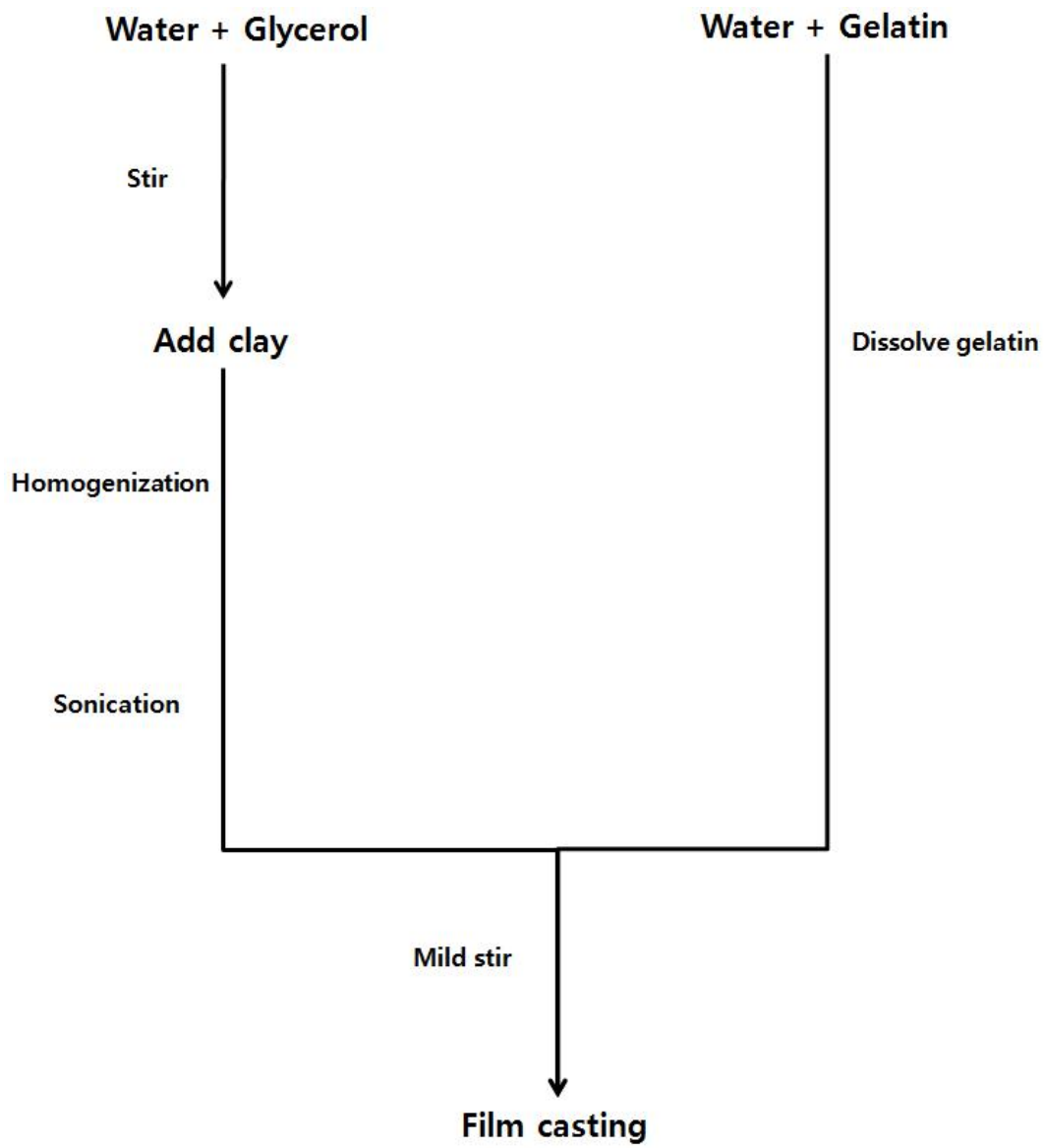


Figure 4.1. Flow diagram for preparation of film casting solution.

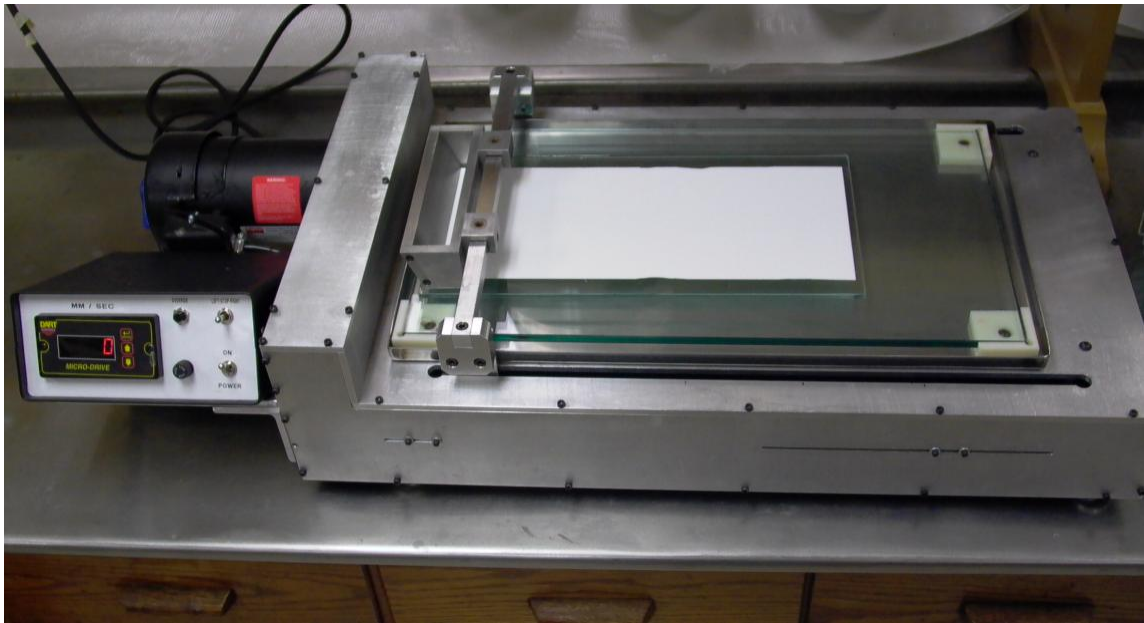


Figure 4.2. Film applicator.

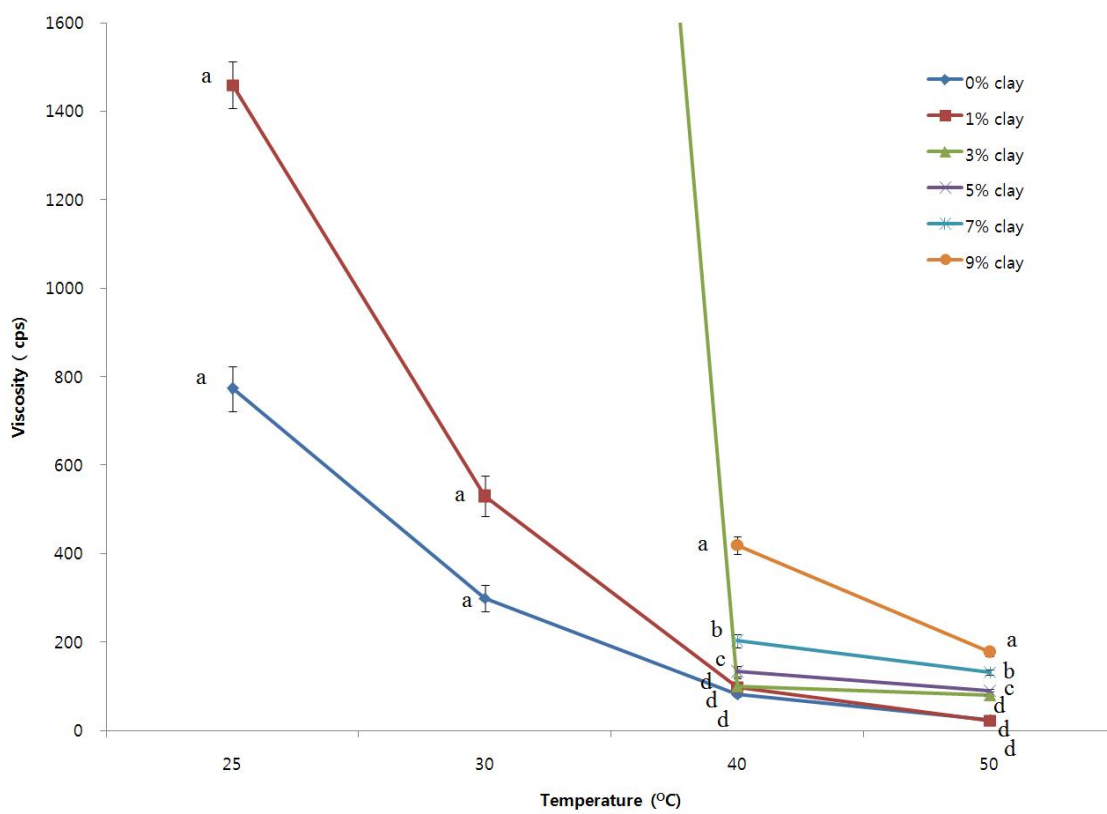


Figure 4.3. Viscosity of film solution as a function of clay content and temperature. Values shown are given as mean±SD from three determinations (n=3).

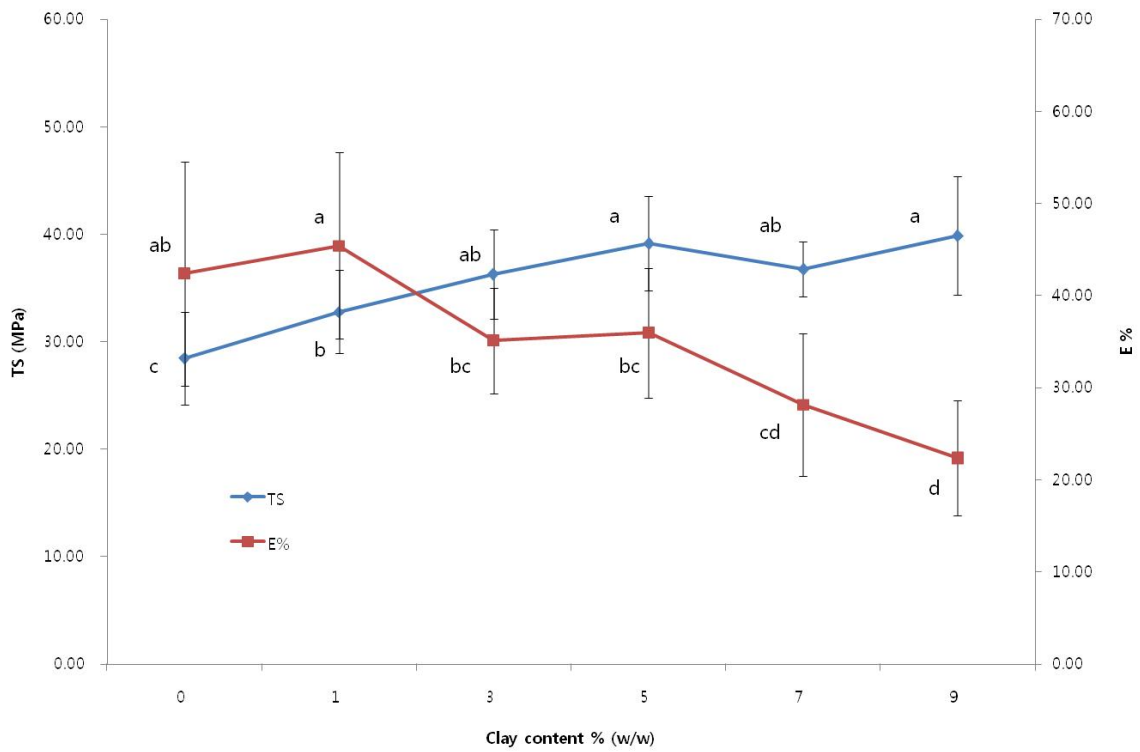


Figure 4.4. Tensile strength and E% of composite film as a function of clay content. Values are given as mean $\pm$ SD from ten determinations (n=10).

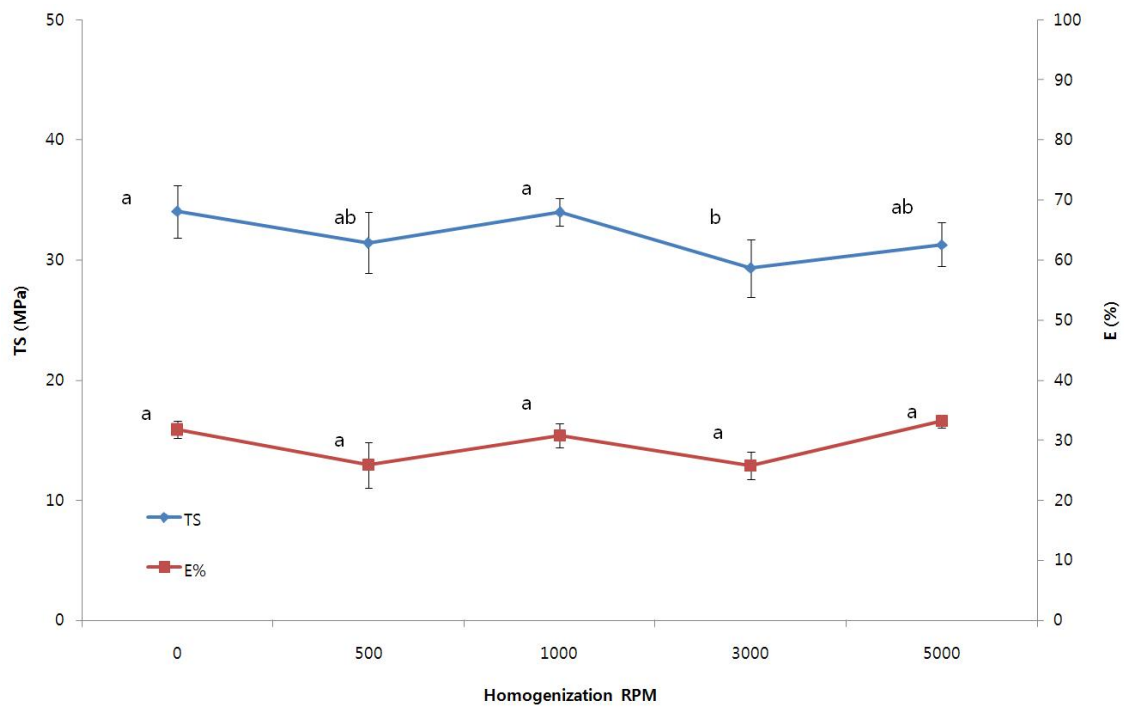


Figure 4.5. Tensile strength and E% of composite film as a function of shear force. Values are given as mean $\pm$ SD from ten determinations (n=10).

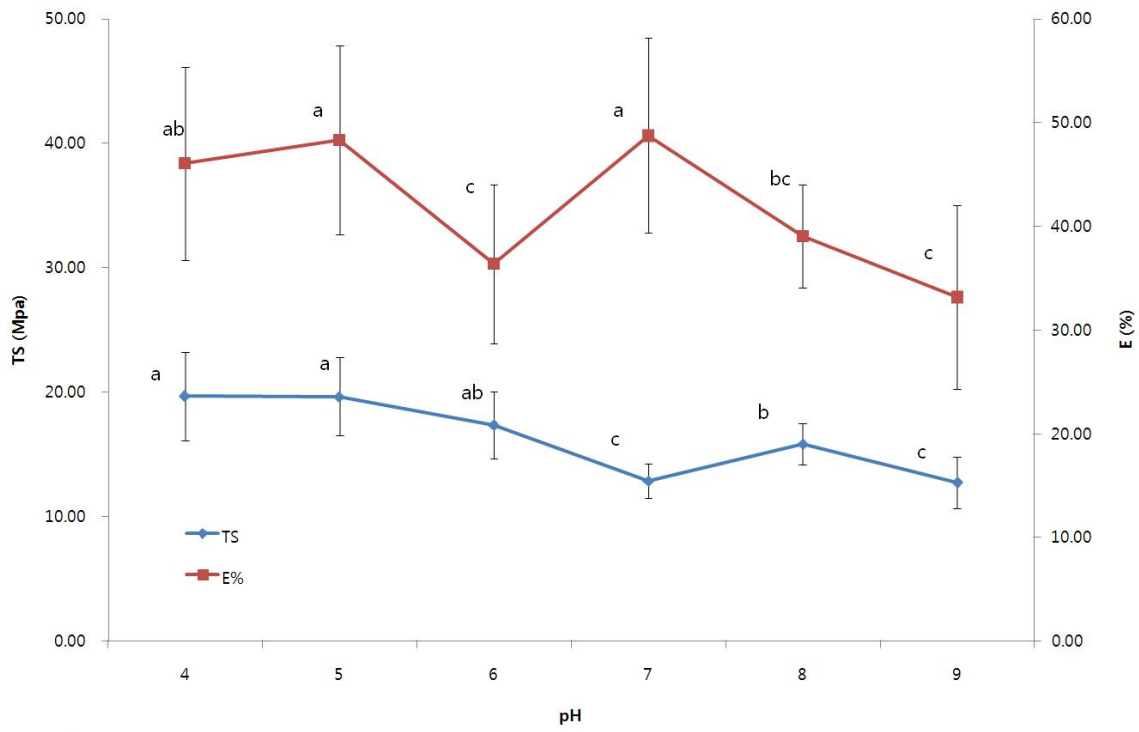


Figure 4.6. Tensile strength and E% of composite film as a function of pH. Values are given as mean±SD from ten determinations (n=10).

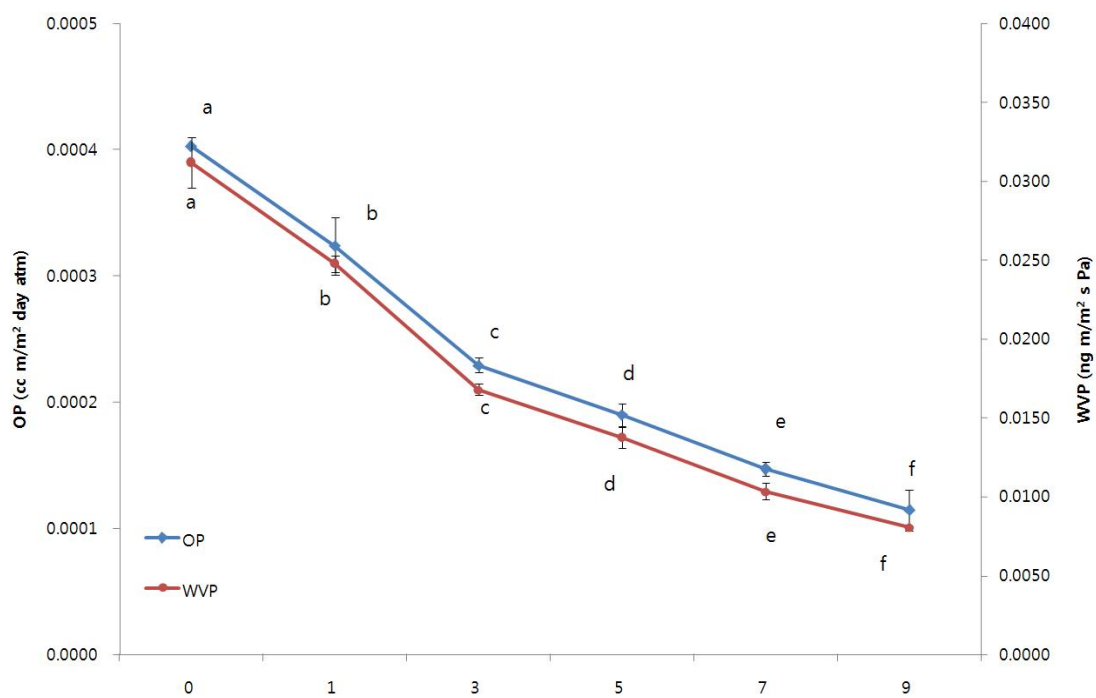


Figure 4.7. Oxygen permeability and water vapor permeability of composite films as a function of clay content. Values are given as mean±SD from three determinations (n=3).



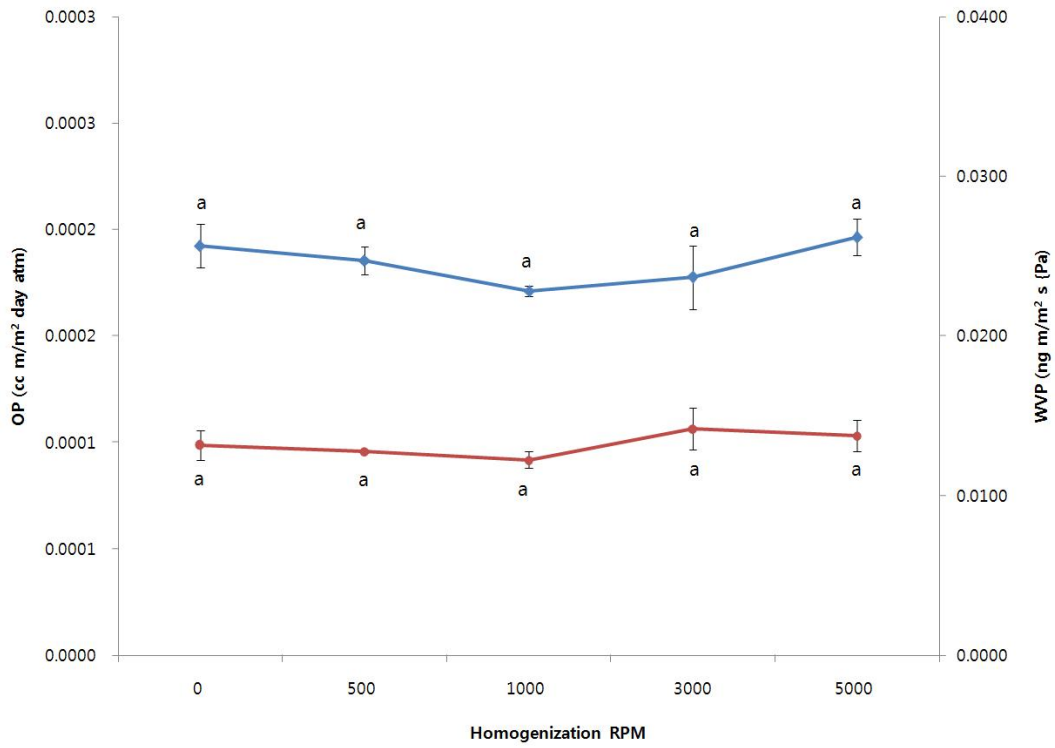


Figure 4.8. Oxygen permeability and water vapor permeability of composite films as a function of shear force. Values are given as mean $\pm$ SD from three determinations (n=3).

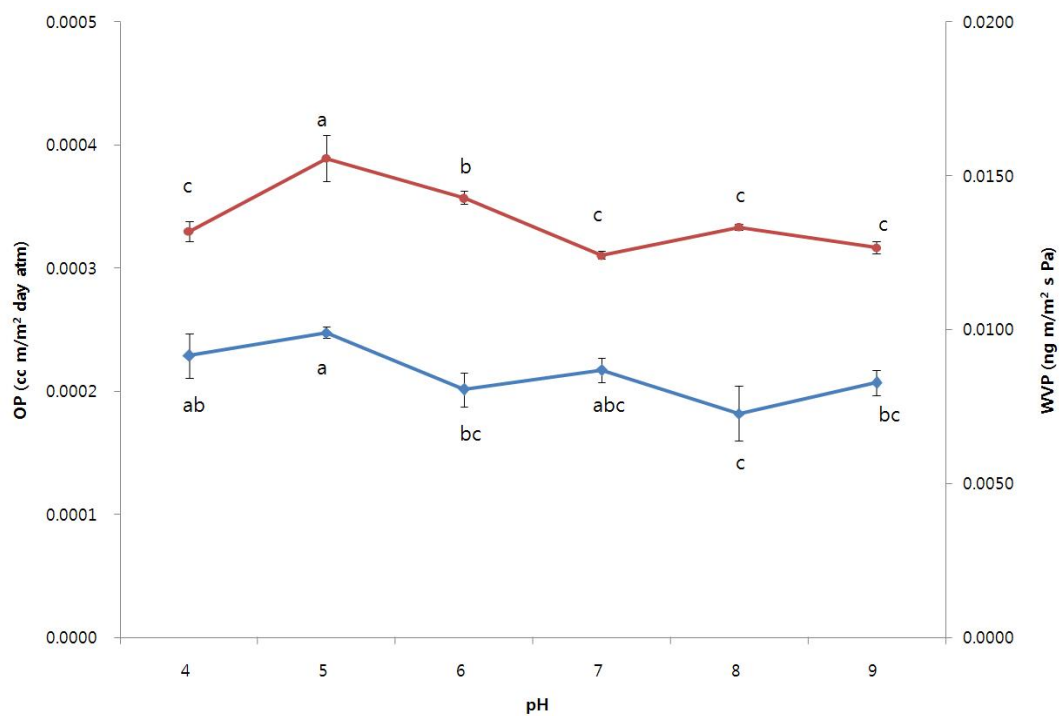


Figure 4.9. Oxygen permeability and water vapor permeability of composite films as a function of pH. Values are given as mean $\pm$ SD from three determinations (n=3).

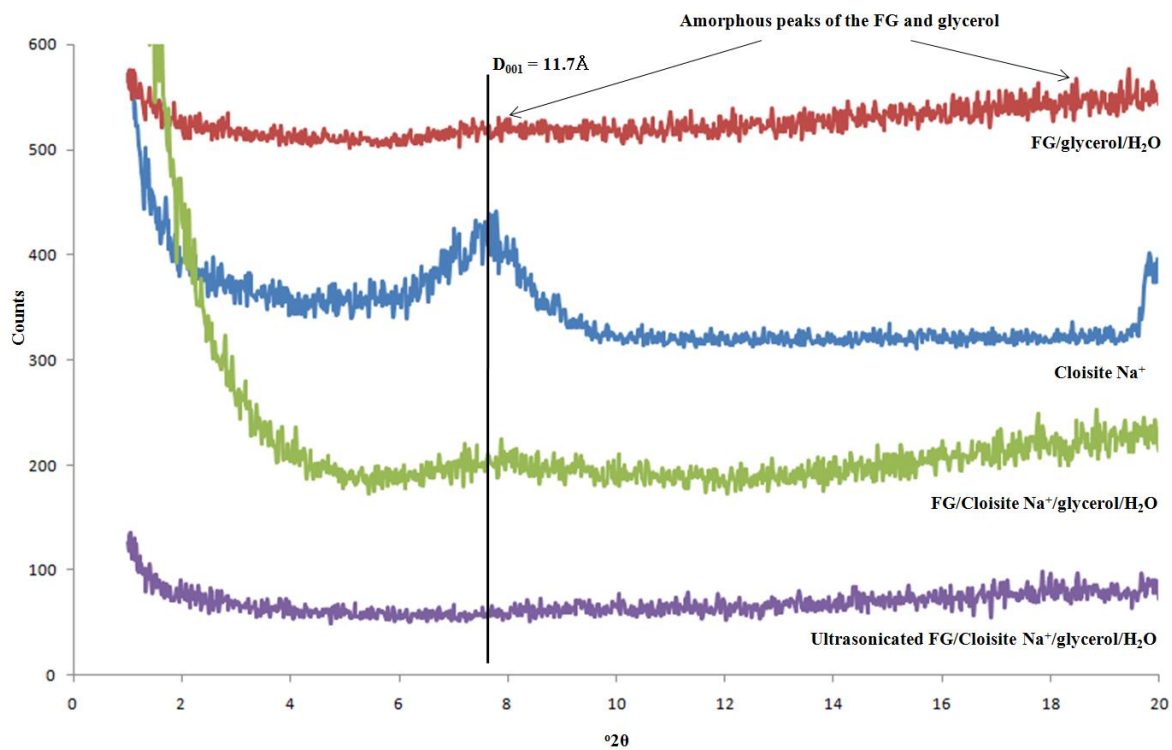
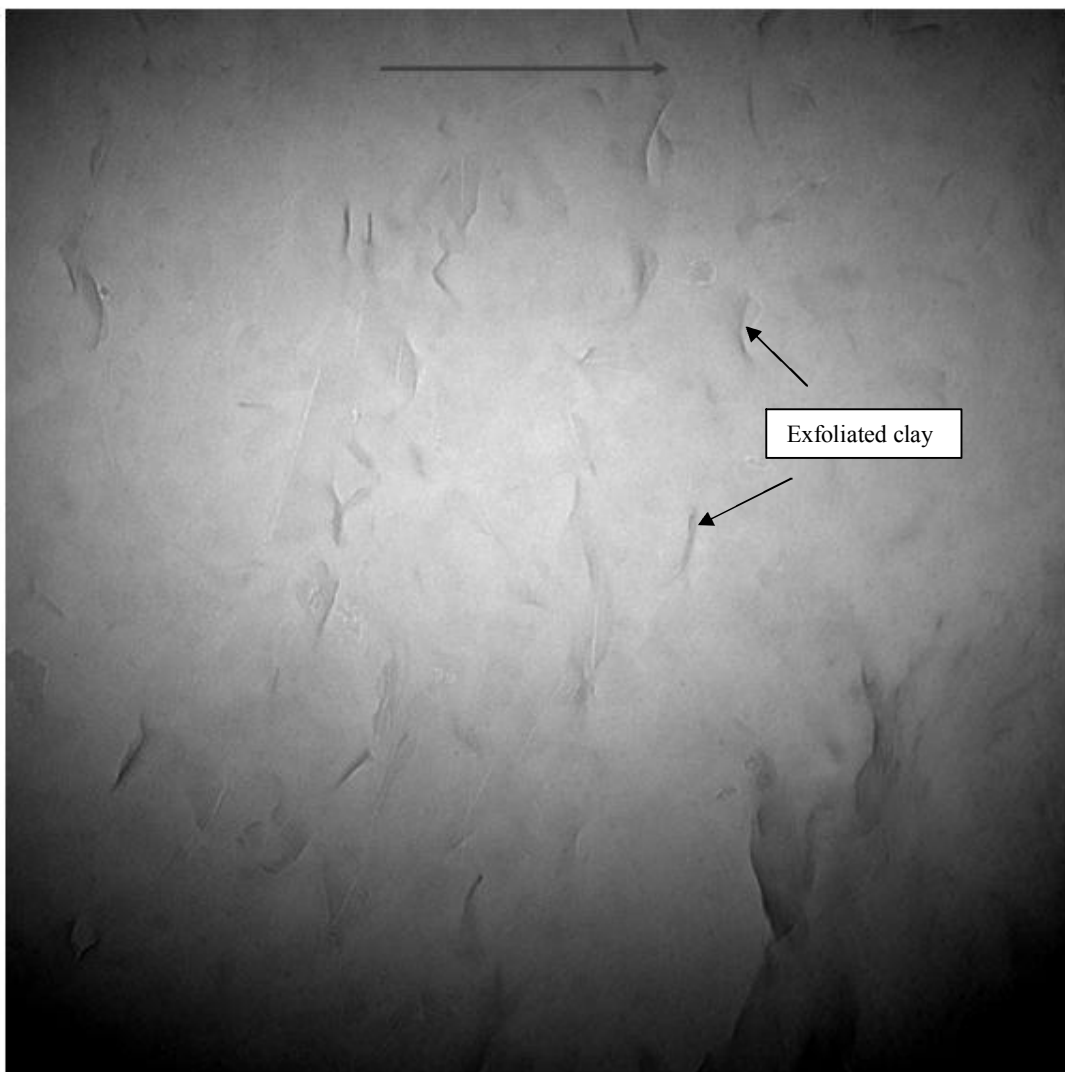


Figure 4.10. SAXS diffractograms of the FG/glycerol, Cloisite Na<sup>+</sup>, and nanocomposite films (FG/Cloisite Na<sup>+</sup>/glycerol, and ultrasonicated FG/Cloisite Na<sup>+</sup>/glycerol).



1-3.tif

1-3

Print Mag: 34400x @ 51 mm

13:52 06/11/07

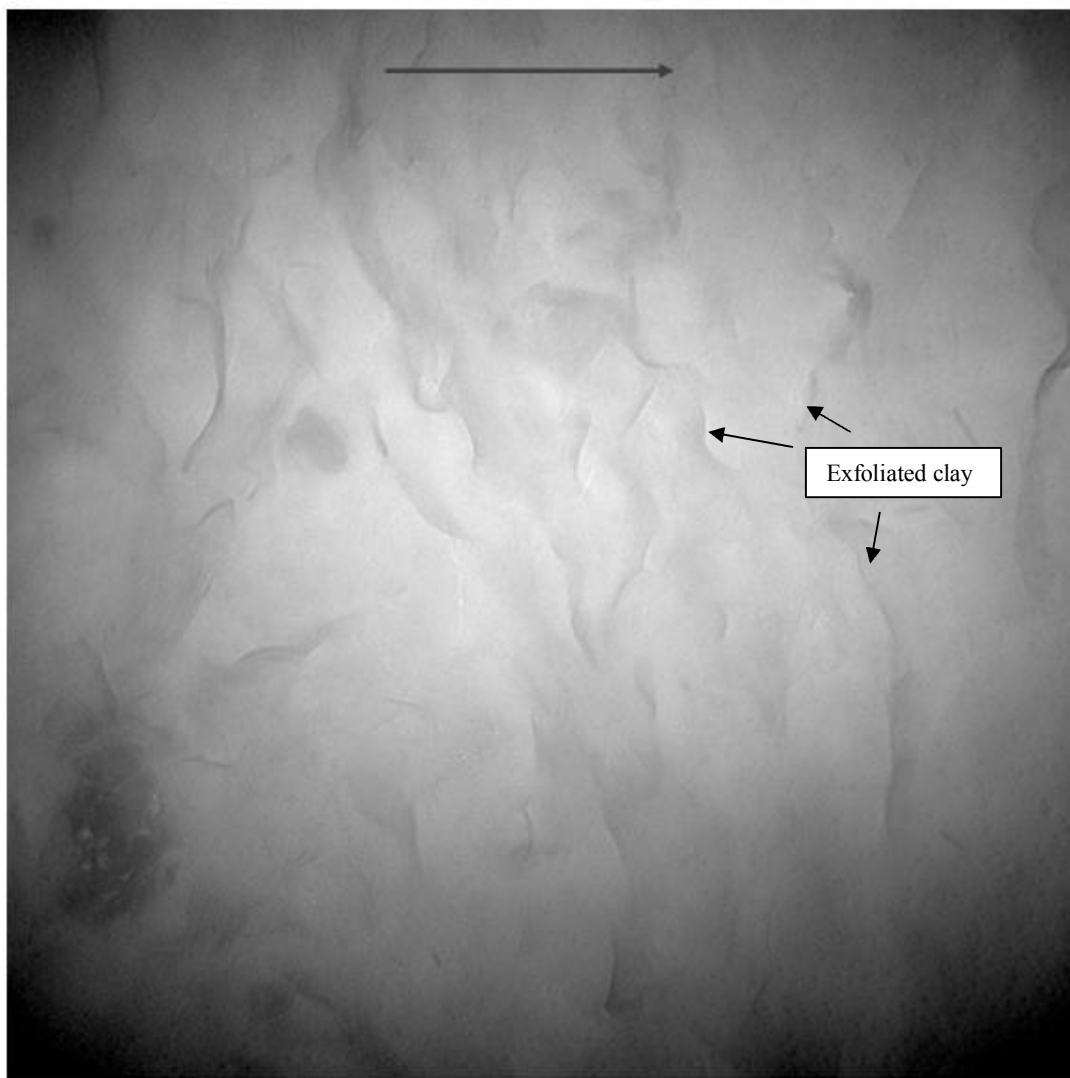
100 nm

HV=120kV

Direct Mag: 100000x

Clemson EM Center

Figure 4.11. TEM observation of ultrasonified FG/Cloisite  $NA^+$  (9% w/w)/glycerol/ $H_2O$  film. The arrow indicates the direction of the film thickness.



1-8.tif

1-8

Print Mag: 34400x @ 51 mm

14:04 06/11/07

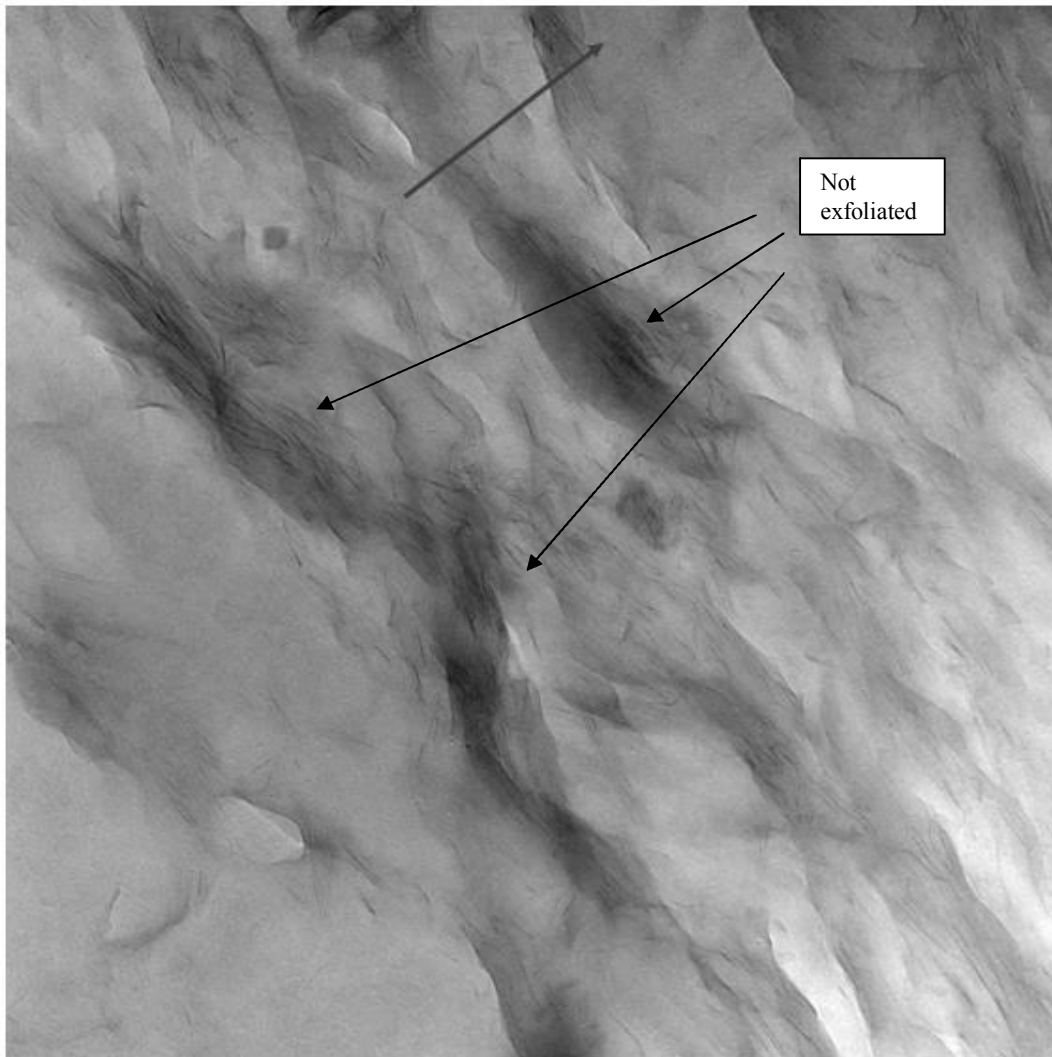
100 nm

HV=120kV

Direct Mag: 100000x

Clemson EM Center

Figure 4.12. TEM observation of ultrasonified FG/Cloisite  $NA^+$  (9% w/w)/glycerol/ $H_2O$  film. The arrow indicates the direction of the film thickness.



3-11.tif

3-11

Print Mag: 34400x @ 51 mm

15:01 06/11/07

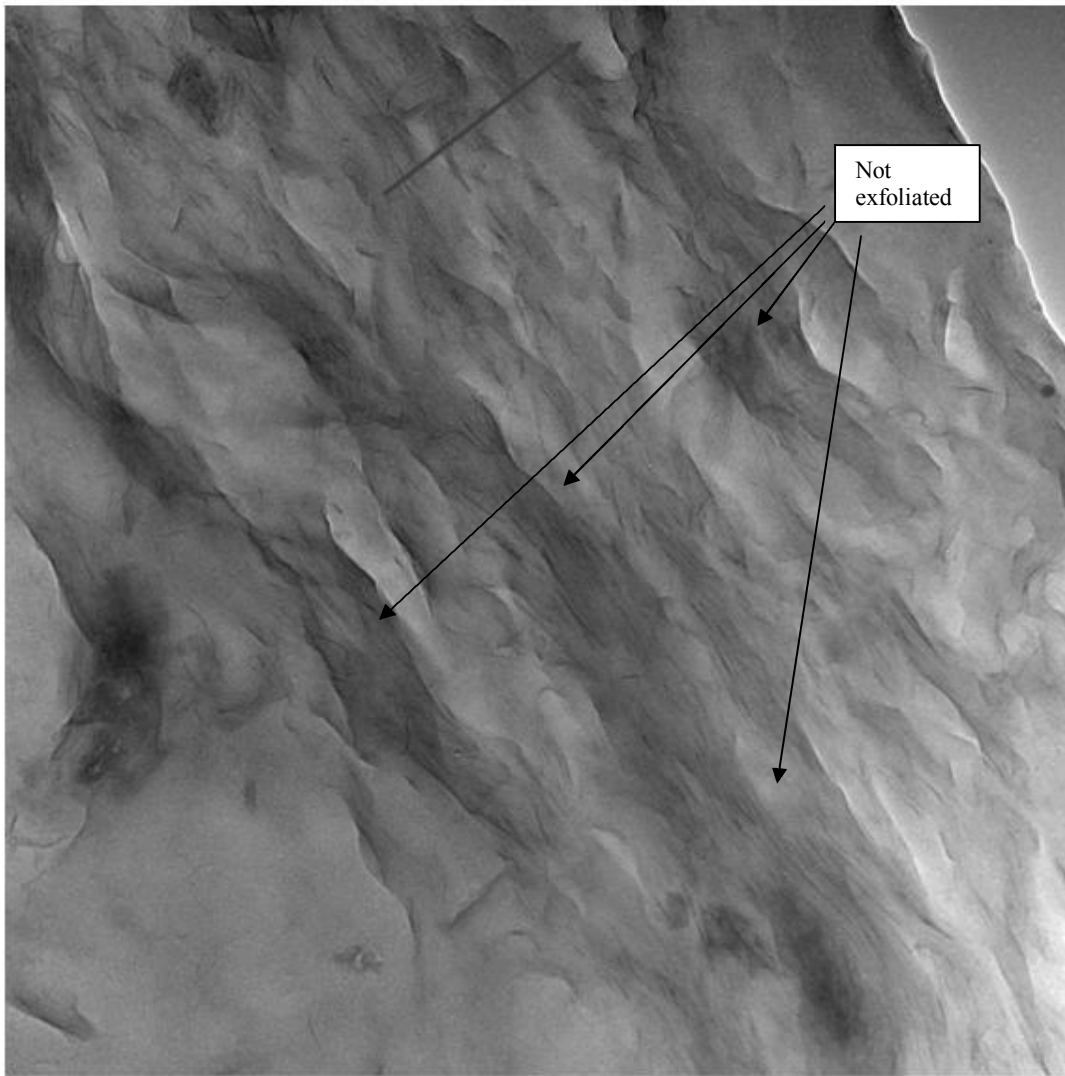
100 nm

HV=120kV

Direct Mag: 100000x

Clemson EM Center

Figure 4.13. TEM observation of unultrasonified FG/Cloisite  $\text{NA}^+$  (9% w/w)/glycerol/ $\text{H}_2\text{O}$  film. The arrow indicates the direction of the film thickness.



3-14.tif

3-14

Print Mag: 34400x @ 51 mm

15:04 06/11/07

100 nm

HV=120kV

Direct Mag: 100000x

Clemson EM Center

Figure 4.14. TEM observation of unultrasonified FG/Cloisite  $\text{NA}^+$  (9% w/w)/glycerol/ $\text{H}_2\text{O}$  film. The arrow indicates the direction of the film thickness.

Table 4.1. Effect of clay content (0~9%) on color and haze of fish gelatin/Cloisite NA<sup>+</sup>/glycerol/H<sub>2</sub>O films. Values are given as mean±SD from three determinations (n=3).

Clay content (%)	Hunter L a b			$\Delta E^D$	Haze <sup>E</sup> (%)
	L <sup>A</sup>	a <sup>B</sup>	b <sup>C</sup>		
0	97.23±0.06 <sup>a,b,c</sup>	0.05±0.01 <sup>a</sup>	-0.14±0.03 <sup>d</sup>	2.13±0.20 <sup>b</sup>	4.53±0.90 <sup>c,d</sup>
1	97.24±0.02 <sup>a,b</sup>	0.06±0.01 <sup>a</sup>	-0.08±0.02 <sup>d</sup>	1.96±0.02 <sup>c,d</sup>	5.87±0.71 <sup>b</sup>
3	97.30±0.02 <sup>a</sup>	0.00±0.01 <sup>b</sup>	0.13±0.01 <sup>c</sup>	1.96±0.03 <sup>c,d</sup>	6.17±0.82 <sup>b</sup>
5	97.01±0.12 <sup>e</sup>	-0.06±0.04 <sup>d</sup>	0.36±0.18 <sup>b</sup>	2.06±0.03 <sup>b,c</sup>	4.11±0.27 <sup>d</sup>
5-no soni	97.15±0.02 <sup>b,c,d</sup>	-0.14±0.01 <sup>e</sup>	1.27±0.04 <sup>a</sup>	2.72±0.02 <sup>a</sup>	7.81±0.12 <sup>a</sup>
7	97.13±0.01 <sup>c,d</sup>	-0.02±0.02 <sup>b,c</sup>	0.32±0.05 <sup>b</sup>	1.82±0.07 <sup>d</sup>	5.20±0.35 <sup>b,c</sup>
9	97.08±0.03 <sup>d,e</sup>	-0.04±0.01 <sup>c,d</sup>	0.44±0.03 <sup>b</sup>	1.82±0.07 <sup>d</sup>	5.78±0.03 <sup>b</sup>

<sup>A</sup> a-e indicate significant differences (P < 0.05) within columns L.

<sup>B</sup> a-e indicate significant differences (P < 0.05) within columns a.

<sup>C</sup> a-d indicate significant differences (P < 0.05) within columns b.

<sup>D</sup> a-d indicate significant differences (P < 0.05) within columns  $\Delta E$ .

<sup>E</sup> a-d indicate significant differences (P < 0.05) within columns Haze.



Table 4.2. Average values of TS, E, OP, and WVP of FG/glycerol/H<sub>2</sub>O, untrasonified FG/Cloisite NA<sup>+</sup> (5% w/w)/glycerol/H<sub>2</sub>O, and ultrasonified FG/Cloisite NA<sup>+</sup> (5% w/w)/glycerol/H<sub>2</sub>O films.

	TS <sup>A,1</sup> (Mpa)	E <sup>B,1</sup> (%)	OP <sup>C,2</sup> (cc·m/m <sup>2</sup> ·day·atm)	WVP <sup>D,2</sup> (ng·m/m <sup>2</sup> ·s·Pa)
FG/glycerol/H <sub>2</sub> O	30.24±2.59 <sup>b</sup>	48.04±4.34 <sup>a</sup>	0.0004028±0.0000007 <sup>a</sup>	0.0312±0.0016 <sup>a</sup>
Non-ultrasonified FG/Cloisite NA <sup>+</sup> /glycerol/H <sub>2</sub> O	37.63±1.82 <sup>a</sup>	36.16±2.25 <sup>b</sup>	0.0002142±0.0000002 <sup>b</sup>	0.0112±0.0005 <sup>b</sup>
Ultrasonified FG/Cloisite NA <sup>+</sup> /glycerol/H <sub>2</sub> O	40.94±3.55 <sup>a</sup>	37.94±3.33 <sup>b</sup>	0.0001899±0.0000091 <sup>c</sup>	0.0137±0.0007 <sup>b</sup>

<sup>A</sup> a-b indicate significant differences (P < 0.05) within columns L.

<sup>B</sup> a-b indicate significant differences (P < 0.05) within columns L.

<sup>C</sup> a-c indicate significant differences (P < 0.05) within columns L.

<sup>D</sup> a-c indicate significant differences (P < 0.05) within columns L.

<sup>1</sup> Values are given as mean±SD from ten determinations (n=10).

<sup>2</sup> Values are given as mean±SD from three determinations (n=3).

CHAPTER FIVE  
EFFECTS OF TRANSGLUTAMINASE INDUCED CROSSLINKING ON  
PROPERTIES OF FISH GELATIN-NANO CLAY COMPOSITE FILM

Ho J. Bae<sup>1</sup>, Duncan. O. Darby<sup>1</sup>, Robert. M. Kimmel<sup>1</sup>,  
and William. S. Whiteside<sup>1</sup>

<sup>1</sup> Department of Packaging Science, Clemson University, Clemson, SC  
29634-0320, USA.

\* To whom all correspondence should be sent:

Dr. William Scott Whiteside, Associate Professor  
Department of Packaging Science,  
Clemson University, Clemson, SC 29634-0370, USA.  
Telephone: +1-864-656-6246, fax: +1-864-656-4395  
e-mail: wwhtsd@clemson.edu

**Abstract**

Nanoclay composite film was produced using warm water fish gelatin as a base material and its physical, mechanical, and molecular weight change properties were observed after treatment with microbial transglutaminase. The viscosity of the MTGase-treated gelatin solution (2% w/w) increased from 86.25±1.77 cp (0 min) to 243±12.37 cp (80 min). SDS-PAGE results showed that the molecular weight of fish gelatin solutions increased after treatment with microbial transglutaminase. The tensile strength decreased from 61.60±1.77 MPa (0 min) to 56.42±2.40 MPa (30 min), while E% increased from

13.94±5.09% (0 min) to 15.78±5.97% (30 min) at 2% (w/w) MTGase concentration. The oxygen permeability and water vapor permeability did not change as a function of treatment time at 2% (w/w) MTGase concentration. The incorporation of nanoclay inhibited increase of oxygen permeability. The color values (L, a, and b) did not change, but haze value increased from 5.24±0.40 (0 min) to 6.44±0.94 (50 min). XRD and TEM results suggested that the nanoclay was exfoliated in fish gelatin film.

Key words: Warm water fish gelatin, nanoclay, film, composite, MTGase

## **5.1. Introduction**

Biodegradable/edible films and coatings from biopolymers have received increasing attention from researches in the past few years. Potential sources of biopolymers have been reviewed by Kester and Fenema (1986), Guilbert (1986), and Gennadios and Weller (1990, 1991). Potential applications of edible films and coatings from biopolymers are to retard transport of gases (O<sub>2</sub>, CO<sub>2</sub>), water vapor, and flavors for fruits and vegetables, confectionaries, frozen foods and meat products. Corn zein and sucrose fatty acid ester coatings have been applied successfully on fresh fruits and vegetables, such as apples, bananas, and tomatoes, as oxygen and water vapor barriers for extending their shelf lives.

Fish gelatin has gained great interest in recent years as the demand for non-bovine and non-porcine gelatin has increased due to religious reasons, social reasons, and the bovine spongiform encephalopathy (BSE) crisis. Production of gelatin from pig skins is

not acceptable for Judaism and Islam and gelatin from beef is acceptable only if it has been prepared according to religious requirements. In contrast, fish gelatin is acceptable for Islam and with minimum restrictions for Judaism. Secondly, fish skin is a major by-product of the fish-processing industry, causing waste and pollution. This byproduct could provide a valuable source of gelatin. However, limited research has been carried out regarding gelatins obtained from different fish species or their behavior in processed foods.

The commercial interests in fish gelatin have been relatively low so far due to sub-optimal physical properties compared to mammalian gelatin. Common problems connected with fish gelatin cold water species, representing the majority of the industrial fisheries, are low gelling and melting temperature and low gel modulus. This makes these gelatins unsuited as mammalian gelatin replacements, especially since they typically gel below 8°C. The differences in the physical properties between mammalian gelatin and from cold water species are due to a lower content of the imino acids proline (Pro) and hydroxyproline (Hyp). Calf skin gelatin contains approximately 94 Hyp and 138 Pro residues per 1000 total amino acid residues, while cod skin gelatin contains approximately 53 and 102 amino acids of Hyp and Pro, respectively, per 1000 total residues. Gelatins from warm water fish species, like fish gelatin from tilapia, contains around 70 and 119 residues of Hyp and Pro, respectively, per 1000 total residues. These gelatins have physical properties more similar to those of mammalian gelatins.

In order to improve mechanical properties and water resistance, many research efforts have been carried out, but physical, thermal, and mechanical properties of fish

gelatins are still not satisfactory, so there are difficulties in many applications. Moreover, in the quest to reduce the amount of material in packages, it is of interest to increase the barrier properties and mechanical strength of the packaging film. In order to obtain packaging films with high mechanical strength and high barrier properties, gelatin films have been filled with layered silicates.

Researchers have investigated various approaches to modify fish gelatin in an effort to improve its functionality. The blending of fish gelatin with other biopolymers, such as  $\kappa$ -carrageenan, chitosan, and pectin, is one possible way to improve the properties of fish gelatin (Chen and others 2003; Uresti and others 2003; Haug and others 2004a). Furthermore, the addition of plasticizers, such as glycerol, sorbitol, sucrose, polyethylene glycol (Tanaka and others 2001; Vanin and others 2005), and salt agents (Fernandez-Diaz and others 2001; Ramirez and others 2002; Haug and others 2004) can improve the mechanical properties of fish gelatin films or gels. The addition of chemical cross-linking agents, such as glutaraldehyde, formaldehyde and glyoxal (Bigi and others 2001; de Carvalho and Grosso 2004) or enzymes, such as microbial transglutaminase, have also been shown to improve the properties of fish gelatin. The chemical cross-linkers are toxic, which limits their use in food systems (Tseng 1990). Therefore, the use of enzymes as a cross-linking agent could be a better alternative for use in food packaging.

Microbial transglutaminases catalyze the displacement of the amide ammonia at the  $\gamma$ -position in glutamine residues by replacing it with another amine, usually a  $\epsilon$ -amino group from a suitable lysine residue. The formation of  $\epsilon$ -( $\gamma$ -glutamyl)lysine isopeptide bonds results in the incorporation of inter- or intramolecular covalent cross-

links into food proteins, leading to improving the physical and textural properties of many food proteins, such as tofu, boiled fish paste, and sausage (Seguro and others 1995; Soeda and others 1995; Nonaka and others 1996; Ni and others 1998; Sharma and others 2002; Shimba and others 2002; Benjakul and others 2004).

In the previous study, fish gelatin has been reinforced with Na-montmorillonite. This has successfully achieved increased mechanical and barrier properties.

The objective of this study was to further increase the mechanical properties of fish gelatin / Na-montmorillonite nanocomposite film by further treating the film solution with MTGase since MTGase have been shown to cross-link gelatin and increase the degree of cross-linking in polymer matrices, enhancing the mechanical properties of polymer molecules.

## **5.2. Experimental Materials and Methods**

### **5.2.1. Materials**

The following raw materials were used to develop gelatin-clay composite films: Gelatin 200 bloom-fish-8 mesh (Vyse Gelatin Company, Illinois, USA); Cloisite® NA<sup>+</sup> (Southern Clay Products, Texas, USA); d-Sorbitol (Sigma, St. Louis, Mo., USA); Activa TG-TI (Ajinomoto Food Ingredients LLC, Chicago, Ill, USA); Commasie Staining Solution (Sigma); Brilliant Blue (Sigma); 7.5% Tris Acetate SDS-PAGE prepared gel (BIORAD).

### 5.2.2. Solution Preparation

The film solution preparation and development procedure is reported in Figure 1. Nanoclay solutions were prepared by first dissolving 8 g of sorbitol in 100 mL of 50°C degassed, distilled, and deionized water and stirred for 30 min at 50±5°C. The concentration of sorbitol was 0.2 g sorbitol/g gelatin. Then 2 g (5% w/w) of clay was added and stirred by magnetic stirrer for 30 min at 50±5°C. The solution was then sonified using Branson sonifier (Model S-450D) to aid intercalation and exfoliation of the clay and plasticizers. A standard 1/2 in diameter tapped flat horn tip was used at approximately 40% output for 30 min. The gelatin solution was prepared separately. Forty grams of biopolymer was dissolved in 100 mL of 60 °C degassed, distilled, and deionized water and stirred for 2 hr at 60±5°C. The solution was cooled to 50 °C to provide favorable conditions for the enzyme reaction. MTGase powder (800 mg) was dissolved into 5 mL of deionized water and was well mixed using Touch Mixer (Fisherbrand, USA) until all powder was in solution. The MTGase solution was then added into the gelatin solution. The enzyme activity was 100 units of enzyme activity per gram of powdered preparation, and consisted of 99% maltodextrin and 1% transglutaminase. MTGase was used without further purification. Deactivation of MTGase was accomplished by heating the enzyme-treated fish gelatin solution at 100 °C for 15 min (Kutemeyer and others, 2005). After the deactivation, the clay solution was added to gelatin solution by droplets and gently stirred for 24 hr at 35±5 °C before casting.

### 5.2.3. Film Casting

Approximately 35 mL of the prepared film solution was cast onto a BYTAC<sup>®</sup> (Norton Performance Plastics Corporation, Wayne, NJ, USA) coated 8" x 16" glass plate which was formed utilizing a custom designed film applicator. After drying, films were peeled off from the glass plates and cut into test specimens. The test specimens were immediately placed into a constant temperature and humidity chamber (25°C, 50% RH) and held for 48 hr prior to testing.

### 5.2.4. Film Thickness

Film thickness was measured with a Digimicro MFC105 micrometer (Nikon, Japan). Measurements for testing mechanical properties were taken at five different locations on the film samples for each test. For testing oxygen and water barrier properties, measurements were made at nine different locations. The mean thickness was used to calculate the mechanical and barrier properties of film.

### 5.2.5. Viscosity

The viscosity of film casting solution was measured by dial reading viscometer (LVT, Brookfield, Mass., USA) at 50 °C. The spindle type used was LV-2C at speed 6, and the amount of the sample used was 500 mL.



### 5.2.6. Color

Hunter L, a, and b values of films were measured by using ColorQuest II Spectrophotometer with Universal Software version 3.73 (Hunter Associates Laboratory, Inc., Reston, VA, USA). The machine was calibrated using a white standard plate (standard no. C6006) and a gray standard plate (standard no. C6006-G). The film specimen was placed on white standard plate (standard no. C6006) having color value of L = 94.62, a = -0.91 and b = 0.64 and mounted at the reflectance port. Color values were measured at three random positions including the center of the film specimen. The L a axis runs from top to bottom. The maximum for L is 100, which would be a perfect reflecting diffuser. The minimum for L would be zero, which would be black. The a and b axes have no specific numerical limits. Positive a is red. Negative a is green. Positive b is yellow. Negative b is blue (HunterLab Applications Note, 1996). Total color difference (E) was calculated by substituting acquired Hunter L, a, and b values into the equation below. The  $\Delta E$  is a single value that takes into account the differences between L, a, and b of the sample and standard (HunterLab Applications Note, 1996).

$$\Delta E = [(L_{\text{film}} - L_{\text{standard}})^2 + (a_{\text{film}} - a_{\text{standard}})^2 + (b_{\text{film}} - b_{\text{standard}})^2]^{0.5} \quad (1)$$

### 5.2.7. Haze

The haze of films was determined using ColorQuest II Spectrophotometer with Universal Software Version 3.73 (Hunter Associates Laboratory, Inc., Reston, VA, USA). The haze measurement was made in transmission mode and calculated using following equation. The white plate (Standard No. C6006, X = 81.77, Y = 86.72, Z =

92.18) provided by the manufacturer was used for calibration and background. The values were expressed by

$$\text{Haze} = \frac{Y \text{ Diffuse transmission}}{Y \text{ Total transmission}} \times 100 \quad (2)$$

#### 5.2.8. Measurement of Mechanical Properties

Tensile strength (TS) and elongation at break (EB) were determined for each film with an Instron Universal Testing Machine (Model 4201, Instron Corp., Canton, MA, U.S.A.). Forty specimen samples, 10 cm x 2.54 cm, were cut from film samples prepared as described above. Samples were conditioned for 48 hr at 25°C and 50% relative humidity (RH) in a constant temperature and humidity chamber before the measurement. Initial grip separation and cross-head speed were set at 5 cm and 25 mm/min, respectively. TS was calculated by dividing the maximum load by the cross-sectional area of the film, and E was calculated and expressed as percentage of change of the original length of a specimen between grips (5 cm) according to the ASTM standard method D882-88 (ASTM 1989).

#### 5.2.9. Oxygen Permeability

Oxygen permeability was measured at 23±1 °C and RH condition of 50% and done in triplicate to get the average mean value. The oxygen transmission rate was determined in an OX-TRAN 2/20 (Mocon, Inc., Minneapolis, MN, USA). The samples were equilibrated at 50±1% relative humidity (23±1 °C) for a period of 48 hr before

analysis. The gas flow rate was fixed at 10 mL/min and the difference in pressure across the film corresponded to atmospheric pressure (101.3 kPa). Oxygen permeability ( $\text{cc}\cdot\text{m}/\text{m}^2\cdot\text{day}\cdot\text{atm}$ ) was calculated by multiplying the oxygen transmission rate by the film thickness.

#### 5.2.10. Water Vapor Permeability (WVP)

Cup method (ASTM standard method E96-80, 1987), was used to determine water vapor permeability (WVP) in a constant temperature and humidity chamber at 25°C and 50% RH. The WVP values were corrected using the WVP Correction Method (Mchugh, Avena-Bustillos, & Krochta, 1993). Poly methyl methacrylate cups (Piedmont Plastics, Inc., Greenville, S.C., U.S.A.) sealed with O-rings were filled with water. Film samples (7cm x 7cm) were mounted over the cups. Weight loss from the cup was measured as a function of time for 12h.

#### 5.2.11. Small angle x-ray diffraction (SAXS)

SAXS studies of the samples were carried out using a Scintag XDS 2000 (Scintag Inc., USA) with a germanium detector equipped with Scintag DMSNT Version 1.37 software. In order to monitor the  $d_{-001}$  spacing corresponding to the interlayer spacing of the clay, the samples were scanned from the start angle of 1° and stop angle of 20° at step size 0.02 and preset time 0.7 sec.

#### 5.2.12. Transmission Electron Microscopy (TEM)

For TEM observation, 70-90 nm sections of the samples were microtomed at room temperature using an Ultracut E microtome at a cutting speed of 0.05 mm/s. The sections were cut perpendicular to the casting direction of the casted film. The observations were made using transmission electron microscopy (H-7600T, HITACHI, Japan) at 120 kV with magnifications from 20,000 to 300,000 times to study dispersions of clay particles..

#### 5.2.14. Sodium dodecyl sulfate polyacrylamide gel electrophoresis (SDS-PAGE)

Fish gelatin solutions were mixed with 2% SDS-containing buffer and reduced with dithiothreitol (Invitrogen Life Technologies) in a 70 °C water bath for 10 min. Electrophoresis (SDS-PAGE) was then performed by adding 2 ug fish gelatin sample in each lane of 7.5% NUPAGE® Tris-Acetate gel with Tris-Acetate SDS running buffer in an ZCell Surelock™ electrophoresis unit (Invitrogen Life Technologies). As a reference marker set, 37 kDa, 50 kDa, 75 kDa, 100 kDa, 150 kDa, and 250 kDa proteins were employed. After this step, the resulting gel was mixed and incubated for 1 h with coomassie staining solution containing brilliant blue, methanol, glacial acetic acid, and distilled water. The gel was then washed with destaining solution containing the same solutions as the staining solution except for the brilliant blue.

### 5.2.15. Statistical Analysis

Measurements were replicated three times for each film, with individually prepared films as the replicated experimental units. Statistics on a completely randomized design were performed with the analysis of variance (ANOVA) procedure in SAS (Release 9.1, SAS Institute Inc., Cary, NC) software. Duncan's Multiple Range Test ( $p < 0.05$ ) was used to detect differences among film property mean values.

## 5.3. Results and Discussion

### 5.3.1. Viscosity

Viscosity values of fish gelatin solutions having different MTGase concentration (0, deactivated, 1, 2, 3% w/w) according to reaction time (0 ~ 100 min) is shown in Figure 2. The viscosity was measured at 20% (w/w) concentration at 50 °C, and at pH 6. According to the manufacturer's specification sheet, the optimum enzyme activity temperature of MTGase is at 50°C and the optimum pH is from 6 to 7. The stability of the enzyme at 50°C is about 90%. The temperature and pH values chosen were based on maximizing the amount of MTGase activity and stability. The viscosity of the solution increased significantly ( $P < 0.05$ ) as both the concentration of MTGase and the reaction time increased, respectively. Rapid gelatinization of the fish gelatin solution was observed within 30 min for samples with greater than 2% (w/w) MTGase. No viscosity change was observed for FG only and deactivated MTGase sample in the function of time. However, there was a significant increase in viscosity for solutions containing 2%

and 3% MTGase concentration after 30 min reaction time. The observed viscosity of solution containing 1% MTGase concentration did increase, but not as significant as higher MTGase concentration.

It has been reported that the treatment of MTGase increased gelatin viscosity from 1 to 100 Pa·s (McDermott and others, 2004) and the viscosity of Type A gelatins from porcine increased after the addition of MTGase. Moreover, gelatin prepared by acid treatment (Type A) was more susceptible to introducing the cross-linking into gelatin matrix than base treatment type (Type B) because base treatment hydrolyzes the amide groups of glutamine residues and suppresses enzymatic cross-linking.

In addition to MTGase, chemical cross-linking agents such as glutaraldehyde, formaldehyde, and glyoxal are used to modify the gelatin structure. These agents have the same effect of reducing the amine contents of gelatin molecules. De Carvalho and Grosso (2004) reported that these chemical cross-linking agents showed similar efficiency with MTGase based on the degree of cross-linking.

### 5.3.2. Color

The MTGase reaction changes the crystallinity or molecular structure of the gelatin matrix, leading to a different response to light (Yi, Kim, Bae, Whiteside, & Park, 2006). Uresti and others (2003) reported that color values were affected by the concentration (0~0.3%) of MTGase in fish gel consisting of fish gelatin and pectin. They reported that the L and b value decreased (from  $80.9 \pm 5.6$  to  $53.3 \pm 1.4$  and from  $12.0 \pm 1.1$

to  $9.1\pm 0.5$ ) as the MTGase concentration increased and the a value increased (from  $-2.91\pm 0.2$  to  $-1.2\pm 0.1$ ) with the increase of MTGase concentration.

However, in this study, the color values of MTGase treated fish gelatin/Cloisite  $\text{Na}^+$ /sorbitol/ $\text{H}_2\text{O}$  films are shown in Table 1. The hunter L (brightness) and a (red/green) values were not affected by an increase in MTGase reaction time. The b value did not differ significantly according to MTGase treatment time. This can be explained by the addition of nanoclay in this experiment. It is possible that the effect of the nanoclay “masked” the effect of MTGase on color properties of the fish gelatin film. From the previous study (Bae, Byun, Hong, Darby, Kimmel, & Whiteside, 2007), the color value of ultrasonified fish gelatin/Cloisite  $\text{Na}^+$  (5% w/w)/glycerol/ $\text{H}_2\text{O}$  were  $97.01\pm 0.12$  (L),  $-0.06\pm 0.04$  (a), and  $0.36\pm 0.18$  and the color value of unultrasonified fish gelatin/Cloisite  $\text{Na}^+$  (5% w/w)/glycerol/ $\text{H}_2\text{O}$  were  $97.15\pm 0.02$  (L),  $-0.14\pm 0.01$  (a), and  $1.27\pm 0.04$ , respectively.

Garcia and Sobral (2005) found that the difference of color in the fish gelatin films derived from tilapia was affected by the gelatin concentration. Moreover, they found that the color of films was affected more by the protein concentration and the amount of plasticizer than by the thermal treatments. They suggested that their results could be related to the concentration of amino acid, which can react with glycerol and produce darkening.

### 5.3.3. Haze

The haze value of fish gelatin composite films are depicted in table 1. The haze value of the MTGase treated films increased as the reaction time increased, and this is most likely due to the cross-linking induced by MTGase. The haze value increases as a function of MTGase treatment time from  $5.41 \pm 0.42$  (0 min) to  $6.44 \pm 0.94$  (50 min).

Zhu and others (2007) reported that islands of crystal domains in the amorphous region did not contribute to higher haze value, but LDPE films with significantly higher molecular weight species (indicating a large population of large, highly long-chain branched LDPE molecules) showed significantly higher haze values.

#### 5.3.4. Mechanical Properties

It is known that the increased degree of cross-linking in polymer matrices enhances the rigidity of polymer molecules and also increases the molecular weight. This leads to an increase in the tensile strength of films and a reduction in the percent elongation due to the depression of molecular mobility.

Bigi and others (1998, 2001, 2004) reported that the use of cross-linking improved the mechanical properties of gelatin and they suggested the application of medical films such as connective tissue, arterial wall, and artificial skin.

Mariniello and others (2003) reported mechanical property improvement of MTGase treated pectin and soy flour mixture film. They reported increase of tensile strength from  $6.8 \pm 0.92$  MPa to  $12.4 \pm 1.05$  MPa and decrease of elongation from  $11.61 \pm 1.09\%$  to  $7.2 \pm 1.03\%$  after the MTGase treatment.



De Carvalho and Grosso (2004) reported minor effect of MTGase on gelatin films, but reported significant effect of chemical cross-linking agents on tensile strength of gelatin films. The chemical cross-linking agents increased tensile strength from  $15.12 \pm 0.75$  MPa to  $23.10 \pm 1.31$  MPa, and decreased the total amine contents of gelatin solution due to the cross-linking reaction.

In this study, tensile strength (figure 3) decreased from  $61.30 \pm 1.90$  MPa to  $57.36 \pm 4.97$  MPa and elongation % was not significantly different as the reaction time with MTGase increased from 0 to 50 min (Figure. 3). These results implied that the film became less stiff and rigid.

Ensminger and Gieseking (1939, 1941) pioneered the systematic investigation into the reactions of clays with proteins. They prepared complexes of montmorillonite with gelatin and examination of the dry complexes using X-ray diffractometry showed that interlayer uptake had appeared and the extent of intercalation increased with a fall in suspension pH (from 7 to 2.7). Since drop of pH would have increased the net positive charge in the protein, they inferred that complex formation primarily involved an exchange between the cationic ( $-\text{NH}_3^+$ ) groups on the amino acid side chains of the protein and the  $\text{Na}^+$  ions occupying exchange sites at the montmorillonite surface. Furthermore, prior treatment of the protein with nitrous acid, formaldehyde, or lignin, all of which would have deactivated the amino groups on the molecule, resulted in a marked decrease in the extent of intercalation.

Since MTGase has the same effect of reducing the amine contents of gelatin molecules as the chemical cross-linking agents mentioned above, it can be inferred that

treatment of the gelatin with MTGase prior to mixing the Cloisite NA<sup>+</sup> solution deactivated the amino group. This would therefore result in decreased interacting groups between protein molecules and the Cloisite NA<sup>+</sup>, which again would result in decreased rigidity and extensibility as the function of MTGase treatment time (0 to 50 min).

Another point of view that can explain the decrease of TS and E% with MTGase treatment time is that its treatment temperature was 50 °C, which is above the helix formation temperature. The cross-linking would take place in the unwound gelatin molecule randomly, and this would hinder the formation of helix structure and resulted in marked decrease of intercalation. Moreover, the increase of molecular weight also would impart steric hindrance to intercalation, which would then result in marked decrease of intercalation.

Theng (1979) reported that among many proteins, notably gelatin and pepsin have ability to unfold when they adsorb at the interlayer surface of montmorillonite and explained that the gelatins which have fibrous properties would tend to adsorb side-on, that is, with its shorter axis perpendicular to the silicate layer. Moreover, this leads to the establishment of maximum contact with the surface, inducing the molecule to unfold and stretch.

#### 5.3.5. Oxygen permeability (OP) and water vapor permeability (WVP)

A motivating factor in developing nanocomposite fish gelatin films is to improve barrier properties. Due to this, the permeability of oxygen and water in fish gelatin composite films was tested. Comparing OP and WVP of the fish gelatin/nanoclay

composites (Figure 4), all the composite films showed lower OP and WVP than that of fish gelatin only films due to barrier properties of the clay. This improvement of oxygen and water vapor barrier properties can be attributed to the better-ordered intercalated structure of the composite film that contained high aspect ratio nano-layers of clay in the film.

The chemical nature of macromolecules, crystallinity, molecular mass, orientation, and the degree of cross-linking typically affects the permeability of films (DeCarvalho & Grosso, 2004). Permeability is also dependent on membrane porosity, the surface absorption and desorption behavior of the permeant, relative humidity, and the amount of plasticizer used (Park, 1991; Kim, 2005). The treatment of MTGase did not affect OP and WVP significantly. The OP and WVP did not increase or decrease as the MTGase treatment time increased. Previous studies reported increases in OP (Yi, Kim, Bae, Whiteside, & Park, 2006) and suggested that new intra- and intermolecular covalent bonds introduced by MTGase hindered the formation of collagen helix structure (Babin & Dickinson, 2001). This resulted in an increase in the free volume of polymer matrix leading to an increase in the oxygen permeability of the films. However, OP in this study should be considered in the view of exfoliation of the nanoclay and thus the more tortuous path that oxygen molecules must travel. It has been observed from the XRD diffractogram and TEM results that added nanoclay in gelatin polymer matrix was exfoliated.

#### 5.3.7. Small angle x-ray diffraction (SAXS)

The assessment of the dispersion of the clays in the fish gelatin-nanoclay composite films was done using XRD (Figure. 5). This allowed monitoring of the  $d_{-001}$  spacing according to the interlayer spacing of the clay and enabled observation of whether the clay was intercalated or exfoliated. The observed  $d_{-001}$  for neat Cloisite  $\text{NA}^+$  was  $11.7\text{\AA}$  as was indicated by the manufacturer. From the diffractogram of the ultrasonified FG/Cloisite  $\text{NA}^+$ /sorbitol/ $\text{H}_2\text{O}$ , a broad series of peaks (from interlayer spacings from about  $10\text{\AA}$  to  $60\text{\AA}$ ) was not observed. It can be suggested from the data that the added nanoclay was exfoliated. Dean and Yu (2005) reported similar diffractogram for ultrasonified soy protein/Cloisite  $\text{NA}^+$  composite film which had been plasticized by glycerol. They reported a broad band from  $10\text{\AA}$  to  $60\text{\AA}$  for unultrasonicated sample and disappearance of this broad band for ultrasonicated sample. Rao (2007) reported that in the exfoliated state, the diffraction from the clay interlayer spacing disappears, and it is believed that the two clay platelets are at least  $70\text{\AA}$  apart.

#### 5.3.8. Transmission Electron Microscopy (TEM)

The TEM images of the FG/sorbitol/Cloisite  $\text{NA}^+$ / $\text{H}_2\text{O}$  composite films are shown in Figure 6 ~ Figure 11. Along with SAXS, TEM is one of the main tools used for determination of the dispersion of the clay.

The acquired TEM image correlated well with the SAXS result. The TEM images of the 0 min and 50 min MTGase treated FG/sorbitol/Cloisite  $\text{NA}^+$ / $\text{H}_2\text{O}$  films are shown

in Figure. 6~Figure. 11. As can be seen in the Figures, large agglomerates are clearly visible along with tactoids (2~3 particles) of silicates in 50 min films sample. However, no large agglomerates were visible from TEM images of 0 min sample. No agglomerates were observed, but mostly single exfoliated silicates were observed. The TEM results are in agreement with the XRD diffractogram results where series of broad peaks were observed in wider (higher) d-spacing values for 0 min film sample.

### 5.3.9. Sodium dodecyl sulfate polyacrylamide gel electrophoresis (SDS-PAGE)

Gomez-Guillen and others (2001) reported that cross-linking could cause an increase in the molecular weight of fish gelatin. Kolodzlejska and others (2004) reported that concentration and reaction time of MTGase treated Baltic cod skin gelatin increased significantly, thus increasing the speed of gel formation. From these results, it can be suggested that gelatin viscosity would increase and gel formation time would decrease during MTGase treatment.

The electrophoretic profile of neat fish gelatin and MTGase treated fish gelatin was obtained by SDS-PAGE shown in Figure 12. Lane 1 and 7 contains standards of known molecular weight (size marker 37, 50, 75, 100, 150, and 250 kDa), lane 2 is neat fish gelatin, and lanes 3 to 6 represents band profile of MTGase treated fish gelatin. As can be observed from lanes 3 to 6, the band intensity below about 75 kDa decreases as the treatment time increases and the band intensity above about 250 kDa increases as the treatment time increases. These results indicate that MTGase induced cross-linking reaction in the fish gelatin matrix, thus causing an increased molecular weight. According to previous research (Dickinson, 1997; Motoki and Seguro, 1998), the molecular weight

of MTGase was confirmed to be 38 kDa with 331 amino acid residues. Therefore, the chance of band overlap is very low and bands showing above 37 kDa should be related to fish gelatin molecules.

Similar results have been reported (Lim, Mine, & Tung, 1999; Gomez-Guillen, Sarabia, Solas, & Montero, 2001), observing decreasing band intensity at the position of around 100 kDa and increasing band intensity in the upper position of the gel when treated with MTGase.

#### **5.4. Conclusion**

In this research, MTGase treated protein-based nanocomposites have been successfully developed from a biopolymer. In the blends, the unmodified sodium montmorillonite clay was initially treated with a high-powered ultrasonifier in a solution of sorbitol and distilled water. The nano-clay solution was then added to a MTGase treated (0 to 50 min) fish gelatin solution and casted using a mechanical film caster. After the MTGase treatment, the viscosity of fish gelatin solution increased because of the cross-linking. MTGase treatment increased molecular weight, but decreased tensile strength and elongation %. MTGase treatment had no significant effect on oxygen permeability and water vapor permeability.

#### **5.5. References**

ASTM. Standard methods for tensile properties of thin plastic sheeting (E 882-88). *Annual Book of ASTM Standards*. American Society for Testing and Materials, Philadelphia, PA. 1989.

- ASTM. Standard methods for water vapor transmission of materials (E 96-80). *Annual Book of ASTM Standards*. American Society for Testing and Materials, Philadelphia, PA. 1987.
- Babin, H. and Dickinson, E. (2001). Influence of transglutaminase treatment on the thermoreversible gelation of gelatin. *Food Hydrocolloid*, 15(3), 271–276.
- Bae, H. J., Byun, Y. J., Hong, S. I., Darby, D. O., Kimmel, R. M., and Whiteside, W. S. (2007). Effect of clay content, homogenization RPM, pH, and ultrasonification on mechanical and barrier properties of fish gelatin/montmorillonite nanocomposites. Dissertation, Clemson University.
- Benjakul, S., Visessanguan, W., and Pecharat, S. (2004). Suwari gel properties as affected by transglutaminase activator and inhibitors. *Food Chem*, 85(1), 91–9.
- Bigi A, Bracci B, Cojazzi G, Panzavolta S, Roveri N. 1998. Drawn gelatin films with improved mechanical properties. *Biomaterials* 19(24):2335–40.
- Bigi, A., Cojazzi, G., Panzavolta, S., Rubini, K., and Roveri, N. (2001). Mechanical and thermal properties of gelatin films at different degrees of glutaraldehyde crosslinking. *Biomaterials*, 22(8), 763.
- Bigi, A., Panzavolta, S., and Rubini, K. (2004). Relationship between triple-helix content and mechanical properties of gelatin films. *Biomaterials*, 25(25), 5675–5680.
- Chen, T., Embree, H., Brown, E., Taylor, M., and Payne, G. (2003). Enzyme-catalyzed gel formation of gelatin and chitosan : potential for in situ applications, *Biomaterials*, 24(17), 2831-2841.
- Dean and Yu (2005). Ch In (R. Smith ed.) *Biodegradable polymers for industrial applications*. Boca Raton : CRC Press; Cambridge: Woodhead.
- De Carvalho, R. A. and Grosso, C. R. F. (2004). Characterization of gelatin based films modified with transglutaminase, glyoxal, and formaldehyde. *Food Hydrocolloid*, 18(5), 717.
- Dickinson, E. (1997). Enzymic crosslinking as a tool for food colloid rheology control and interfacial stabilization. *Trends Food Sci Tech*, 8(10), 334–339.
- Ensminger, L. E. and Giesecking, J. E. (1939). The adsorption of proteins by montmorillonitic clays. *Soil Science*, 48, 467-471.
- Ensminger, L. E. and Giesecking, J. E. (1941). The adsorption of proteins by montmorillonitic clays and its effect on base-exchange capacity. *Soil Science*, 51, 125-132.

- Fernandez-Diaz, M., Montero, P., and Gomez-Guillen, M. (2001). Gel properties of collagens from skins of cod (*Gadus morhua*) and hake (*Merluccius merluccius*) and their modification by the coenhancers magnesium sulphate, glycerol, and transglutaminase. *Food Chem*, 74(2), 161-167.
- Garcia, F. T., and Sobral, P. (2005). Effect of the thermal treatment of the filmogenic solution on the mechanical properties, color and opacity of films based on muscle proteins of two varieties of tilapia. *Food Sci Tech*, 38(3), 289–296.
- Gennadios, A. and Weller, C. L. (1990). Edible films and coatings from wheat and corn proteins. *Food Technology*, 44(10), 63-69.
- Gennadios, A. and Weller, C. L. (1991). Edible films and coatings from soy milk and soy protein. *Cereal Foods World*, 36(12), 1004-1009.
- Gomez-Guillen, M. C., Sarabia, A. I., Solas, M. T., Montero, P. (2001). Effect of microbial transglutaminase on the functional properties of megrim (*Lepidorhombus bosci*) skin gelatin. *J Sci Food Agr*, 81(7), 665–673.
- Guilbert, S. Technology and application of edible protective films in Food Packaging and Preservation, Elsevier Applied Science, London, 1986, 371-394.
- Haug, I. J., Draget, K. I., and Smidsrod, A. (2004). Physical behavior of fish gelatin-kapp-carrageenan mixtures, *Carbohydr Polym*, 56(1), 11-19.
- Hunter Lab applications note. (1996). September 1-15, Vol. 8, No. 11.
- Kester, J. J. and Fennema, O. R. (1986). Edible films and coatings – a review. *Food Technology*, 40(12), 47-59.
- Kim, Y. T. (2005). Development and characterization of gelatin film as active packaging layer. Clemson: Clemson University.
- Kolodziejska, I., Kaczorowski, K., Piotrowska, B., and Sadowska, M. (2004). Modification of the properties of gelatin from skins of Baltic cod (*Gadus morhua*) with transglutaminase. *Food Chem*, 86(2), 203–209.
- Kutemeyer, C., Froeck, M., Werlein, H., and Watkinson, B. (2005). The influence of salts and temperature on enzymatic activity of microbial transglutaminase. *Food Control*, 16(8), 735–737.



- Lim, L., Mine, Y., and Tung, M. (1999). Barrier and tensile properties of transglutaminase crosslinked gelatin films as affected by relative humidity, temperature, and glycerol content. *J Food Sci*, 64(4), 616–622.
- Mariniello, L., Di Pierro, P., Esposito, C., Sorrentino, A., Masi, P., and Porta, R. (2003). Preparation and mechanical properties of edible pectin-soy flour films obtained in the absence or presence of transglutaminase. *J Biotechnol*, 102(2), 191–198.
- McDermott, M., Chen, T., Williams, C., Markley, K., and Payne, G. (2004). Mechanical properties of biomimetic tissue adhesive based on the microbial transglutaminase-catalyzed crosslinking of gelatin. *Biomacromol*, 5(4), 1270–1279.
- Mchugh, T. H., Avena-Bustillos, R., and Krochta, J. M. (1993). Hydrophilic edible films: Modified procedure for water vapor permeability and explanation of thickness effects. *J Food Sci*, 58, 899-903.
- Motoki, M. and Seguro, K. (1998). Transglutaminase and its use for food processing. *Trends Food Sci Tech*, 9(5), 204–210.
- Ni, S., Nozawa, H., and Seki, N. (1998). Effect of microbial transglutaminase on thermal gelation of carp actomyosin sol. *Fisheries Sci*, 64(3), 434–438.
- Nonaka, M., Sakamoto, H., Toiguchi, S., Yamagiwa, K., Soeda, T., and Motoki, M. (1996). Retortresistant tofu prepared by incubation with microbial transglutaminase. *Food Hydrocolloid*, 10(1), 41–44.
- Park, H. J. (1991). Edible coating for fruits and vegetables: determination of gas diffusivities, prediction of internal gas composition and effects of the coating on shelf life. Athens: University of Georgia. p 23–30.
- Ramirez, J., Uresti, R., Tellex, S., and Vazquez, M. (2002). Using salt and microbial transglutaminase as binding agents in restructured fish products resembling hams. *J Food Sci*, 67(5), 1778-1784.
- Rao, Y. (2007). Gelatin-clay nanocomposites of improved properties, *Polymer*, 48, 5369-5375.
- Seguro, K., Kumazawa, Y., Ohtsuka, T., Toiguchi, S., Motoki, M. (1995). Microbial transglutaminase and epsilon-(gamma-glutamyl)lysine cross-link effects on elastic properties of kamaboko gels. *J Food Sci*, 60(2), 305–311.
- Sharma, R., Zakora, M., and Qvist, K. (2002). Susceptibility of an industrial alpha-lactalbumin concentrate to cross-linking by microbial transglutaminase. *Int Dairy J*, 12(12), 1005–1012.

- Shimba, N., Shinohara, M., Yokoyama, K., Kashiwagi, T., Ishikawa, K., Ejima, D., and Suzuki, E. (2002). Enhancement of transglutaminase activity by NMR identification of its flexible residues affecting the active site. *Febs Lett*, 517(1–3), 175–179.
- Soeda, T., Ishii, T., Yamazaki, K., Murase, K. (1995). The functionalities of microbial transglutaminase for food application. 1. The effect of transglutaminase on texture of tofu. *J Jpn Soc Food Sci*, 42(4), 254–61.
- Tanaka, M., Iwata, K., Sanguandeeikul, R., Handa, A., and Ishizaki, S. (2001). Influence of plasticizers on the properties of edible films prepared from fish water-soluble proteins, *Fisheries Sci*, 67(2), 346-351.
- Theng, B. K. G. (1979). Formation and properties of clay-polymer complexes. Amsterdam; New York: Elsevier Scientific Publishing. Company.
- Tseng, Y. C., Tabata, Y., Yyon, S. H., and Kiada, Y. (1990). In vitro toxicity test of 2-cyanoacrylate polymers by cell culture method. *J Biomed Mater Res*, 24(10), 1355-1367.
- Uresti, R., Ramirez, J., Lopez-Arias, N., and Vazquez, M. (2003). Negative effect of combining microbial transglutaminase with low methoxyl pectins on the mechanical properties and colour attributes of fish gels, *Food Chem*, 80(4), 551-556.
- Yi, J. B., Kim, Y. T., Bae, H. J., Whiteside, W. S., and Park, H. J. (2006). Influence of Transglutaminase-Induced Cross-Linking on Properties of Fish Gelatin Films. *J Food Sci*, 71(9), 376-383.
- Zhu, H. J., Wang, Y. F., Zhang, X. Q., Su, Y. F., Dong, X., Chen, Q. K., Zhao, Y., Geng, C., Zhu, S. N., Han, C. C., Wang, D. J. (2007). Influence of molecular architecture and melt rheological characteristic on the optical properties of LDPE blown films. *Polymer*, 48(17), 5098-5106.

## 5.6. Figure Captions

**Figure 5.1.** Flow diagram for preparation of film casting solution.

**Figure 5.2.** Effect of MTGase on viscosity as a function of MTGase concentration and time at 50 °C.

**Figure 5.3.** Tensile strength and E% of film as a function MTGase treatment time (2% MTGase)

**Figure 5.4.** Oxygen permeability and water vapor permeability of composite films as a function of clay content.

**Figure 5.5.** XRD diffractograms of the FG/sorbitol/H<sub>2</sub>O, Cloisite Na<sup>+</sup>, and MTGase treated (0 and 50 min) nanocomposite films (ultrasonified FG/Cloisite Na<sup>+</sup>/sorbitol/H<sub>2</sub>O).

**Figure 5.6.** TEM observation of MTGase treated (0 min) FG/Cloisite NA<sup>+</sup> (5% w/w)/sorbitol/H<sub>2</sub>O film. The arrow indicates the direction of the film thickness.

**Figure 5.7.** TEM observation of MTGase treated (0 min) FG/Cloisite NA<sup>+</sup> (5% w/w)/sorbitol/H<sub>2</sub>O film. The arrow indicates the direction of the film thickness.

**Figure 5.8.** TEM observation of MTGase treated (0 min) FG/Cloisite NA<sup>+</sup> (5% w/w)/sorbitol/H<sub>2</sub>O film. The arrow indicates the direction of the film thickness.

**Figure 5.9.** TEM observation of MTGase treated (50 min) FG/Cloisite NA<sup>+</sup> (5% w/w)/sorbitol/H<sub>2</sub>O film. The arrow indicates the direction of the film thickness.

**Figure 5.10.** TEM observation of MTGase treated (50 min) FG/Cloisite NA<sup>+</sup> (5% w/w)/sorbitol/H<sub>2</sub>O film. The arrow indicates the direction of the film thickness.

**Figure 5.11.** TEM observation of MTGase treated (50 min) FG/Cloisite NA<sup>+</sup> (5% w/w)/sorbitol/H<sub>2</sub>O film. The arrow indicates the direction of the film thickness.

**Figure 5.12.** Electrophoretic profile of fish gelatin and MTGase treated fish gelatin. Lane 1 and 7 is size marker, lane 2 is fish gelatin, and lane 2 to 6 are enzyme treated fish gelatin according to the reaction time.

## 5.7. Table Captions

**Table 5.1.** Effect of MTGase (2% w/w) on color and haze of fish gelatin/Cloisite NA<sup>+</sup>/glycerol/H<sub>2</sub>O films.

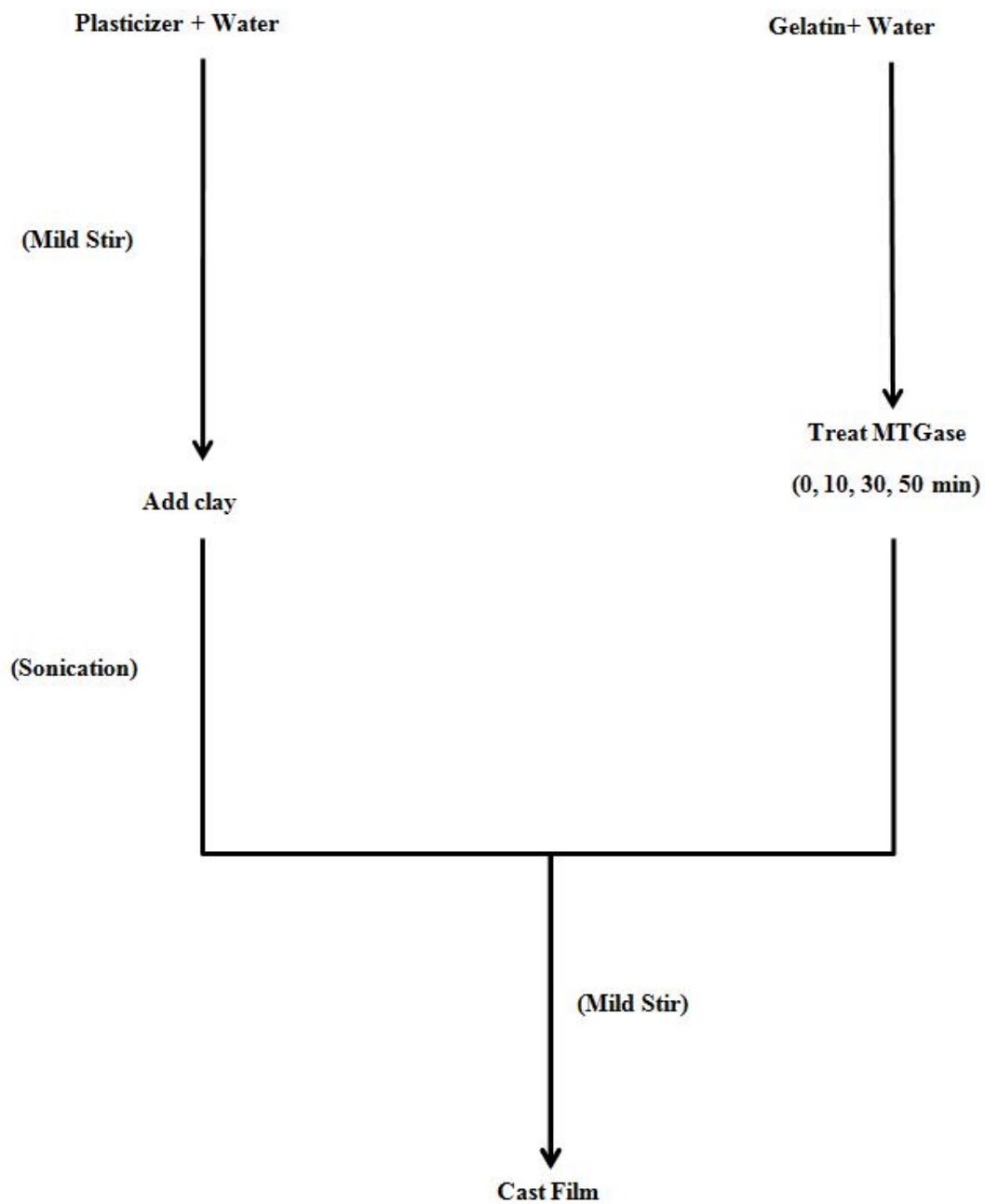


Figure 5.1. Flow diagram for preparation of film casting solution.

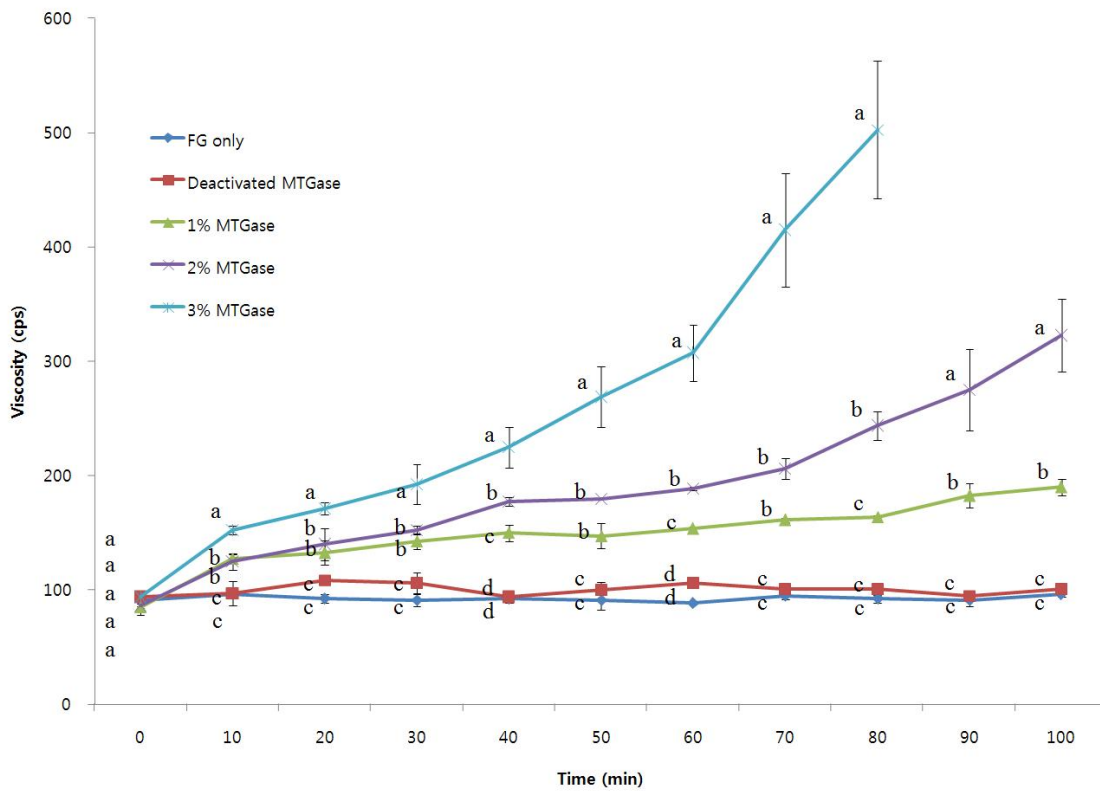


Figure 5.2. Effect of MTGase on viscosity as a function of MTGase concentration and time at 50 °C. Values are given as mean±SD from three determinations (n=3).

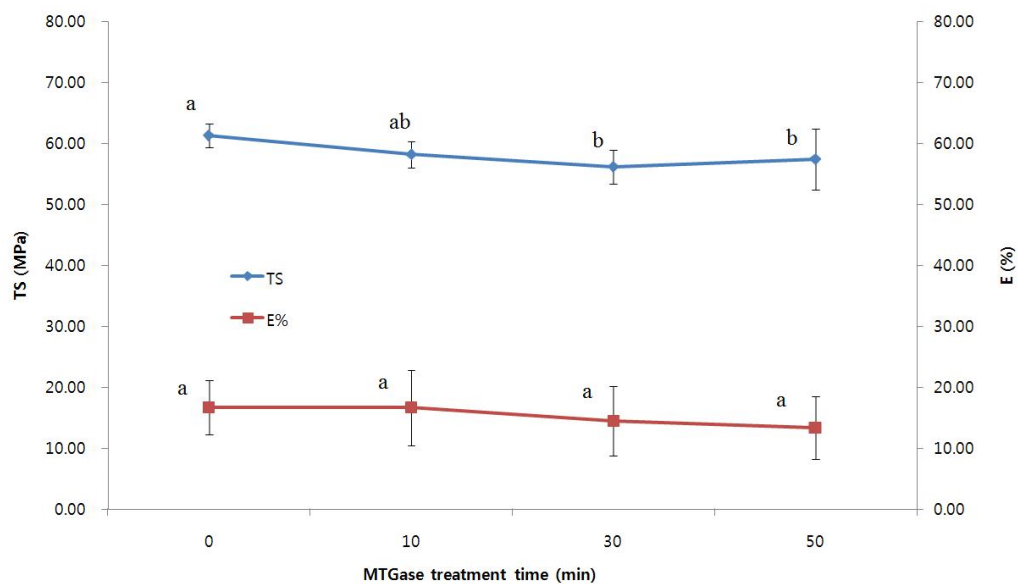


Figure 5.3. Tensile strength and E% of film as a function MTGase treatment time (2% MTGase). Values are given as mean $\pm$ SD from ten determinations (n=10).

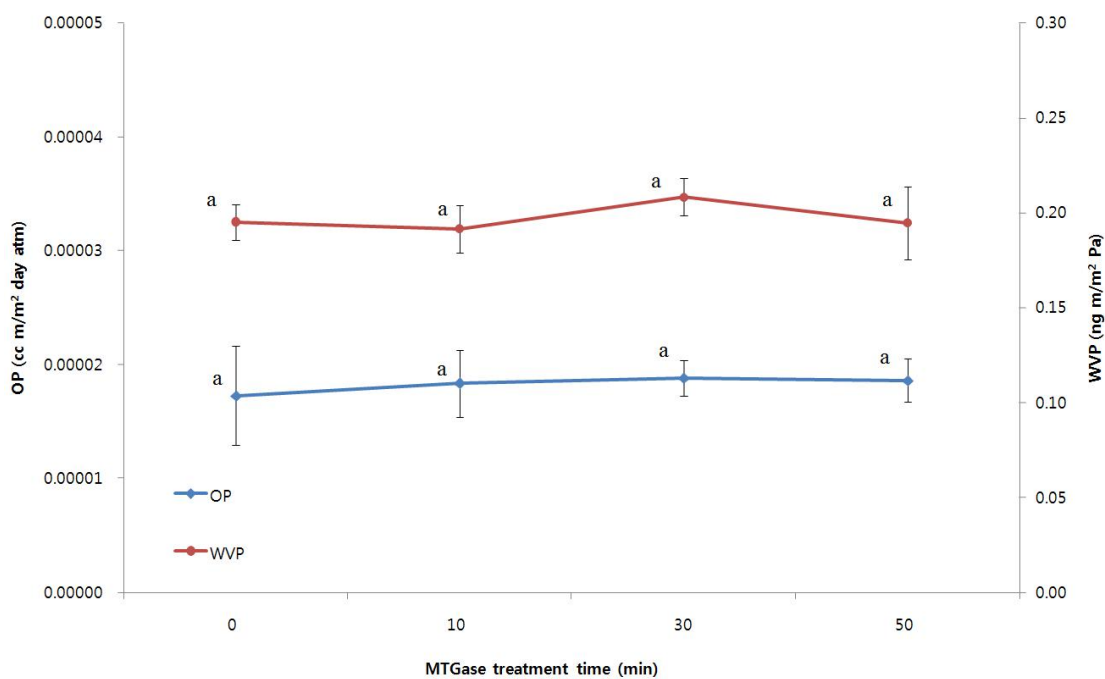


Figure 5.4. Oxygen permeability and water vapor permeability of composite films as a function of clay content. Values are given as mean $\pm$ SD from three determinations (n=3).

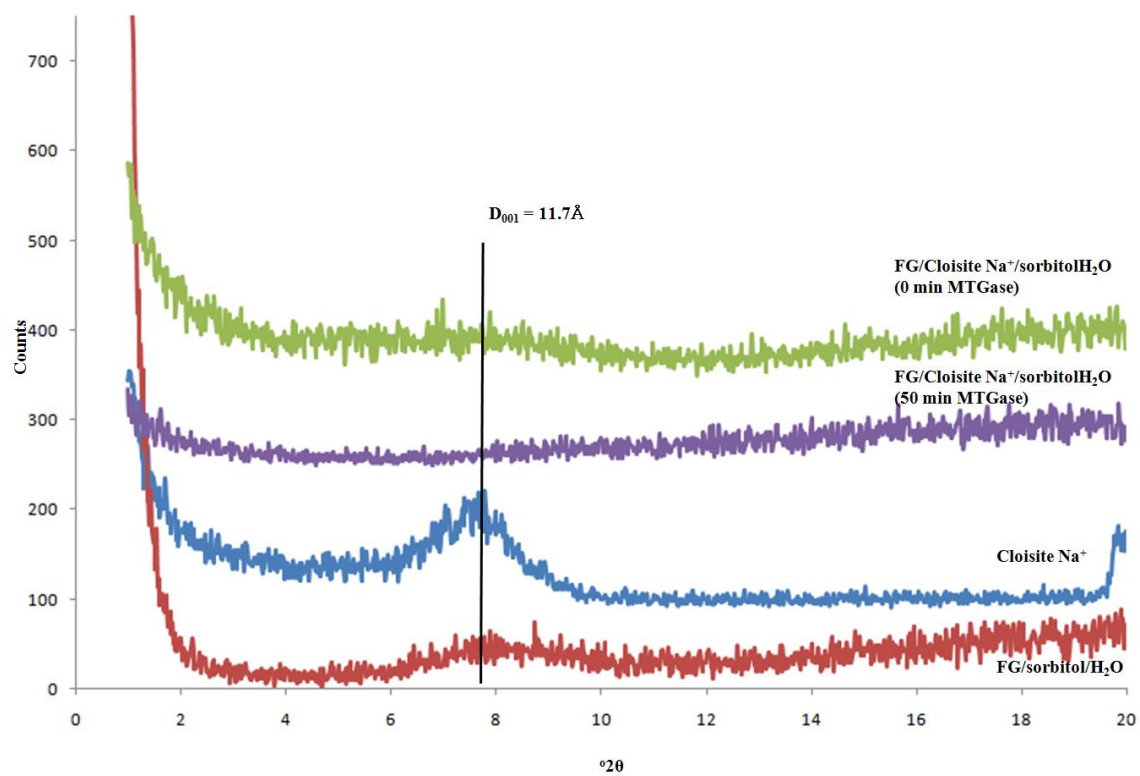
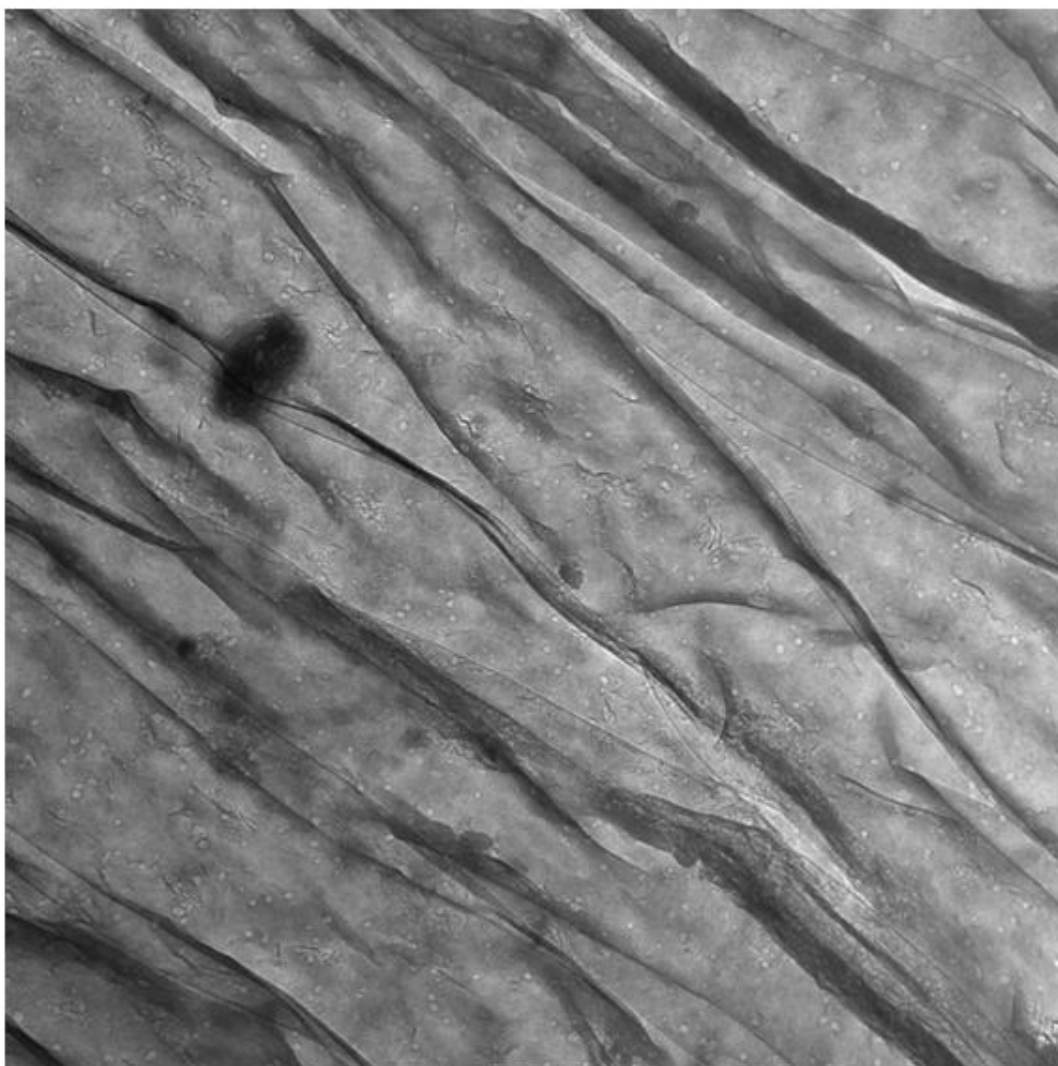


Figure 5.5. XRD diffractograms of the FG/sorbitol/H<sub>2</sub>O, Cloisite Na<sup>+</sup>, and MTGase treated (0 and 50 min) nanocomposite films (ultrasonified FG/Cloisite Na<sup>+</sup>/sorbitol/H<sub>2</sub>O).





9.tif

2-0-9

Print Mag: 17200x @ 51 mm

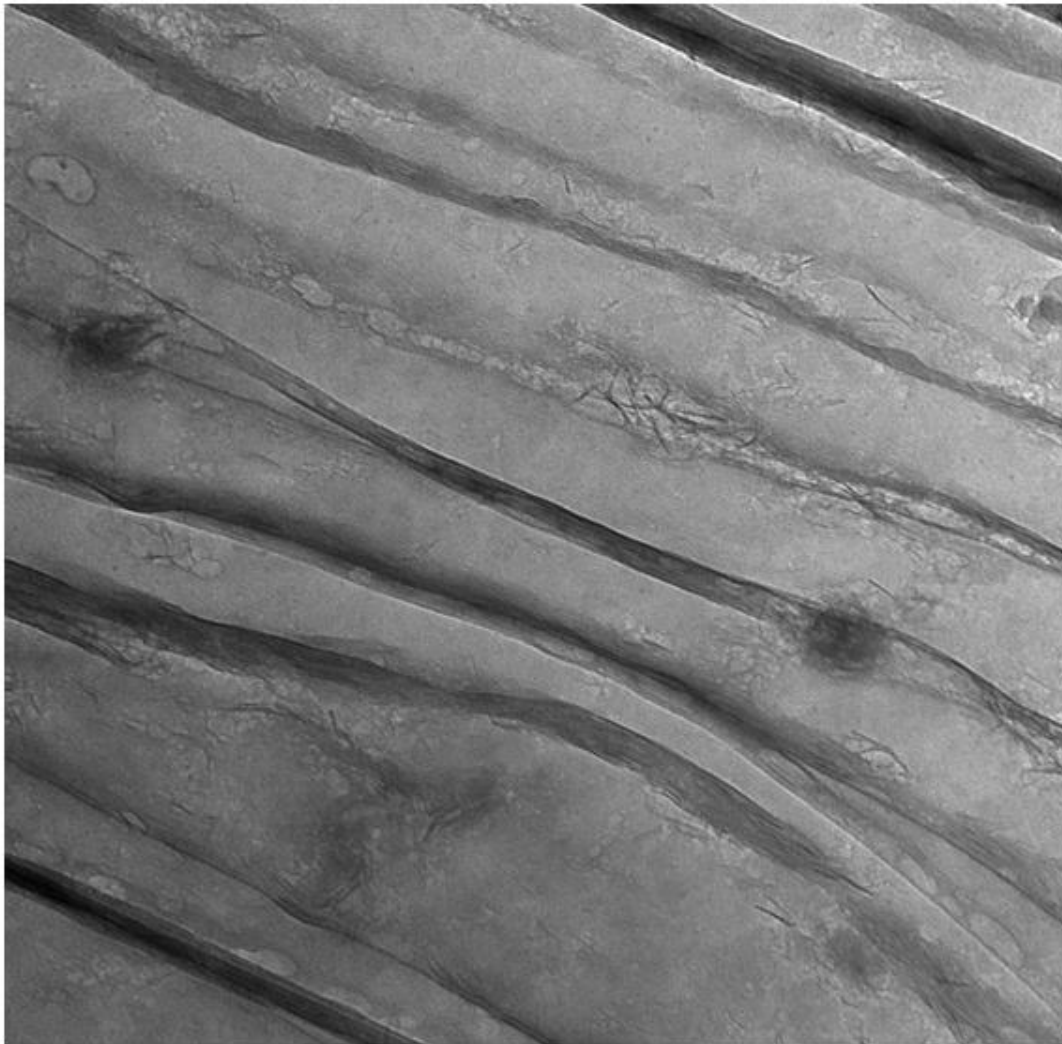
16:47 09/25/07

500 nm

HV=110kV

Direct Mag: 50000x

Figure 5.6. TEM observation of MTGase treated (0 min) FG/Cloisite  $\text{NA}^+$  (5% w/w)/sorbitol/ $\text{H}_2\text{O}$  film. The arrow indicates the direction of the film thickness.



19.tif

2-0-19

Print Mag: 51700x @ 51 mm

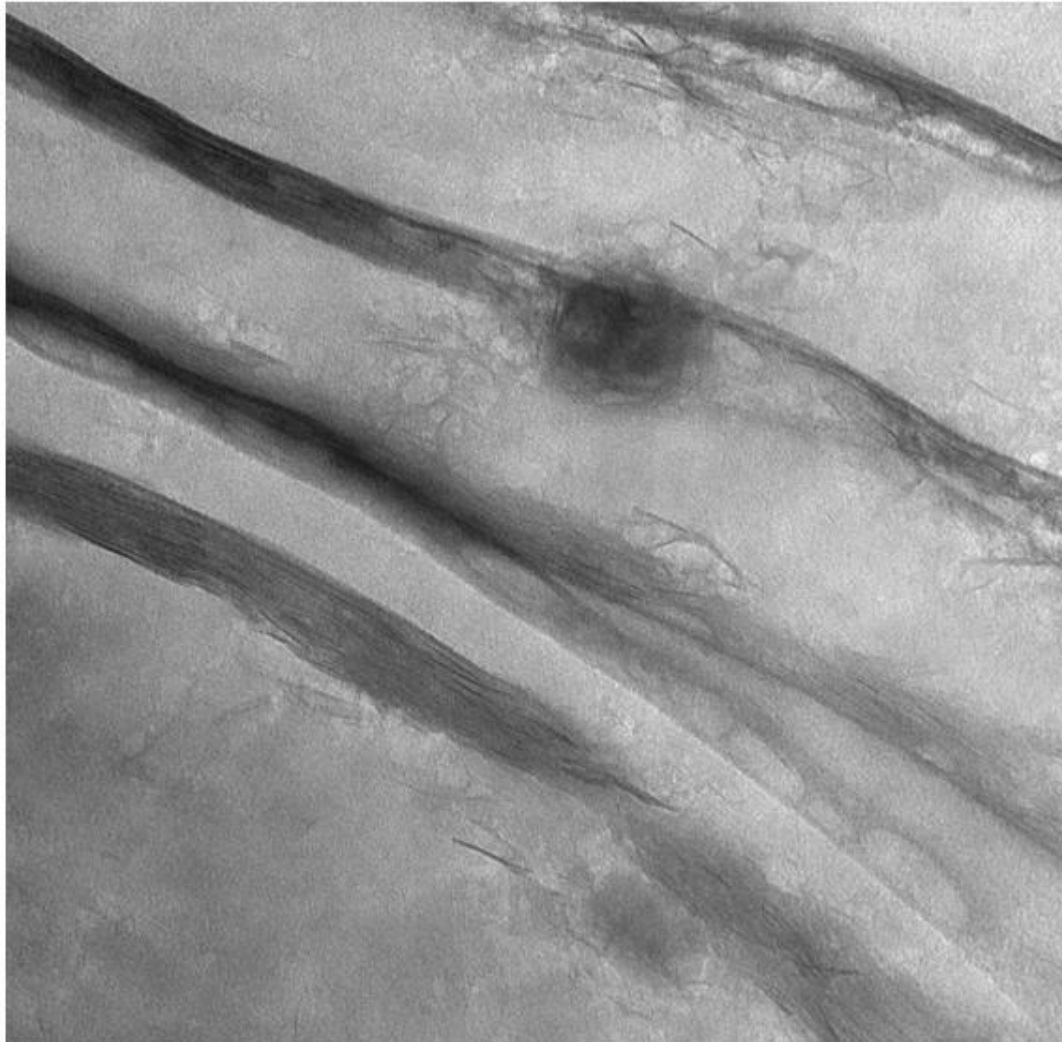
16:56 09/25/07

100 nm

HV=110kV

Direct Mag: 150000x

Figure 5.7. TEM observation of MTGase treated (0 min) FG/Cloisite  $\text{NA}^+$  (5% w/w)/sorbitol/ $\text{H}_2\text{O}$  film. The arrow indicates the direction of the film thickness.



20.tif

2-0-20

Print Mag: 103000x @ 51 mm

16:57 09/25/07

100 nm

HV=110kV

Direct Mag: 300000x

Figure 5.8. TEM observation of MTGase treated (0 min) FG/Cloisite  $\text{NA}^+$  (5% w/w)/sorbitol/ $\text{H}_2\text{O}$  film. The arrow indicates the direction of the film thickness.



17.tif

2-50-17

Print Mag: 17200x @ 51 mm

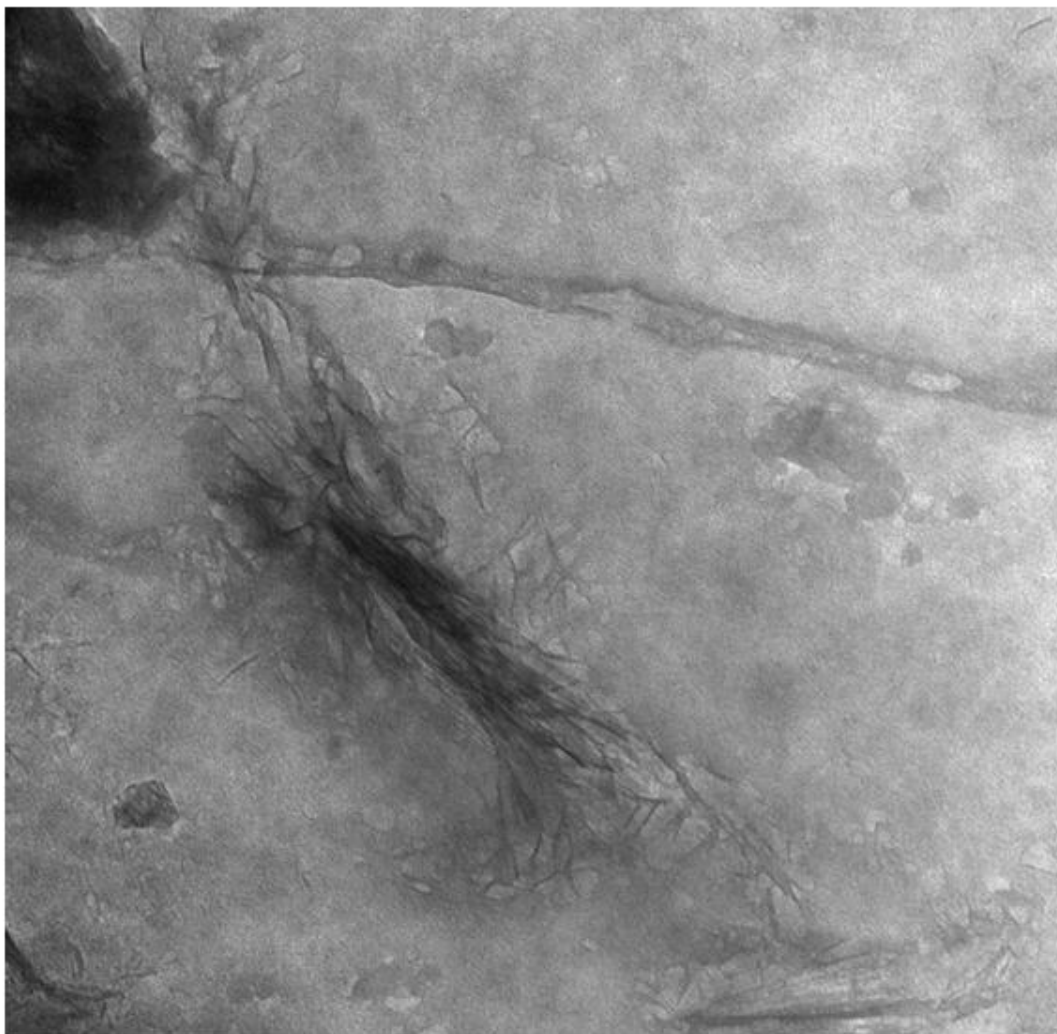
15:38 09/25/07

500 nm

HV=110kV

Direct Mag: 50000x

Figure 5.9. TEM observation of MTGase treated (50 min) FG/Cloisite  $\text{NA}^+$  (5% w/w)/sorbitol/ $\text{H}_2\text{O}$  film. The arrow indicates the direction of the film thickness.



26.tif

2-50-26

Print Mag: 51700x @ 51 mm

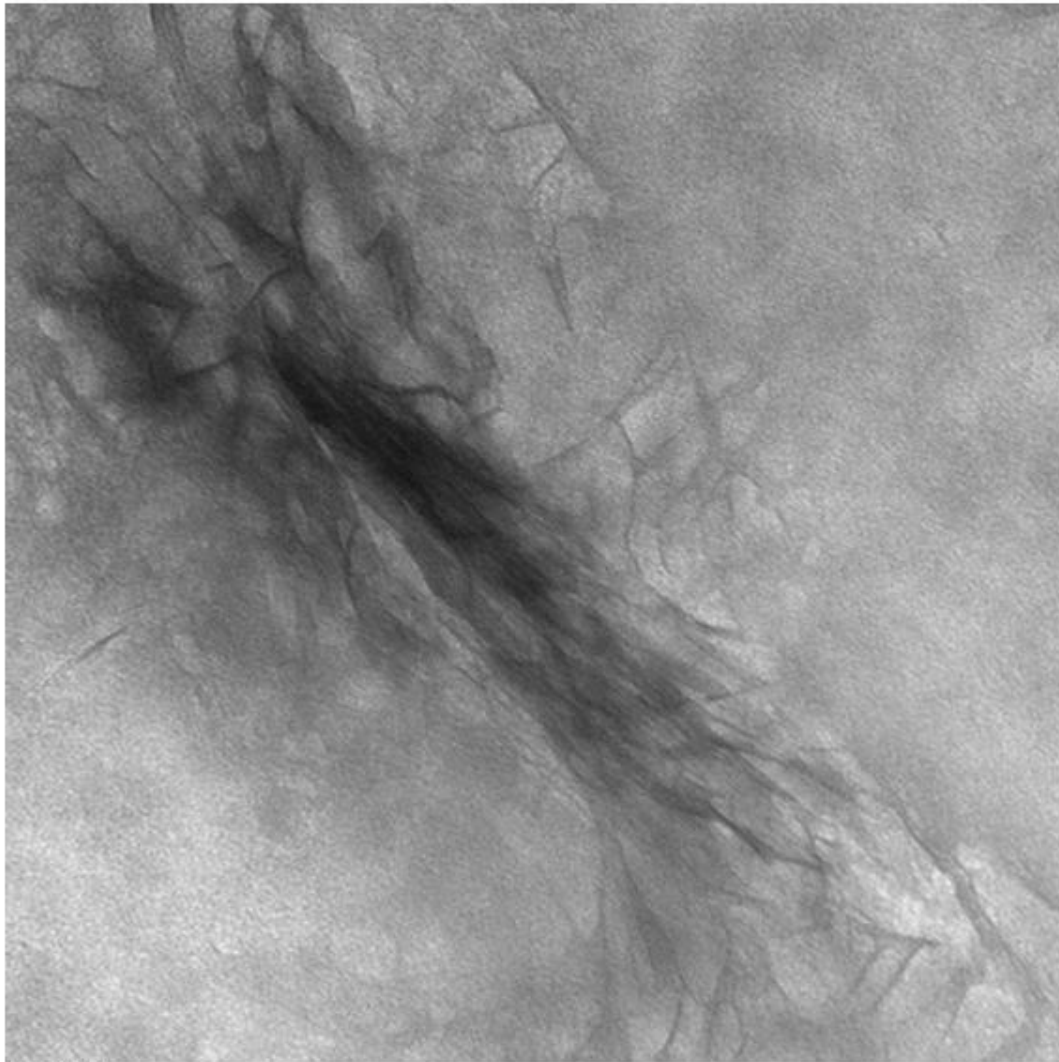
15:52 09/25/07

100 nm

HV=110kV

Direct Mag: 150000x

Figure 5.10. TEM observation of MTGase treated (50 min) FG/Cloisite  $\text{NA}^+$  (5% w/w)/sorbitol/ $\text{H}_2\text{O}$  film. The arrow indicates the direction of the film thickness.



28.tif

2-50-28

Print Mag: 103000x @ 51 mm

15:55 09/25/07

100 nm

HV=110kV

Direct Mag: 300000x

Figure 5.11. TEM observation of MTGase treated (50 min) FG/Cloisite  $\text{NA}^+$  (5% w/w)/sorbitol/ $\text{H}_2\text{O}$  film. The arrow indicates the direction of the film thickness.

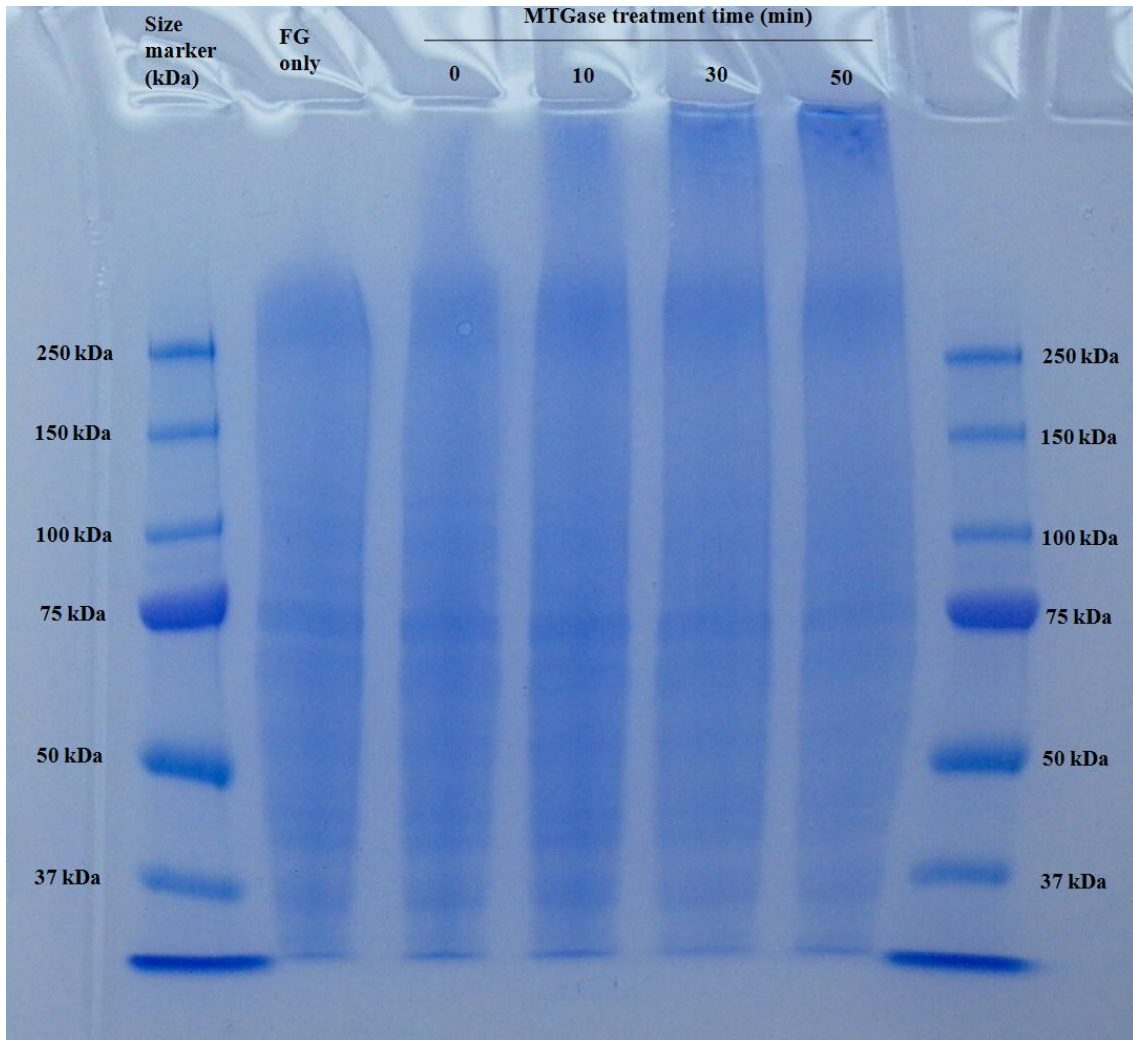


Figure 5.12. Electrophoretic profile of fish gelatin and MTGase treated fish gelatin. Lane 1 and 7 is size marker, lane 2 is fish gelatin, and lane 2 to 6 are enzyme treated fish gelatin according to the reaction time.

Table 5.1. Effect of MTGase (2% w/w) on color and haze of fish gelatin/Cloisite NA<sup>+</sup>/glycerol/H<sub>2</sub>O films. Values are given as mean±SD from three determinations (n=3).

MTGase Treat Time (min)	Hunter L a b			$\Delta E^D$	Haze <sup>E</sup> (%)
	L <sup>A</sup>	a <sup>B</sup>	b <sup>C</sup>		
FG only	97.02±0.06a	-0.04±0.01 <sup>a</sup>	0.82±0.07 <sup>a</sup>	2.56±0.06 <sup>a</sup>	3.03±0.19 <sup>c</sup>
No MTGase	96.92±0.05 <sup>b</sup>	-0.04±0.05 <sup>a</sup>	0.76±0.55 <sup>a</sup>	2.50±0.07 <sup>a</sup>	5.24±0.40 <sup>b</sup>
0	96.92±0.03 <sup>b</sup>	-0.07±0.01 <sup>a</sup>	1.01±0.06 <sup>a</sup>	2.48±0.03 <sup>a</sup>	5.41±0.42 <sup>b</sup>
10	96.94±0.04 <sup>ab</sup>	-0.05±0.01 <sup>a</sup>	0.95±0.03 <sup>a</sup>	2.49±0.04 <sup>a</sup>	5.63±0.27 <sup>ab</sup>
30	96.95±0.02 <sup>ab</sup>	-0.06±0.01 <sup>a</sup>	1.00±0.02 <sup>a</sup>	2.50±0.02 <sup>a</sup>	6.03±0.14 <sup>ab</sup>
50	97.02±0.06 <sup>a</sup>	-0.04±0.00 <sup>a</sup>	0.92±0.03 <sup>a</sup>	2.57±0.06 <sup>a</sup>	6.44±0.94 <sup>a</sup>

<sup>A</sup> a-e indicate significant differences (P < 0.05) within columns L.

<sup>B</sup> a-e indicate significant differences (P < 0.05) within columns a.

<sup>C</sup> a-d indicate significant differences (P < 0.05) within columns b.

<sup>D</sup> a-d indicate significant differences (P < 0.05) within columns  $\Delta E$ .

<sup>E</sup> a-d indicate significant differences (P < 0.05) within columns Haze.



## CHAPTER SIX

### DEVELOPMENT AND CHARACTERIZATION OF PET/FISH GELATIN- NANOCLAY COMPOSITE/LDPE LAMINATE : GELATIN-NANOCLAY FILM AS A FUNCTIONAL BARRIER LAYER

Ho J. Bae<sup>1</sup>, Duncan. O. Darby<sup>1</sup>, Robert. M. Kimmel<sup>1</sup>,  
and William. S. Whiteside<sup>1\*</sup>

<sup>1</sup> Department of Packaging Science, Clemson University, Clemson, SC 29634-0320,  
USA.

\* To whom all correspondence should be sent:

Dr. William Scott Whiteside, Associate Professor  
Department of Packaging Science,  
Clemson University, Clemson, SC 29634-0370, USA.  
Telephone: +1-864-656-6246, fax: +1-864-656-4395  
e-mail: wwhtsd@clemson.edu

#### **Abstract**

A three layer laminate film was developed which constitute PET/fish gelatin-nanoclay composite/LDPE. The fish gelatin-nanoclay composite was used as an oxygen barrier layer and showed excellent oxygen barrier property when compared to EVOH. The introduction of nanometer-sized filler clay into the fish gelatin matrix improved the barrier property due to the tortuosity effect of the clay particles. Moreover, the fish

gelatin-nanoclay composite film showed good bond strength to both LDPE and PET.

Therefore, these developed laminates are suited as functional barrier layers in laminates for food packaging.

Key words: Fish gelatin, nanoclay, laminate, EVOH, tortuosity, food, packaging

## **6.1. Introduction**

One of the most important issues in food packaging is the oxygen permeability. Protection of contents against oxygen is critical in order to prolong shelf-life of many packaged products. The high barrier property is achieved by formation of multilayer packaging film containing functional barrier layers against gas transmission. However, conventional functional barrier layers used in multilayer packaging films usually consists of expensive barrier polymers such as ethylene-vinyl alcohol copolymers (EVOH), poly(vinylidene chloride) (PVDC) which require complex processing technology, or surface modification processes (aluminum evaporation or plasma deposition of inorganic layer etc.) which require high technical efforts and expensive materials. Moreover, many of these functional barrier materials are not biodegradable and therefore environmental concerns still may prevail. Packaging materials account for approximately 30% by weight of municipal solid waste and two-thirds of the volume in trash cans due to their bulk (Han, 2001).

Biodegradable/edible films and coatings from biopolymers have received increasing attention and potential sources of biopolymers have been reviewed by Kester

and Fenema (1986), Guilbert (1986), and Gennadios and Weller (1990, 1991). Natural biopolymers have the advantage of being biodegradable, renewable, and often edible. Furthermore, some of them exhibit high oxygen barrier and good mechanical strength (Forsell, lahtinen, Lahelin, & Myllärinen, 2002; Gilleland, Turner, Patton, & Harrison, 2001; Lawton, 1996; Lee & Rhim, 2000). Numerous studies have been conducted investigating the properties of various protein, polysaccharide, and lipid-based biopolymer materials. These materials have successfully been formed into films or coatings (Gontard, Guilbert, & Cuq, 1993; Park & Chinnan, 1995; Kim, Ko, & Park, 2002; Lawton, 1996; Arvanitoyannis, Nakayama, & Aiba, 1998; McHugh & Krochta, 1994; Gontard, Thibault, Cuq, & Guilbert, 1996; Chen, 1995; Lourdin, Valle, & Colonna, 1995; Gennadios, Weller, & Testin, 1993; Mchugh, Aujard, & Krochta, 1994; Park, Weller, Vergano, & Testin, 1993).

Gelatin is a complex polypeptide widely used in food, pharmaceutical, photographic, and cosmetic products. Gelatin was one of the initial materials used for the formation of biopolymer films. Gelatin continues to be used in edible film studies given the abundance of raw material, low production cost, global availability, and excellent film forming properties (Vanin, Sobral, Menegalli, Carvalho, & Habitante, 2005). Traditional sources of gelatin have been primarily pig skin and cowhide. For a number of reasons such as religious prohibition and concerns over the spreading of bovine spongiform encephalopathy (commonly known as mad cow disease), fish gelatin has been along with other possible alternatives (Park & Chinnan, 1995; Park, Lee, Jung, & Park, 2001; Kim, Ko, & Park, 2002). The characteristics and properties of fish gelatin

have been studied in recent years as a potential mammalian gelatin alternative (Yi, Kim, Bae, Whiteside, & Park, 2006).

In order to obtain a packaging film with high mechanical strength and high barrier properties, fish gelatins have been filled with layered silicates. Low gas permeation of nanocomposites was long considered as one of the most important technological advantages (Ruiz-Hitzky & Meerbeek, 2006). It had been shown that polymer nanocomposites have excellent barrier properties against gases and water vapor. This is due to the presence of ordered dispersed silicate layers with large aspect ratios which are impermeable to gases and water vapor in the polymer matrix (Yano, Usuki, & Okad, 1997). Qian and others (2001) reported oxygen transmission rate of PP nanocomposites containing 6% organoclay about half than that of the neat PP. Gilmer and others (2002) reported aromatic-aliphatic polyamide nanocomposites (Imperm<sup>TM</sup>) which shows superb barrier properties. Moreover, after final degradation, only inorganic, natural clay will be left over (Sinha & Okamoto, 2003)

In this study, a multilayer lamination made of PET/fish gelatin-nanoclay composite/LDPE was developed and compared with a PET/EVOH/LDPE lamination. A fish gelatin-nanoclay film layer was used as the oxygen barrier layer and its possibility as an alternative oxygen barrier was investigated.

## 6.2. Experimental Material and Method

### 6.2.1. Materials

The following raw materials were used to develop gelatin-clay composite films: Gelatin 200 bloom-fish-8 mesh (Vyse Gelatin Company, Illinois, USA); Cloisite® NA<sup>+</sup> (Southern clay Products, Texas, USA); Glycerol, Anhydrous (J. T. Baker, New Jersey, USA); d-Sorbitol (Sigma, St. Louis, Mo., USA); Liofol ® Tycel® 393™ Single Component Adhesive (Düsseldorf, Germany). The EVOH films (EF-F and EF-XL) were kindly donated from EVALCA (Houston, Texas, USA).

### 6.2.2. FG-Nanoclay Composite Film Casting Solution Preparation

The film solution preparation and development procedure is reported in Figure 1. Nanoclay solutions were prepared by first dissolving 10 g of plasticizer in 100 mL of 50 °C degassed, distilled, and deionized water and stirred for 30 min at 50±5°C. The concentration of plasticizer was 0.2 g plasticizer/g gelatin. Clay (20% w/w) were added and stirred by magnetic stirrer for 30 min at 50±5 °C. The solution was then ultrasonified using Branson sonifier (Model S-450D) to aid intercalation and exfoliation of the clay and plasticizers. A standard 1/2 in diameter tapped flat horn tip was used at approximately 40% output for 30 min. Gelatin solution was prepared separately. Fifty grams of biopolymer was dissolved in 100 mL of 60 °C degassed, distilled, and deionized water and stirred for 2 hr at 60±5 °C. Finally, the clay solution was added to gelatin solution in droplets and gently stirred for 24 hr at 35±5 °C before casting.

### 6.2.3. Fish Gelatin-Nanoclay Composite Film Casting

Approximately 30 mL of the prepared film solution was cast onto a BYTAC<sup>®</sup> (Norton Performance Plastics Corporation, Wayne, NJ, USA) coated 8" x 16" glass plate which was formed utilizing a custom designed film applicator as shown in Figure 2. After drying, films were peeled off from the glass plates and cut into test specimens. The test specimens were immediately placed back into a constant temperature and humidity chamber (25 °C, 50% RH) and held for 48 hr prior to testing.

### 6.2.4. Film Lamination

PET/FG-nanoclay composite/LDPE and PET/EVOH/LDPE laminates were produced using an adhesive laminator equipped with computerized drive and control systems. The line included process parameter controls for the control of web tension and guiding of the individual plies. The laminate production step is depicted in Figure 1.

Dry bond laminating was used to bond the layers. The coating (adhesive:ethyl acetate 50:50) was coated on the PET layer and the FG or EVOH films were fed into the machine after the substrate coated PET passed through a heater/dryer and before the LDPE web was combined to form the laminate. The coating applied had a basis weight of 1.65 pounds/ream. Then the PET/FG or PET/EVOH laminates were cut from the roll and the unbound LDPE layer was discarded. The 2<sup>nd</sup> lamination was done by feeding PET/FG or PET/EVOH laminates with FG or EVOH layer facing up (to result in contact with LDPE layer) before the substrates were applied on a PET layer. The adhesive therefore

was applied on either FG or EVOH side, went through the heater dryer for the removal of the ethyl acetate, and then combined with LDPE web for the final lamination.

#### 6.2.5. Film Thickness

Film thickness was measured with a Digimicro MFC105 micrometer (Nikon, Japan). Measurements for testing mechanical properties were taken at five different locations on the film samples for each test. For testing oxygen and water barrier properties, measurements were made at nine different locations. The mean thickness was used to calculate the mechanical and barrier properties of film.

#### 6.2.6. Color Values and Haze

Hunter L, A, and B values of films were measured by using ColorQuest II Spectrophotometer with Universal Software version 3.73 (Hunter Associates Laboratory, Inc., Reston, VA, USA). The machine was calibrated using a white standard plate (standard no. C6006) and a gray standard plate (standard no. C6006-G). The film specimen was placed on white standard plate (standard no. C6006) having color value of  $L = 94.62$ ,  $a = -0.91$  and  $b = 0.64$  and mounted at the reflectance port. Color values were measured at three random positions including the center of the film specimen. The L axis runs from top to bottom. The maximum for L is 100, which would be a perfect reflecting diffuser. The minimum for L would be zero, which would be black. The a and b axes have no specific numerical limits. Positive a is red. Negative a is green. Positive b is yellow. Negative b is blue (HunterLab Applications Note, 1996). Total color difference

(E) was calculated by substituting acquired Hunter L, a, and b values into the equation below.

The haze of films was determined using ColorQuest II Spectrophotometer with Universal Software Version 3.73 (Hunter Associates Laboratory, Inc., Reston, VA, USA). The haze measurement was made in transmission mode and calculated using following equation. The standard white plate (Standard No. C6006, X = 81.77, Y = 86.72, Z = 92.18) provided by the manufacturer was used for calibration and background. The values were expressed by

$$\text{Haze} = \frac{\text{Y Diffuse transmission}}{\text{Y Total transmission}} \times 100$$

#### 6.2.7. Bond Strength

The bond strength of the lamination was determined with an Instron Universal Testing Machine (Model 5566, Instron Corp., Canton, MA, U.S.A.). Ten specimen samples, 25.4 cm x 2.54 cm, were cut in machine direction and transverse directions from multilayer film samples prepared from the laminator. Samples were conditioned for 48 hr at 25°C and 50% relative humidity (RH) in a constant temperature and humidity chamber before the measurement. Initial grip separation and cross-head speed were set at 2.54 cm and 280 mm/min, respectively. The force required to separate 3 in of the test specimen at 280 mm/min was recorded. Bond strength was calculated by first disintegrating the initial peak and then the average force to separate the next 2 inches of each specimen was



determined according to the ASTM standard method F904-98 (ASTM 2003). Bond strength was expressed in  $\text{g}/25.4 \text{ mm}$ . The mechanism of failure is important in bond measurement, so this was observed also.

#### 6.2.8. Oxygen Permeability

Oxygen permeability was measured at  $23 \pm 1 \text{ }^\circ\text{C}$  and RH condition of 50% and done in triplicate to get the average mean value. The oxygen transmission rate was determined in an OX-TRAN 2/20 (Mocon, Inc., Minneapolis, MN, USA). The samples were equilibrated at  $50 \pm 1\%$  relative humidity ( $23 \pm 1 \text{ }^\circ\text{C}$ ) for a period of 48 hr before analysis. The gas flow rate was fixed at (10 mL/min) and the difference in pressure across the film corresponded to atmospheric pressure (101.3 kPa). Oxygen permeability ( $\text{cc}\cdot\text{m}/\text{m}^2\cdot\text{day}\cdot\text{atm}$ ) was calculated by multiplying the oxygen transmission rate by the film thickness.

#### 6.2.9. Microscopy Observation

The cross section of the laminate was observed using Nikon OPTIPHOT (Nikon, Japan) equipped with Color Camera (NC-8 CCD, NEC, Japan) and *For-a* Video Micro Scaler IV-550. The scale on the video micro scaler was calibrated using 0.04"/0.001" scale stage micrometer. The 40X objective lens was used for the observation of the cross section of the laminates. The cut samples were treated with iodine before the observation in order to induce clear distinction between layers.

#### 6.2.10. Transmission Electron Microscopy (TEM)

For TEM observation, 70-90 nm sections of the samples were microtomed at room temperature using an Ultracut E microtome at a cutting speed of 0.05 mm/s. The sections were cut perpendicular to the casting direction of the casted film. The observations were made using the transmission electron microscopy (H-7600T, HITACHI, Japan) at 120 kV using magnifications from 20,000 to 300,000 times to study dispersions of clay particles..

#### 6.2.11. Statistical Analysis

Measurements were replicated three times for each film, with individually prepared films as the replicated experimental units. Statistics on a completely randomized design were performed with the analysis of variance (ANOVA) procedure in SAS (Release 9.1, SAS Institute Inc., Cary, NC) software. Duncan's Multiple Range Test ( $p < 0.05$ ) was used to detect differences among film property mean values.

### **6.3. Results and Discussion**

#### 6.3.1. Color Values and Haze

In this observation, the color and haze was significantly different between laminate films containing EVOH and FG clay composite films. The lightness ( $L$ ) of the laminations varied from  $96.43 \pm 0.16$  to  $95.78 \pm 0.04$ . Laminate films containing FG clay composite showed lower  $L$  values than EVOH samples which suggests that FG containing laminate films were darker. The red/green values ( $a$ ) and yellow/blue values

(b) varied from  $0.07 \pm 0.01$  to  $-0.21 \pm 0.01$  and  $0.65 \pm 0.01$  to  $2.46 \pm 0.04$ , respectively. These results suggested that the color of films became more greenish and bluish when FG clay composite film was used as an oxygen barrier layer. The color difference between gelatin composite and EVOH films was visible to the naked eye.

Like color value, the haze value was significantly different between laminate films containing EVOH and FG clay composite film. The haze value ranged from  $7.25 \pm 0.10$  to  $8.07 \pm 0.10$  with laminate film containing FG clay composite films showing higher haziness. Although significantly different, it can be suggested that addition of 20% (w/w)  $\text{Na}^+$  montmorillonite did not alter the film's haziness in great extent. This result suggested that high degree of exfoliation resulted in relatively narrow distinction of haziness between samples with EVOH and FG clay composite. The haze difference between gelatin composite and EVOH films was visible to the naked eye.

### 6.3.2. Bond Peel Strength

The objective of this test was to compare adhesion strength between different layers of the laminate films produced. It is interesting to note that the bond peel behavior between layers made of FG based films and EVOH films showed different behavior. In the case of LDPE/FG (sorbitol or glycerol), delamination occurred followed by elongation, then tearing, of LDPE. However, for LDPE/EVOH sample (F or XL), the mode of failure was due to mostly delamination, then elongation of LDPE layer, with no tearing. The tearing initiated at the beginning of the bond test with short strings coming

off the interface between LDPE and FG film surface. This suggests that adhesion strength was stronger between LDPE/FG film layer.

The test results of bonds to the PET layer showed similar behavior between laminate films which contained FG based films (sorbitol and glycerol) and EVOH (F and XL) films. The failure for PET/FG and PET/EVOH film samples was due to break of PET film. This was caused by tensile failure of the PET film layer. The failure for all PET/FG and PET/EVOH samples occurred shortly after the beginning of the test (within 0.3 inches of separation). The numbers before and after break are included in the average load values ( $g_f$ ). However, after the PET breaks, we are no longer measuring the actual bond between layers. To cause the PET break, the bond strength between the layers was apparently stronger than the breaking force of PET film. Thus, in this case, it may be more appropriate to use maximum load which occurred before the PET failed. Overall, acquired maximum load ( $g_f$ ) values ranged from  $334.02 \pm 41.05$  g/25.4 mm to  $997.66 \pm 53.26$  g/25.4 mm. PET/FG maximum bonds were stronger than PET/EVOH bonds.

### 6.3.3. Oxygen Permeability

The oxygen permeability of PET/FG/LDPE and PET/EVOH/LDPE laminate films are depicted in Table 4.

The performance of the PET/FG/LDPE laminate films changed according to the different RH conditions. The laminations exhibited good oxygen barrier properties under low RH conditions, but their applications under high RH environments would be limited

due to hydrophilicity of fish gelatin. Therefore, specific RH conditions during end-use applications must be considered. Rico-Pena and Torres (1990) examined the effect of relative humidity on the oxygen transmission rate through methylcellulose-palmitic acid edible films. No significant increase in oxygen transmission rate was observed between 0 and 57% relative humidity. However, above 57% relative humidity an exponential increase in oxygen transmission rate resulted.

Liebman and Gilbert (1973) reported significant increase of OP of collagen films when relative humidity was increased from 63 to 93%.

Lim and others (1999) reported large increase in oxygen permeabilities above 50% RH for MTGase cross-linked gelatin films. They reported that as the polymer continued to gain moisture, the concomitant large-scale molecular motion and swelling of the film caused a diminished resistance to transport of the relatively small O<sub>2</sub> molecules.

#### 6.3.4. Microscopy Observation

The cross sectional images of PET/FG/LDPE and PET/EVOH/LDPE laminate films are depicted in Figure 2. The adhesive layer was observed at both sides of the middle layer (FG or EVOH). The adhesive layer was evenly distributed across the section observed. The thickness measured by the micro scaler of PET, LDPE, FG (sorbitol and glycerol), and EVOH (F and XL) were 0.5, 1.25, 1.4, 0.45 mil, respectively.

#### 6.3.5. Transmission electron microscopy (TEM)

TEM is one of the main tools used for determination of the dispersion of clay nanoparticles in the polymer matrix. The TEM images of the ultrasonified fish gelatin-clay composite film containing 20 wt % clay plasticized using glycerol or sorbitol are shown in Figure. 3~Figure. 6. As can be seen in the Figures, no large agglomerates were visible, there were some smaller tactoids (2~3 particles), but the dominant structure observed consisted of single exfoliated silicates.

#### 6.4. Conclusion

The biodegradable barrier layer based on fish gelatin-nanoclay composite film have been developed in this study. Even after lamination, the fish gelatin-nanoclay composite film show a great oxygen barrier properties at RH under 50% of which were comparable to EVOH barrier films. Furthermore, the fish gelatin-nanoclay composite film possess good adhesion characteristics. Therefore, it can be suggested that fish gelatin-nanoclay composite can be suitable for barrier layers in laminates for food packaging.

#### 6.5. References

- Arvanitoyannis, I. S., Nakayama, A., Aiba, S. Chitosan and gelatin based edible films: state diagrams, mechanical and permeation properties. *Carbohydr Polym*, 1998, 37, 371-382.
- Chen, H. Functional Properties and Applications of Edible Films Made of Milk Proteins. *J Dairy Sci*, 1995, 78, 2563-2583.

- Forssell, P., Lahtinen, R., Lahelin, M., and Myllärinen, P. Oxygen Permeability of Amylose and Amylopectin Films. *Carbohydr Polym*, 2002, 47, 125-129.
- Gennadios, A. and Weller, C. L. (1990). Edible films and coatings from wheat and corn proteins. *Food Technology*, 44(10), 63-69.
- Gennadios, A. and Weller, C. L. (1991). Edible films and coatings from soy milk and soy protein. *Cereal Foods World*, 36(12), 1004-1009.
- Gilleland, G. M., Turner, J. L., Patton, P. A., and Harrison, M. D. Modified Starch As A Replacement For Gelatin In Soft Gel Films And Capsules, *World Intellectual Property Organization*, International Patent Number 2001, WO 01/91721 A2.
- Gennadios, A., Weller, C. L., and Testin, R. F. Temperature Effect on Oxygen Permeability of Edible Protein-based Films. *J Food Sci*, 1993, 58, 212-219.
- Gilmer, J. W., Germinario, L. T., and Bagrodia, S. (2002). Structure-property relationships in polyamide based nanocomposites. *ABSTRACTS OF PAPERS OF THE AMERICAN CHEMICAL SOCIETY*, 223, D90-D90 215-PMSE Part 2.
- Gontard, N., Guilbert, S., and Cuq, J. Water and Glycerol as Plasticizers Affect Mechanical and Water Vapor Barrier Properties of an Edible Wheat Gluten Film, *J Food Sci*, 1993, 58(1), 206-211.
- Gontard, N., Thibault, R., Cuq, B., and Guilbert, S. Influence of Relative Humidity and Film Composition on Oxygen and Carbon Dioxide Permeabilities of Edible Films, *Journal Agr Food Chem*, 1996, 44, 1064-1069.
- Guilbert, S. Technology and application of edible protective films in Food Packaging and Preservation, Elsevier Applied Science, London, 1986, 371-394.
- Han, J. H. Design of Edible and Biodegradable Films/Coatings Containing Active Ingredients. Pre-Congress Short Course of IUFOST 'Active Biopolymer Films and Coatings for Food and Biotechnological Uses', Korea University, Seoul, Korea. 2001.
- Kester, J. J. and Fennema, O. R. (1986). Edible films and coatings – a review. *Food Technology*, 40(12), 47-59.
- Kim, K. W., Ko, C. J., and Park, H. J. (2002). Mechanical Properties, Water Vapor Permeabilities and Solubilities of Highly Carboxymethylated Starch-Based Edible Films. *J Food Sci*, 67(1), 218-222.

- Lawton, J. W. Effect of Starch Type on the Properties of Starch Containing Films, *Carbohydr Polym*, 1996, 29, 203-208.
- Lee, J. J. and Rhim, J. W. Characteristics of Edible Films Based with Various Cultivars of Sweet Potato Starch, *Korean J Food Sci and Technol*, 2000, 32(4), 834-842.
- Lieberman, E. R. and Gilbert, S. G. (1973). Gas permeation of collagen films as affected by cross-linkage, moisture, and plasticizer content. *J Polym Sci*, 41, 33-43.
- Lim, L. T., Mine, Y., and Tung, M. A. (1999). Barrier and Tensile Properties of Transglutaminase Cross-linked Gelatin Films as Affected by Relative Humidity, Temperature, and Glycerol Content. *J Food Sci*, 64(4), 616-622.
- Lourdin, D., Valle, G. D., and Colonna, P. Influence of amylose content on starch films and foams, *Carbohydr Polym*, 1995, 27, 261-270.
- McHugh, T. H., Aujard, J. F., and Krochta, J. M. Plasticized Whey Protein Edible Films: Water Vapor Permeability Properties, *J Food Sci*, 1994, 59(2), 416-419.
- McHugh, T. H. and Krochta, J. M. Sorbitol- vs Glycerol-Plasticized Whey Protein Edible Films: Integrated Oxygen Permeability and Tensile Property Evaluation, *J Agr Food Chem*, 1994, 42, 841-845.
- Park, H. J., Chinnan, M. S. (1995). Gas and Water Vapor Barrier Properties of Edible Films from Protein and Cellulosic Materials. *Journal of Food Engineering*, 25, 497-507.
- Park, H. J., Weller, C. L., Vergano, P. J., and Testin, R. F. (1993). Permeability and Mechanical Properties of Cellulose-Based Edible Films. *J Food Sci*, 58(6), 1361-1370.
- Park, S.Y., Lee, B.I., Jung, S.T., and Park, H.J. (2001). Biopolymer composite films based on k-carrageenan and chitosan. *Mater Res Bull*, 36, 511-519.
- Rico-Pena, D. C., and Torres, J. A. (1990). Oxygen transmission rates of an edible methylcellulose-palmitic acid film. *J Food Process Eng*, 13, 125-133.
- Ruiz-Hitzky, E. and Meerbeek, A. V. (2006). Chapter 10.3: Clay Mineral-and Organoclay-Polymer Nanocomposite, In: Bergaya, F, Theng, B. K. G., and Lagaly, G. (eds) Handbook of clay science, pp. 583-622. Elsevier, Academic Press.



- Sinha Ray, S. and Okamoto, M. (2003). Polymer/layered silicate nanocomposites: areview from preparation to processing. *Progress in Polymer Science* 28(11), 1539-1641.
- Qian, X. F., Yin, J., Yang, Y. F., Lu, Q. H., Zhu, Z. K., and Lu, J. (2001). Polymer-inorganic nanocomposites prepared by hydrothermal method: Preparation and characterization of PVA-transition-metal sulfides. *JOURNAL OF APPLIED POLYMER SCIENCE*, 82(11), 2744-2749.
- Vanin, F. M., Sobral, P. J. A., Menegalli, F. C., Carvalho, R. A., and Habitante, A. M. Q. B. (2005). Effects of plasticizers and their concentrations on thermal and functional properties of gelatin-based films. *Food Hydrocolloid*, 19, 899-907.
- Yano, K., Usuki, A., and Okada, A. (1997). Synthesis and properties of polyimide-clay hybrid films. *JOURNAL OF POLYMER SCIENCE PART A-POLYMER CHEMISTRY*, 35(11), 2289-2294.
- Yi, J. B., Kim, Y. T., Bae, H. J., Whiteside, W. S., and Park, H. J. (2006). Influence of Transglutaminase-Induced Cross-Linking on Properties of Fish Gelatin Films. *J Food Sci*, 71(9), 376-383.

## 6.6. Figure Captions

**Figure 6.1.** Flow chart of PET/FG/LDPE and PET/EVOH/LDPE laminate preparation.

**Figure 6.2.** Observation of cross section of the laminates. (a) PET/FG(sorbitol)/LDPE (0.5/1.4/1.25 mil), (b) PET/FG(glycerol)/LDPE (0.5/1.4/1.25 mil), (c) PET/EF-F/LDPE (0.5/0.45/1.25 mil), and (d) PET/EF-XL/LDPE (0.5/0.45/1.25 mil).

**Figure 6.3.** TEM observation at 50,000 magnification of FG (glycerol) film containing 20% w/w clay content.

**Figure 6.4.** TEM observation at 100,000 magnification of FG (glycerol) film containing 20% w/w clay content.

**Figure 6.5.** TEM observation at 50,000 magnification of FG (sorbitol) film containing 20% w/w clay content.

**Figure 6.6.** TEM observation at 100,000 magnification of FG (sorbitol) film containing 20% w/w clay content.

**Figure 6.7.** Oxygen permeability of PET/FG/LDPE and PET/EVOH/LDPE laminates

### **6.7. Table Captions**

**Table 6.1.** Color and haze of produced laminate films.

**Table 6.2.** Bond peel strength of LDPE / FG and LDPE / EVOH laminates.

**Table 6.3.** Bond peel strength of PET / FG and PET / EVOH laminates

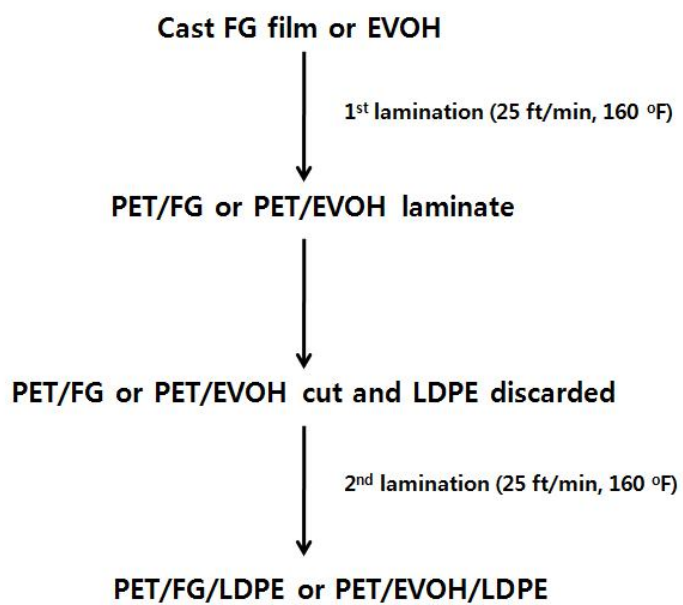


Figure 6.1. Flow chart of PET/FG/LDPE and PET/EVOH/LDPE laminate preparation.

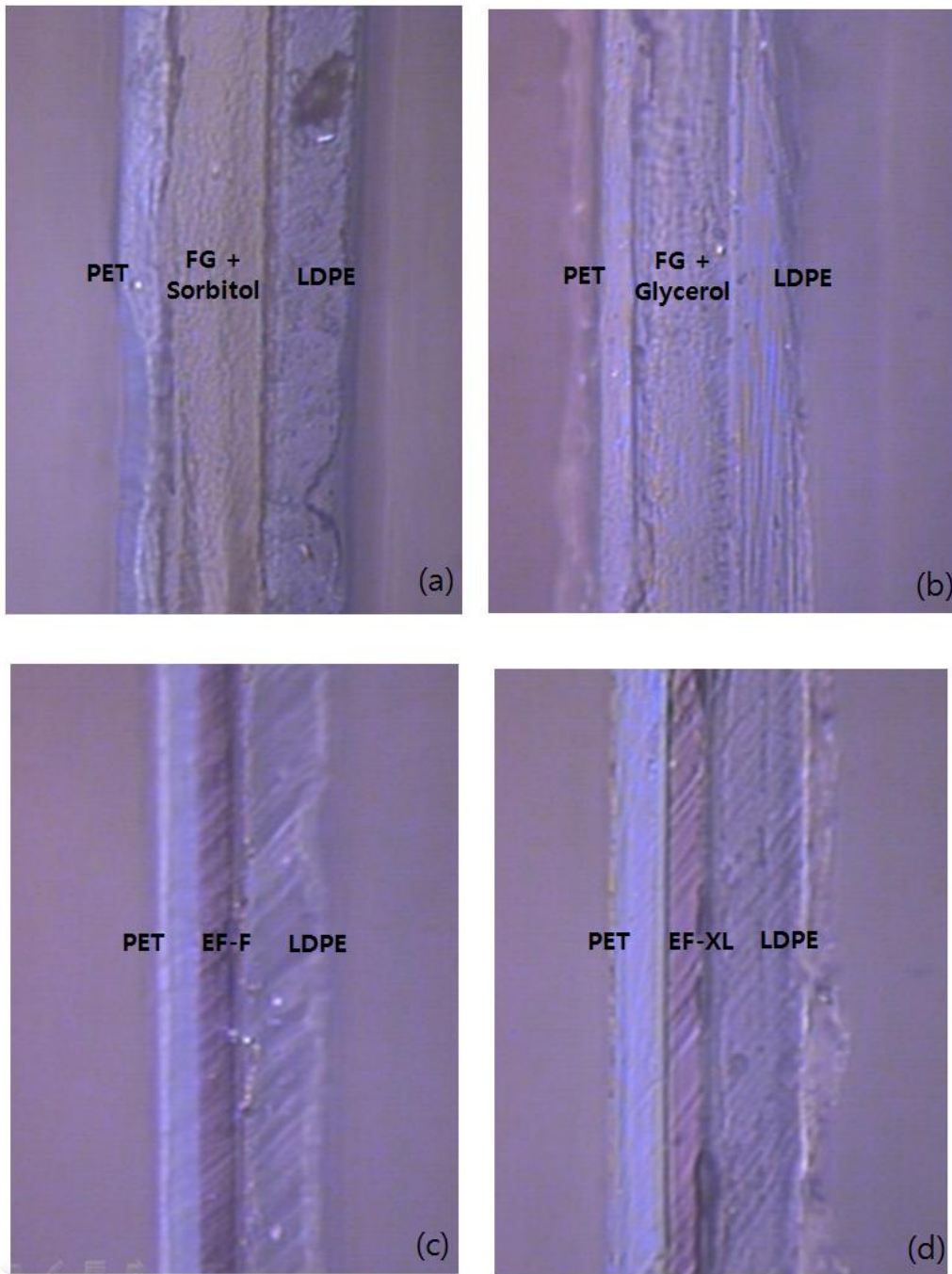
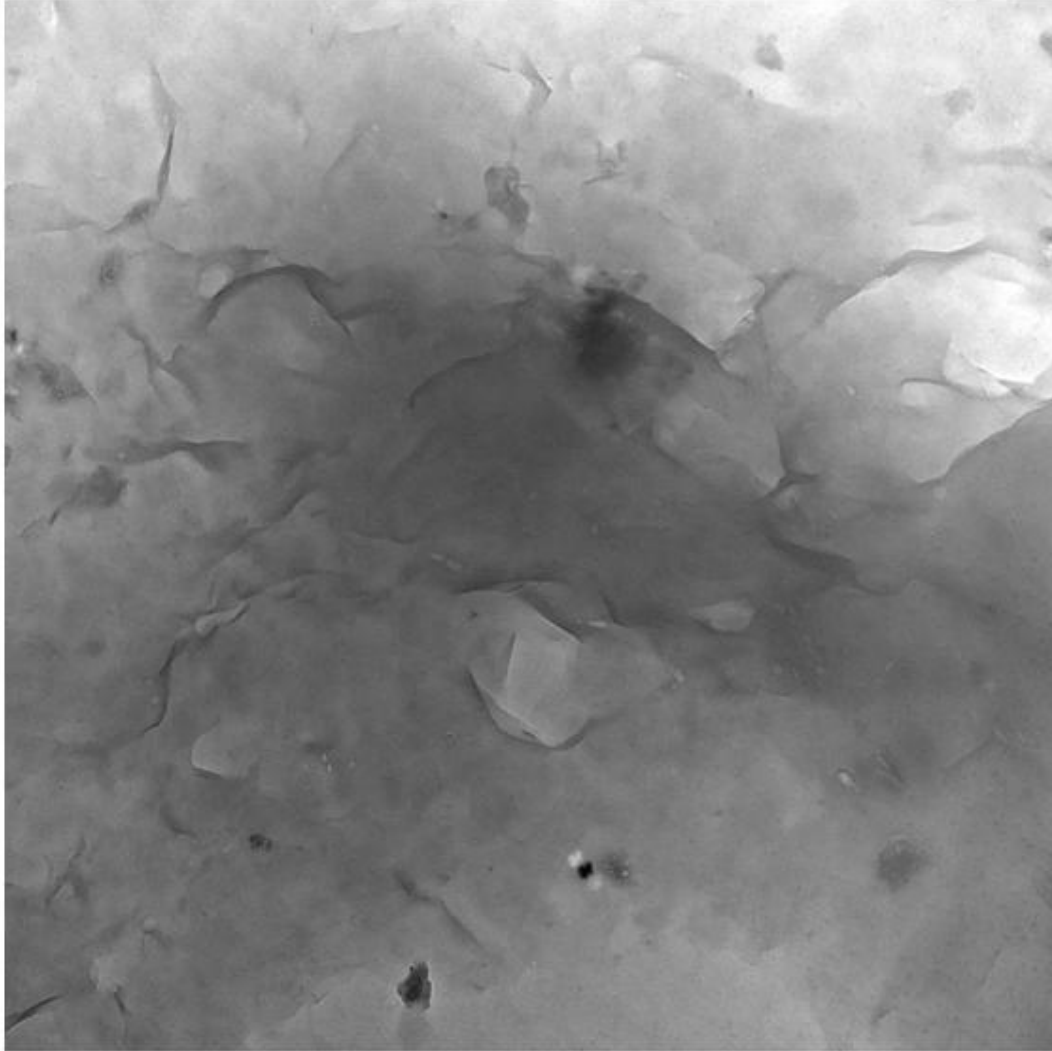


Figure 6.2. Observation of cross section of the laminates. (a) PET/FG(sorbitol)/LDPE (0.5/1.4/1.25 mil), (b) PET/FG(glycerol)/LDPE (0.5/1.4/1.25 mil), (c) PET/EF-F/LDPE (0.5/0.45/1.25 mil), and (d) PET/EF-XL/LDPE (0.5/0.45/1.25 mil).



8.tif

Print Mag: 17200x @ 51 mm

15:44 10/30/07

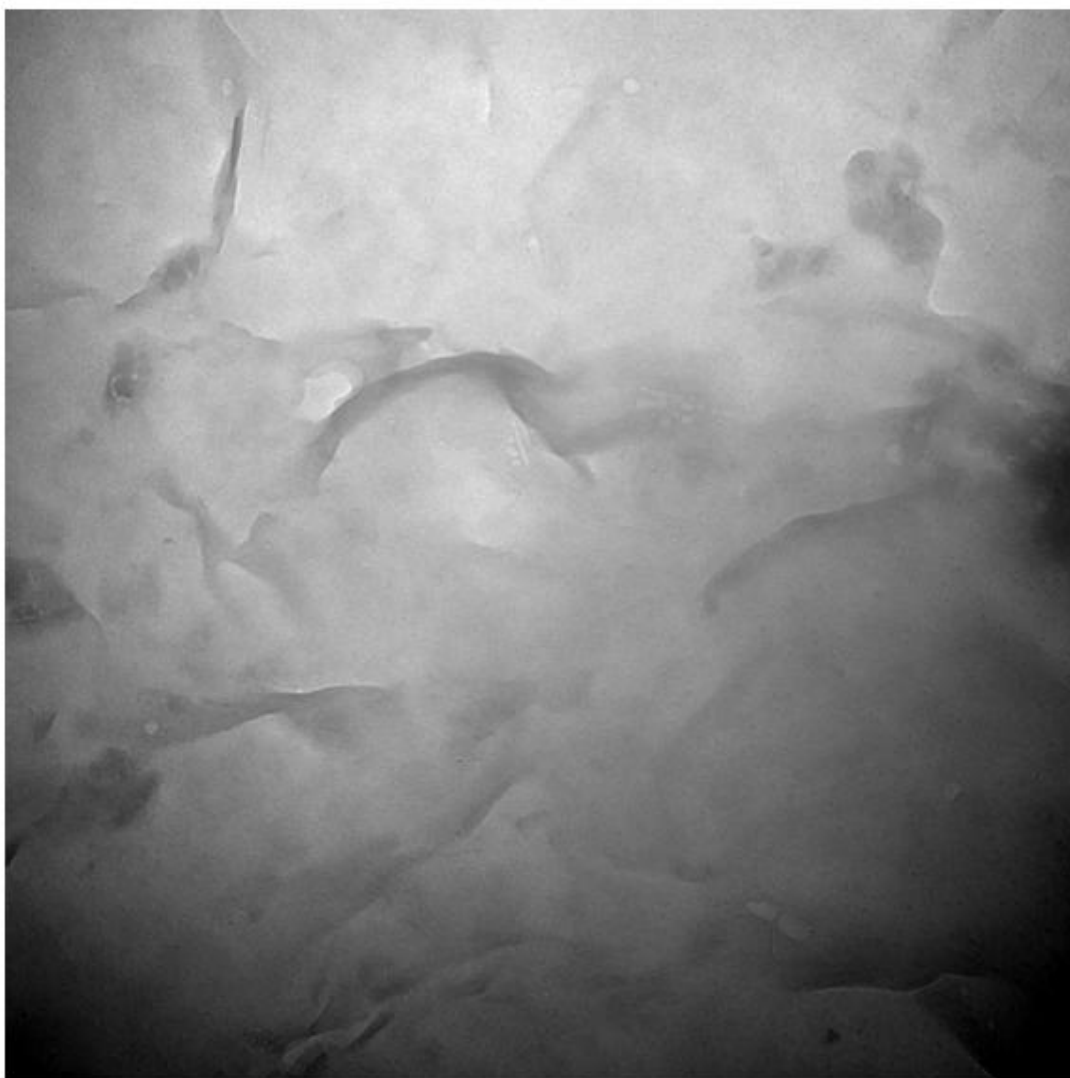
500 nm

HV=120kV

Direct Mag: 50000x

Clemson EM Center

Figure 6.3. TEM observation at 50,000 magnification of FG (glycerol) film containing 20% w/w clay content.



15.tif

Print Mag: 34400x @ 51 mm

15:55 10/30/07

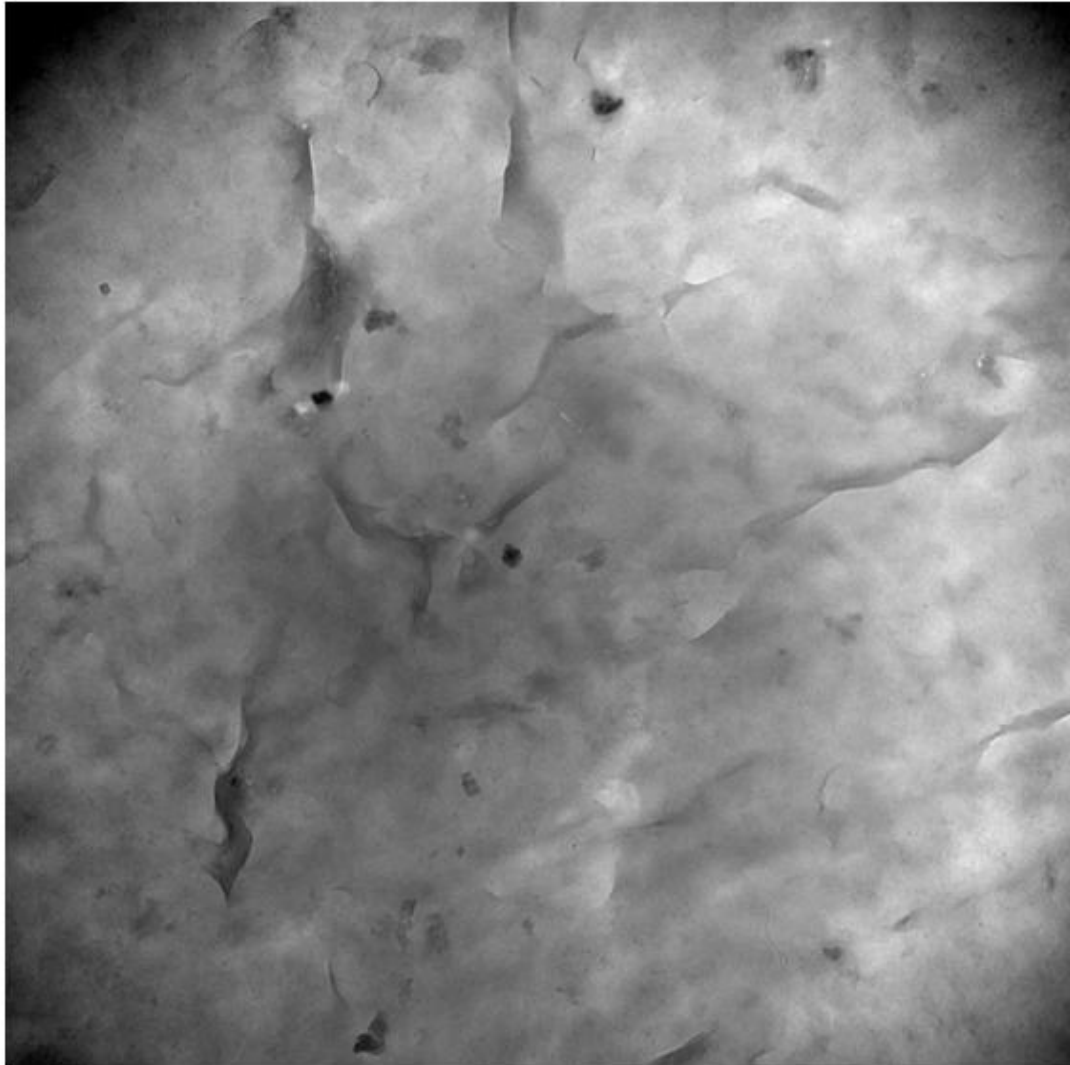
100 nm

HV=120kV

Direct Mag: 100000x

Clemson EM Center

Figure 6.4. TEM observation at 100,000 magnification of FG (glycerol) film containing 20% w/w clay content.



3.tif

Print Mag: 17200x @ 51 mm

14:36 10/30/07

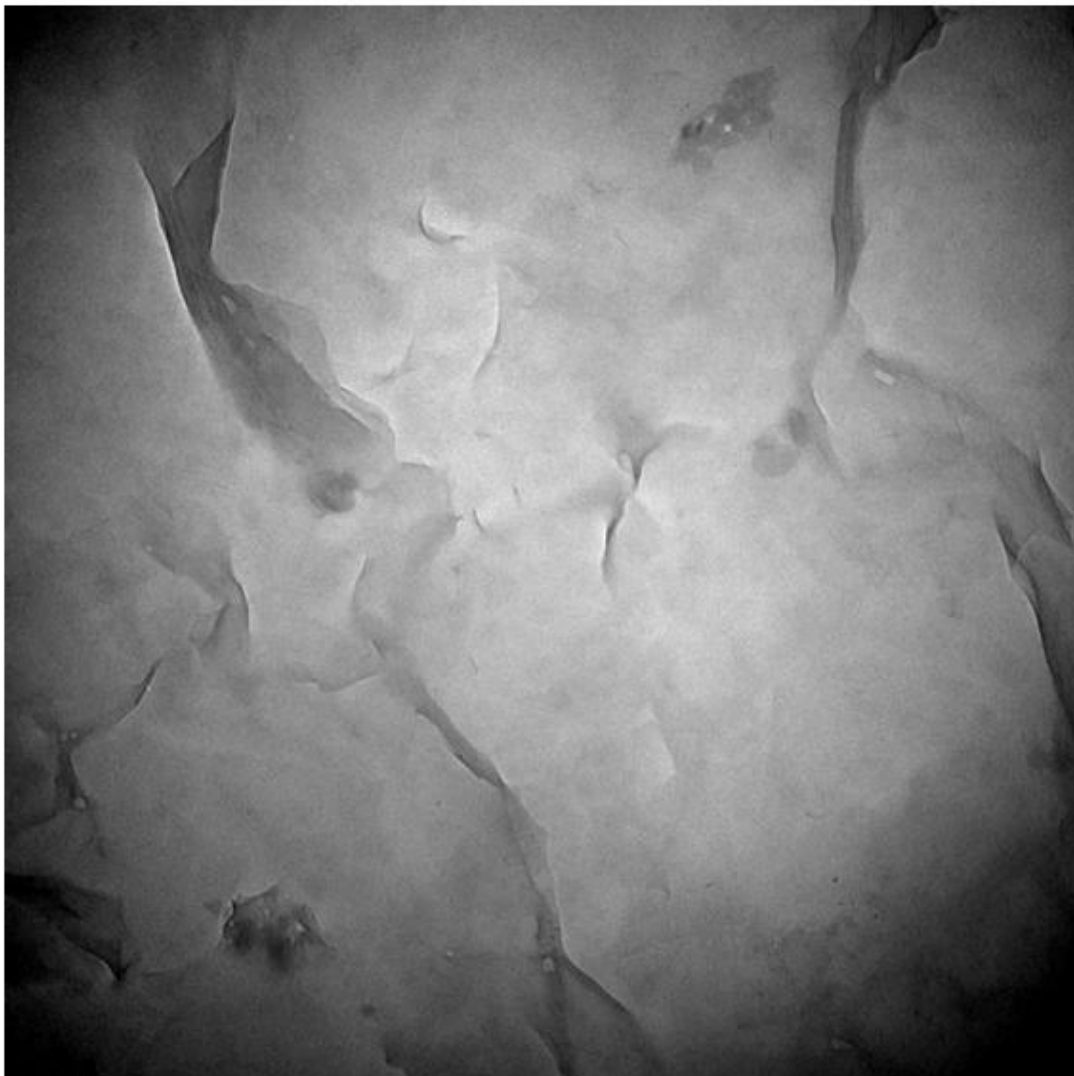
500 nm

HV=120kV

Direct Mag: 50000x

Clemson EM Center

Figure 6.5. TEM observation at 50,000 magnification of FG (sorbitol) film containing 20% w/w clay content.



6.tif

Print Mag: 34400x @ 51 mm

14:42 10/30/07

100 nm

HV=120kV

Direct Mag: 100000x

Clemson EM Center

Figure 6.6. TEM observation at 100,000 magnification of FG (sorbitol) film containing 20% w/w clay content.



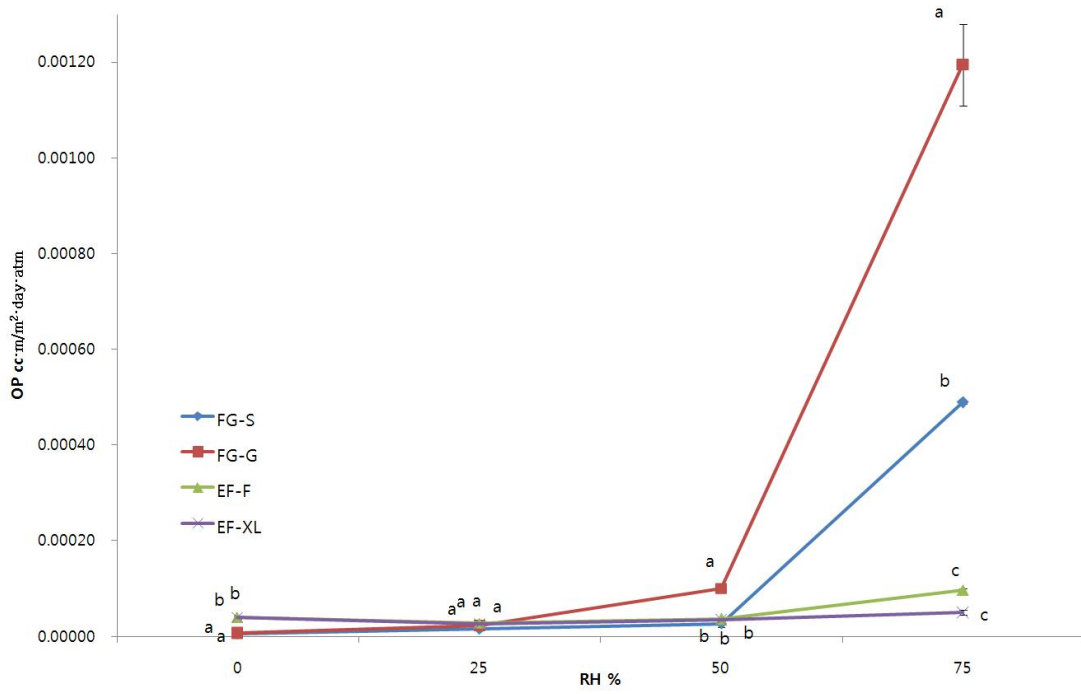


Figure 6.7. Oxygen permeability of PET/FG/LDPE and PET/EVOH/LDPE laminates.

Table 6.1. Hunter L, a, b and haze (%) of produced PET/FG-nanoclay composite/LDPE and PET/EVOH/LDPE laminate films. Values given as mean $\pm$ SD from three determinations (n=3).

Laminate Type	Hunter L a b			Haze <sup>D</sup> (%)
	L <sup>A</sup>	a <sup>B</sup>	b <sup>C</sup>	
LDPE/PET	96.43 $\pm$ 0.16 <sup>a</sup>	0.07 $\pm$ 0.01 <sup>a</sup>	0.65 $\pm$ 0.01 <sup>c</sup>	7.06 $\pm$ 0.05 <sup>b</sup>
LDPE/EVOH EF-F/PET	96.38 $\pm$ 0.08 <sup>a,b</sup>	0.06 $\pm$ 0.00 <sup>a</sup>	0.64 $\pm$ 0.02 <sup>c</sup>	7.25 $\pm$ 0.10 <sup>b</sup>
LDPE/EVOH EF-XL/PET	96.21 $\pm$ 0.07 <sup>b</sup>	0.06 $\pm$ 0.01 <sup>b</sup>	0.63 $\pm$ 0.01 <sup>c</sup>	7.23 $\pm$ 0.43 <sup>b</sup>
LDPE/FG-clay-glycerol/PET	96.00 $\pm$ 0.06 <sup>c</sup>	-0.14 $\pm$ 0.02 <sup>b</sup>	1.82 $\pm$ 0.16 <sup>b</sup>	7.70 $\pm$ 0.11 <sup>a</sup>
LDPE/FG-clay-sorbitol/PET	95.78 $\pm$ 0.04 <sup>d</sup>	-0.21 $\pm$ 0.01 <sup>c</sup>	2.46 $\pm$ 0.04 <sup>a</sup>	8.07 $\pm$ 0.10 <sup>a</sup>

<sup>A</sup> a-e indicate significant differences ( $P < 0.05$ ) within columns L.

<sup>B</sup> a-e indicate significant differences ( $P < 0.05$ ) within columns a.

<sup>C</sup> a-d indicate significant differences ( $P < 0.05$ ) within columns b.

<sup>D</sup> a-d indicate significant differences ( $P < 0.05$ ) within columns Haze.

Table 6.2. Bond peel strength of LDPE / FG and LDPE / EVOH laminates. Values given as mean±SD from three determinations (n=3).

Sample	Mode of Failure	AVG Load <sup>A</sup> (gf)	Maximum Load/width <sup>B</sup> (gf/25 mm)
LDPE / FG + sorbitol	Delamination, elongation, partial tear of LDPE	806.88 ± 165.33 <sup>a</sup>	934.12 ± 68.90 <sup>a,b</sup>
LDPE / FG + glycerol	Delamination, elongation, partial tear of LDPE	917.79 ± 44.40 <sup>a</sup>	997.66 ± 53.26 <sup>a</sup>
LDPE / EF-F	Delamination, elongation of LDPE	870.73 ± 28.20 <sup>a</sup>	912.65 ± 33.16 <sup>a,b</sup>
LDPE / EF-XL	Delamination, elongation of LDPE	781.55 ± 53.07 <sup>a</sup>	887.54 ± 3.58 <sup>b</sup>

<sup>A</sup> a-e indicate significant differences ( $P < 0.05$ ) within columns AVG Load.

<sup>B</sup> a-e indicate significant differences ( $P < 0.05$ ) within columns Maximum Load/width.

Table 6.3. Bond peel strength of PET / FG and PET / EVOH laminates Values given as mean±SD from three determinations (n=3).

Sample	Mode of Failure	AVG Load <sup>A</sup> (gf)	Maximum Load/width <sup>B</sup> (gf/25 mm)
PET / FG + sorbitol	Break (cohesive) of PET	64.82 ± 13.05 <sup>a</sup>	504.58 ± 57.97 <sup>a,b</sup>
PET / FG + glycerol	Break (cohesive) of PET	56.02 ± 23.66 <sup>a,b</sup>	614.69 ± 137.63 <sup>a</sup>
PET / EF-F	Break (cohesive) of PET	41.85 ± 2.10 <sup>a,b</sup>	370.33 ± 52.93 <sup>b,c</sup>
PET / EF-XL	Break (cohesive) of PET	30.88 ± 7.75 <sup>b</sup>	334.02 ± 41.05 <sup>c</sup>

<sup>A</sup> a-e indicate significant differences (P < 0.05) within columns AVG Load.

<sup>B</sup> a-e indicate significant differences (P < 0.05) within columns Maximum Load/width.

## CHAPTER SEVEN

### GENERAL CONCLUSION

The high-powered ultrasonifer treated nanocomposite film exhibited an exfoliated type structure with improved tensile strength and barrier properties and the films produced were uniform in thickness and relatively transparent. Nanocomposite film without the ultrasonifer treatment exhibited an intercalated type structure and showed improved tensile strength and barrier properties although not as good as exfoliated type. The result gathered by XRD and TEM observations confirms the difference in clay dispersion. Improvement of mechanical and barrier properties were achieved as a function of the clay content. The effect of homogenization on clay solution did not impart any changes in mechanical or barrier properties of produced nanocomposite films. At higher pH ( $\text{pH} > \text{pI}$ ), the produced films showed poor mechanical and barrier properties compared to samples at lower pH and this due to electrostatic repulsion between the protein anion and the negatively charged montmorillonite surface. This study promotes the fact that clean ultrasonic energy contributes to the intercalation and exfoliation of unmodified montmorillonite clays. The complete exfoliation of clay silicates without the use of chemical modification is significant both in terms of cost and biodegradability.

MTGase treated protein-based nanocomposites have been successfully developed from a biopolymer. In the blends, the unmodified sodium montmorillonite clay was initially treated with a high-powered ultrasonifer in a solution of sorbitol and distilled water. The nano-clay solution was then added to a MTGase treated (0 to 50 min) fish gelatin solution and casted using a mechanical film caster. After the MTGase treatment,

the viscosity of fish gelatin solution increased because of the cross-linking. MTGase treatment increased molecular weight, but decreased tensile strength. MTGase treatment had no significant effect on oxygen permeability, water vapor permeability, and elongation %. This can be explained by the fact that high molecular weight and large molecular dimension may cause failure to intercalate. Studies show that the MTGase modification did not significantly affect the mechanical and barrier properties as compared to native film.

The biodegradable barrier layer based on fish gelatin-nanoclay composite film have been developed using conventional laminating machine. Even after lamination, the fish gelatin-nanoclay composite film show great oxygen barrier properties at RH up to 50% of which were comparable to EVOH barrier films. Significant increase of OP can be observed for biopolymer films when the relative humidity increases from 60% to 90%. The fish gelatin-nanoclay composite film showed good adhesion characteristics. The laminate film can be produced using very simple, relatively rapid, and low cost technology that does not require expensive instrumentation. Therefore, it can be suggested that fish gelatin-nanoclay composite can be suitable for barrier layers in laminates for food packaging.

For future studies, investigation of fish gelatin-nanoclay composite film using thermoanalytical techniques : differential thermal analysis (DTA), thermogravimetry (TG), differential scanning calorimetry, dynamic mechanical analysis (DMA), differential scanning calorimetry (DSC), and derivative thermogravimetry (DTG) etc. in order to investigate relationship between polymer and clay. Simultaneous recording of

thermal curves obtained using multiple techniques can be of great significance due to the much greater possibilities for a fuller interpretation of results obtained.

Transmission electron microscopy can be another field that requires further study. TEM investigation according to different degree of ultrasonification treatment and clay : water : plasticizer ratio can be a significant study in this field. To date, sufficient TEM image is not provided in order to thoroughly show difference in clay dispersion behavior.

It has been proposed that intercalation of proteins into montmorillonite may produce important distortions and other conformational changes in both the secondary and the tertiary structure of proteins due to their confinement in the interlayer space of smectites. Using advanced spectroscopic techniques such as solid state high resolution NMR, any loss of entropy associated to the intercalation process.